New theories of relativistic hydrodynamics in the LHC era

Wojciech Florkowski[*1,2,3], Michal P. Heller[†4,5], and Michał Spaliński[‡5,6]

[1] *Institute of Nuclear Physics, Polish Academy of Sciences, PL-31-342 Krakow, Poland*
[2] *Jan Kochanowski University, PL-25-406 Kielce, Poland*
[3] *ExtreMe Matter Institute EMMI, GSI, D-64291 Darmstadt, Germany*
[4] *Max Planck Institute for Gravitational Physics D-14476 Potsdam-Golm, Germany*
[5] *National Center for Nuclear Research, PL-00-681 Warsaw, Poland*
[6] *Physics Department, University of Białystok, PL-15-245 Białystok, Poland*

Abstract

The success of relativistic hydrodynamics as an essential part of the phenomenological description of heavy-ion collisions at RHIC and the LHC has motivated a significant body of theoretical work concerning its fundamental aspects. Our review presents these developments from the perspective of the underlying microscopic physics, using the language of quantum field theory, relativistic kinetic theory, and holography. We discuss the gradient expansion, the phenomenon of hydrodynamization, as well as several models of hydrodynamic evolution equations, highlighting the interplay between collective long-lived and transient modes in relativistic matter. Our aim to provide a unified presentation of this vast subject – which is naturally expressed in diverse mathematical languages – has also led us to include several new results on the large-order behaviour of the hydrodynamic gradient expansion.

---

[*]wojciech.florkowski@ifj.edu.pl
[†]michal.p.heller@aei.mpg.de
[‡]m.spalinski@uwb.edu.pl

Contents

3

1 Introduction and outline

The heavy-ion collision program pursued in recent years at the Relativistic Heavy Ion Collider (RHIC)[1] and the Large Hadron Collider (LHC) explores properties of nuclear matter under extreme conditions, close to those existing shortly after the Big Bang. The theoretical interpretation of its results requires a wide variety of methods which are needed to bridge the gap between the fundamental theory of the strong interactions in the form of Quantum Chromodynamics (QCD) and the experimentally accessible observables.

It was established at RHIC and confirmed at the LHC that the nuclear matter produced in heavy-ion collisions at ultrarelativistic energies exhibits clear signatures of collective behaviour. They are interpreted as experimental evidence for the creation of strongly-coupled Quark-Gluon Plasma (QGP), an equilibrium phase of QCD formed of deconfined quarks and gluons. The successful phenomenological description of collective behaviour in the soft observables sector is based on relativistic hydrodynamics [1] with a small viscosity to entropy density ratio, initiated very early, perhaps as soon as a fraction of fermi/c after the collision.

The unfolding of this story throughout the last 15 years or so has led to a great deal of progress in relativistic hydrodynamics. This period constitutes a veritable golden age for this discipline. Despite many excellent review articles [2–6] and books [7–9] devoted to these developments, we believe that there is a need for a systematic presentation of new ideas in the approach to relativistic hydrodynamics.

The key novelty of our present review is to recognize at the outset that hydrodynamic behaviour is a property of the underlying, microscopic descriptions of physical systems evolving toward equilibrium. This behaviour is captured by the truncated gradient expansion of the expectation value of the energy-momentum tensor, and possibly other conserved currents. The role of hydrodynamics is to mimic this behaviour at the level of a classical effective theory. The goal in this respect is to seek formulations of hydrodynamics which incorporate such degrees of freedom and such dynamics that they capture in the best way critical aspects of the evolution toward equilibrium. An important point is that, in general, such an effective description is not derived from a microscopic theory. Rather, it is posited in accordance with very general principles such as symmetry and conservation laws and is then reconciled with the underlying microscopic model by matching the gradient expansion at the hydrodynamic level with the gradient expansion at the microscopic level.

The inspiration for this attitude is the effective field theory paradigm which dominates our thinking in high-energy physics. An important milestone was the formulation of the Baier, Romatschke, Son, Starinets, Stephanov (BRSSS) theory in 2007 [10], which guarantees that the

---

[1]For the list of acronyms, symbols, and notation conventions used in this work see Secs. A, B, and C.

hydrodynamic description can be matched with any microscopic dynamics up to second order in the gradient expansion. Since then, the importance of effects which govern the applicability of hydrodynamics has come to be appreciated. This development has led to the realization that the hydrodynamic description can be accurate under much more extreme conditions than earlier seemed reasonable [11–13]. In particular, from this perspective it is not outrageous to apply models of relativistic hydrodynamics even for very anisotropic, inhomogeneous or small systems naturally created in collisions. It has in fact puzzled practitioners for a while that hydrodynamics can be used successfully in conditions which cannot plausibly be viewed as close even to local equilibrium. This has led to usage of the term "hydrodynamization" to mean the onset of the regime where a hydrodynamic description is useful. An extensive recent discussion of this and its phenomenological consequences can be found in Ref. [14].

Our goal is to review attempts to formulate new hydrodynamic theories which try to capture effects at the edge of what would traditionally be considered the domain of applicability of hydrodynamics. Important questions here concern the role of higher order terms in the gradient expansion [15–19], as well as the role of collective degrees of freedom not explicitly included in hydrodynamics and their relation to causality [10, 20]. We discuss approaches to formulating effective hydrodynamic descriptions taking inspiration from kinetic theory, quantum field theory and string theory.

Historically, methods based on the AdS/CFT correspondence, or gauge-gravity duality, more generally referred to as holography, have played an important role in understanding many of the points discussed in this article. On the other hand, most of these ideas can also be understood without reference to string theory. In particular, many essential aspects of the story can also be seen from the perspective of kinetic theory, even though some are more complex in that setting. We aim at presenting a unified picture which makes it easier to see similarities and differences between different microscopic frameworks in the context of applicability of hydrodynamics and hydrodynamic theories. Because of this, and also because there are many excellent specialized reviews, we have refrained from a comprehensive presentation of each individual framework or aspect. This has led to necessary omissions. Certainly, among the most important ones are: the anomalous transport phenomena reviewed in Ref. [21], progress on understanding the entropy production constraint in the hydrodynamic gradient expansion [22], the question of transport in the vicinity of a critical pole (see, e.g., Ref. [23]), detailed analysis of the effects of conformal symmetry breaking in hydrodynamics and beyond (see, e.g., Refs. [24–30]), the issue of thermal fluctuations in hydrodynamics (see, e.g., Ref. [31–33]), entropy production by horizons in holography (see, e.g., Refs. [34–37]) and holographic collisions (see Ref. [38] for a comprehensive picture of early developments and Ref. [39] for a state-of-the-art presentation).

This review is structured as follows. We begin with an overview of the theoretical challenges

raised by the heavy-ion collisions programme in Sec. 2. In Sec. 3 we use linear response theory to introduce the notion of a mode of equilibrium plasma and describe how modes manifest themselves in quantum field theory and kinetic theory. We introduce basic kinetic theory notions and signal the importance of string theory methods for the development of the field. In Sec. 4 we describe the relevant details on how holography works and demonstrate the connection between quasinormal modes of black branes and modes of strongly-coupled plasmas. Certainly, these developments significantly influenced the way we shaped our presentation in the preceding section. The main point made in Secs. 3 and 4 is the idea of a separation between imaginary parts of frequencies of long-lived (hydrodynamic) modes and transient (non-hydrodynamic) modes, which makes the former dominate the late time dynamics. This leads up to Sec. 5, which is devoted to a detailed presentation of the application of microscopic frameworks to the case of Bjorken flow, which simplifies the problem immensely while keeping many essential features. We review the results of holographic calculations which have led to the idea of hydrodynamization, that is, the emergence of quasi-universal features in the late-time behaviour at times when, superficially, the system is still far from local equilibrium. We also review subsequent results leading to similar conclusions obtained in the framework of kinetic theory. In Sec. 6 we turn to the issue of finding an effective description of late time behaviour in the language of relativistic hydrodynamics. We emphasise the need to maintain causality, which leads to the appearance of non-hydrodynamic modes also at the level of the effective theory. Section 7 reviews the notion of the gradient expansion in hydrodynamics and the idea that it may be used to match microscopic calculations. This is the central point which we emphasise in this review: hydrodynamic theories are engineered to match aspects of calculations in microscopic theories. We discuss this notion in detail for the case of Müller-Israel-Stewart (MIS) theory and its generalizations which attempt to capture some features of early time behaviour. This line of reasoning is continued in Sec. 8, which discusses how models of kinetic theory can be used as a guide in constructing hydrodynamic theories. An important example is the case of anisotropic hydrodynamics which is presented in detail. The question of large order behaviour of gradient expansions is reviewed in Sec. 9, where we explain how the gradient series encodes information about both the hydrodynamic and non-hydrodynamic sectors at the level of fundamental theories as well as for their hydrodynamic descriptions. We close with an outlook in Sec. 10.

This review contains also some new results which have not been published earlier but significantly complement or improve earlier presentations of the reviewed material. Among the ones that we would like to highlight are a unified presentation of holographic and RTA kinetic theory calculation of large order gradient expansion in Sec. 9.2 and the demonstration of the presence of a subleading transient mode in the Borel transform of the gradient expansion in holography in Fig. 17.

2 Motivation: ultrarelativistic heavy-ion collisions

2.1 Overview

The physical system which is the subject of this review is a lump of hot, dense, strongly interacting matter consisting of quarks and gluons. This type of matter existed in the Early Universe but at about 10 microseconds after the Big Bang, due to the expansion of the Universe and cooling, it transformed itself into hadrons. Similar physical conditions are now realized in Earth laboratories by colliding heavy atomic nuclei at the highest possible energies.

The first experiments with ultra-relativistic heavy ions (i.e., with energies exceeding 10 GeV per nucleon in the projectile beam) took place at BNL and at CERN in 1986. In 2000 the first data from RHIC at BNL was analysed. The LHC at CERN completed its first heavy-ion running period in the years 2010–2013. At the moment, the second period is taking place (2015–2018), while the third one is planned for the years 2021–2023.

Of particular importance in the heavy-ion program are experimental searches for theoretically predicted new phases of matter, description of the phase transitions between such phases (deconfinement, chiral symmetry restoration) and, ultimately, a possible reconstruction of the entire phase diagram of strongly interacting matter in a wide range of thermodynamic parameters such as temperature and baryon chemical potential. In this context, new experiments done at lower energies and with different colliding systems are also very much important, as this allows us to study the beam energy and baryon number density dependence of many aspects of particle production.

2.2 Phenomenology: the standard model of heavy ion collisions

The current understanding of heavy-ion collisions typically separates their evolution into three stages: i) the initial or pre-equilibrium stage, presumably dominated by gluons; ii) the hydrodynamic stage, in which the dynamics can be successfully described by relativistic viscous hydrodynamics and where the phase transition back to hadronic matter takes place; iii) the freeze-out stage where hadrons form a gas, first dense and then dilute, and in the end, the final state particles are created. Different physical processes play a role as the system evolves and it is one of the challenges in the field to identify the dominant effects at each stage.

From the theoretical point of view, the fact that the collision process can be modelled as a sequence of distinct stages as outlined above is attractive, since it allows for independent modifications and/or improvements of each stage. For example, different versions of hydrodynamics can be used for the second stage of evolution. For example, by moving from perfect-fluid hydrodynamics to viscous hydrodynamics and developing the necessary formalism we are able

to make progress in our description and understanding of the collision dynamics.

2.2.1 The initial stage

The very early stages of heavy-ion collisions are most often described with the help of microscopic models which refer to the presence of coherent colour fields at the moment when the two nuclei pass through each other. Such models refer directly to QCD and to the phenomenon of gluon saturation, which allows for treatment of gluons as the classical fields obeying the Yang-Mills (YM) equations [40, 41]. When quantum effects are incorporated, this framework is generally known as the Color-Glass-Condensate (CGC) model. An alternative to QCD-based models, which are now being intensively studied (see for example [42]), is the approach based on the AdS/CFT correspondence, which will be widely discussed later in this review.

Any microscopic model of the early stages requires assuming certain initial conditions which usually refer to the initial distribution of matter in the colliding nuclei. Such geometric concepts are very often introduced in the framework of the Glauber model where the nucleon distributions in nuclei are random and given by the nuclear density profiles, whereas the elementary nucleon-nucleon collision is characterized by the total inelastic cross section $\sigma_{\rm in}$. The Glauber model allows for introducing the concepts of participants or wounded nucleons (nucleons that at least once interacted inelastically) and of binary nucleon-nucleon collisions [43]. Densities of the numbers of wounded nucleons and binary collisions (in the transverse plane with respect to the beam axis) serve to make the estimates of the initial energy-density profiles of the colliding system.

Early applications of relativistic hydrodynamics to model the RHIC data very often used the Glauber model estimates as a direct input for the subsequent hydrodynamic stage. With perfect-fluid codes at hand, this approach means that one assumes (implicitly) local thermalisation of matter at the moment of initialisation of hydrodynamic evolution. Since successful description of the data was achieved with the initialisation times on the order of a fraction of fermi/c, the conclusions were drawn from these calculations that matter produced in heavy-ion collisions undergoes a process of very fast thermalisation.

2.2.2 The hydrodynamic stage

The presence of the hydrodynamic stage with a low shear viscosity to entropy density ratio in the space-time evolution of matter produced in heavy-ion collisions is crucial for the explanation of several physical effects, including the elliptic-flow phenomenon [44]. In particular, the hydrodynamic expansion explains the momentum anisotropy of the final-state hadrons, which turns out to be the hydrodynamic response to an initial spatial anisotropy of matter.

An attractive feature of using the hydrodynamic approach is that it easily and consistently incorporates the phase transition into a global picture of the collisions. The phase transition is included directly by the use of a specific equation of state (EOS). Different forms of EOS can be used in model calculations and one can check which one leads to the best description of the data. Interestingly, such studies support the lattice QCD EOS indicating the presence of a crossover phase transition at finite temperature and zero baryon chemical potential [45].

2.2.3   The freeze-out of hadrons

In the late stages of evolution, the system density decreases and the mean free path of hadrons increases. This process eventually leads to the decoupling of particles which become non-interacting objects moving freely toward the detectors. Since after this stage the momenta of particles do not change anymore, this process is referred to as the thermal freeze-out (the momenta of particles become frozen). Apart from the decrease in density, also the growing rate of the collective expansion favours the process of decoupling. If the expansion rate is much larger than the scattering rate, the freeze-out may occur even at relatively large densities. Generally speaking, the process of decoupling is a complicated non-equilibrium process which should be studied with the help of the kinetic equations. In particular, different processes and/or different types of particles may decouple at different times, so one often introduces a hierarchy of different freeze-outs. In particular, one freqently distinguishes between the chemical and thermal freeze-outs. The former is the stage where the hadronic abundances are established. The chemical freeze-out precedes the thermal freeze-out.

2.2.4   RHIC vs. LHC

The first hydrodynamic models used to interpret the heavy-ion data from RHIC were based on 2+1 [2] perfect-fluid hydrodynamics (Huovinen, Kolb, Heinz, Ruuskanen, and Voloshin [46], Teaney and Shuryak [47], Kolb and Rapp [48]). These works assumed the bag equation of state for QGP and the resonance gas model for the hadronic phase. The two phases were connected by a first-order phase transition with the latent heat varying from 0.8 GeV/fm^3 in Ref. [47] to 1.15 GeV/fm^3 in Ref. [46,48]. The initialization time for hydrodynamics was 1 fm/c in Ref. [47] and 0.6 fm/c in [46,48]. The models differed also in their treatment of the hadronic phase. In Ref. [47] the hydrodynamic evolution was coupled to the hadronic rescattering model RQMD, while in Ref. [48] partial chemical equilibrium was incorporated into the hydrodynamic framework. On the other hand, in Ref. [46] full chemical equilibrium was assumed. The use of a very short initialization time for perfect-fluid hydrodynamics triggered ideas about early equilibration time

---

[2]The 2+1 denotes in this case two space and one time dimensions, the 2+1 codes assume that the longitudinal dynamics is determined completely by the boost symmetry.

of matter produced in heavy-ion collisions and shaped our way of thinking about these processes in the following years.

As the experimental program was continued at RHIC, theoretical models based on the use of viscous hydrodynamics with a realistic QCD equation of state at zero baryon density have been developed. This allowed for the first quantitative estimates of the shear viscosity to entropy density ratio, $\eta/\mathcal{S}$, that turned out to be very close to the value $\hbar/(4\pi k_B)$ obtained from the AdS/CFT correspondence [49]. Recent comparisons between hydrodynamical calculations and the data lead to the range $1 \leq \eta/\mathcal{S} \leq 2.5$ in units of $\hbar/(4\pi k_B)$ [50]. This value is smaller than that of any other known substance, including superfluid liquid helium.

Although the $\eta/\mathcal{S}$ ratio is small in viscous codes describing experimental data, dissipative corrections to equilibrium values of thermodynamic variables turn out to be quite large in such models at early stages of the collisions. This is so, because initially there exist large gradients of flow in the produced systems and non-equilibrium corrections are proportional to the products of kinetic coefficients and such gradients. Large values of the latter compensate smallness of the former. This results in substantial values of the shear stress tensor and modification of the pressure components — with the transverse component of the pressure much larger than the longitudinal one. Such a pressure anisotropy has motivated investigations aiming at generalization of the standard viscous hydrodynamic framework on one hand and at extension of the validity of viscous hydrodynamics on the other. All these issues are discussed in our review.

The initial energy density in central PbPb collisions at the LHC, inferred from the number of produced particles via Bjorken's formula at the beam energy $\sqrt{s_{\mathrm{NN}}} = 2.76$ TeV, is more than an order of magnitude larger than that of the deconfinement transition predicted by lattice QCD. The viscous hydrodynamic codes including fluctuating initial conditions showed very remarkable agreement with the measured flow harmonic coefficients v_n. The odd flow harmonics [51] were found to have a weak centrality dependence, which is typical for initial state geometric fluctuations. In the coming years, the bulk viscosity to entropy ratio, $\zeta/\mathcal{S}$, may be estimated from experimental data, so that the two main viscosity coefficients of QGP can be determined [52]. In the future, the shear and bulk viscosities might be also found directly from QCD and one will use these values in the hydrodynamic calculations in order to check the overall consistency of the theoretical frameworks.

3 Microscopic approaches

The point of departure for the theoretical progress reviewed in this article is the fact that the basic condition for a description in terms of hydrodynamic variables to be useful is that the underlying microscopic theory should display quasi-universal behaviour at late stages of its
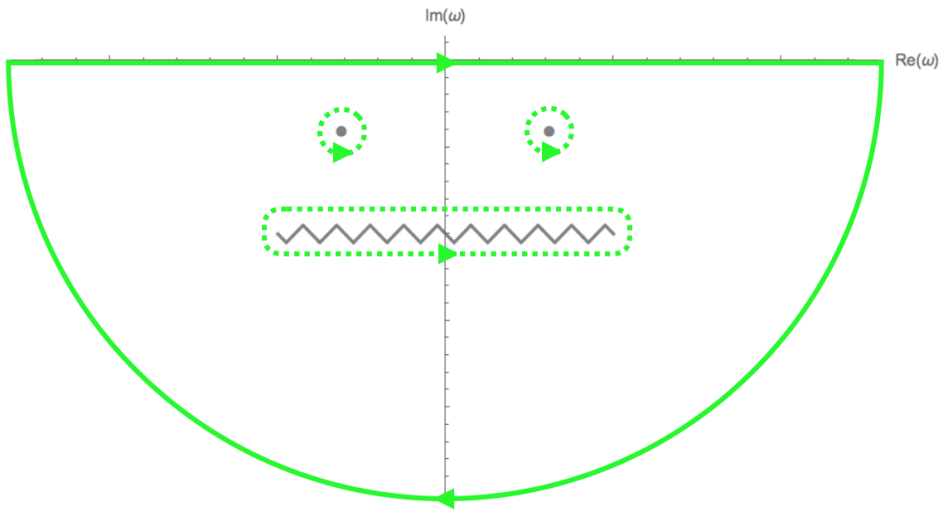
Figure 1: The contour integral computing the integral over frequencies in Eq. (3.2), for a generic value of momentum **k**, is a sum of contributions from singularities, single poles and branch points, of $G_R^{\mu\nu,\alpha\beta}(\omega,\mathbf{k})$ in the lower half of frequency plane. Each such contribution we call a mode. Depending on a microscopic model there can be a finite or an infinite number of modes and at late times the one which corresponds to the singularity closest to the real axis dominates the response, since it is the least-damped.

dynamical evolution. Such behaviour is a sign of a significant reduction of the number of degrees of freedom and constitutes the final stretch on the way to local thermodynamic equilibrium. In this Section we review, in general terms, various approaches to late-time behaviour relevant for the dynamics of QGP. We start with perhaps the most general approach to this problem in the context of quantum field theory, which is the theory of linear response.

3.1 Linear response and degrees of freedom of relativistic collective states

From the point of view of phenomenological applications to hydrodynamic evolution in heavy-ion collisions, the most important quantity to consider is the one-point function of the energy-momentum tensor, $\langle \hat{T}^{\mu\nu} \rangle$, of a microscopic model[3] in a non-equilibrium state. The simplest such states can be described within linear response theory, i.e., starting with an equilibrium state and subjecting it to a weak perturbation.

The source that directly couples to the energy-momentum tensor is the background metric $g_{\mu\nu}$.

---

[3]Although our presentation here aims at QFT applications, in particular we refer to the energy-momentum tensor as to an operator, the methods from this section also apply directly in the context of relativistic kinetic theory, see Sec. 3.3.4, or hydrodynamic theories, see Sec. 6.5.

Within the linear response theory one has, see e.g. [53],

$$\delta\langle\hat{T}^{\mu\nu}\rangle(x) = -\frac{1}{2}\int d^4x\, G_R^{\mu\nu,\alpha\beta}(x^0 - y^0, \mathbf{x} - \mathbf{y})\,\delta g_{\alpha\beta}(y), \tag{3.1}$$

where $\delta\langle\hat{T}^{\mu\nu}\rangle(x)$ is the change in the expectation value of the energy-momentum tensor after perturbing the flat background metric with $\delta g_{\alpha\beta}(y)$ and $G_R^{\mu\nu,\alpha\beta}(x^0 - y^0, \mathbf{x} - \mathbf{y})$ is the retarded two-point correlator of the energy-momentum tensor evaluated in global thermal equilibrium with temperature T,

$$G_R^{\mu\nu,\alpha\beta}(x^0 - y^0, \mathbf{x} - \mathbf{y}) = -i\,\theta(x^0 - y^0)\langle[\hat{T}^{\mu\nu}(x), \hat{T}^{\alpha\beta}(y)]\rangle_T.$$

Let us now rewrite the right-hand side of Eq. (3.1) in Fourier space

$$\delta\langle\hat{T}^{\mu\nu}\rangle(x) = -\frac{1}{2 \times (2\pi)^4}\int d^3k \int d\omega\, e^{-i\omega x^0 + i\mathbf{k}\cdot\mathbf{x}}\, G_R^{\mu\nu,\alpha\beta}(\omega, \mathbf{k})\,\delta g_{\alpha\beta}(\omega, \mathbf{k}), \tag{3.2}$$

where the Fourier-transformed quantities can be recognized by their arguments. In Eq. (3.2), the integral over momenta $\mathbf{k}$ is taken over $\mathbb{R}^3$ and the integral over frequencies ω is taken over $\mathbb{R}$. Furthermore, due to the rotational symmetry of the thermal state the retarded two-point function of the energy-momentum tensor decomposes into a sum of three independent terms, see e.g. Ref. [53], which results in three sets of independent components of the energy-momentum tensor evolving independently. Assuming the momentum $\mathbf{k}$ is aligned along the x^3 direction, these are

- scalar channel: $\delta\langle\hat{T}^{12}\rangle$);

- shear channel: $\delta\langle\hat{T}^{0a}\rangle$ and $\delta\langle\hat{T}^{3a}\rangle$ with $a = 1, 2$;

- sound channel: $\delta\langle\hat{T}^{00}\rangle$, $\delta\langle\hat{T}^{03}\rangle$ and $\delta\langle\hat{T}^{33}\rangle$.

For vanishing spatial momentum, $\mathbf{k} = 0$, or at zero temperature all three channels are equivalent to each other. In the following, to keep the presentation as compact as possible, we review the physics of the sound channel in more detail and we refer the reader to the relevant literature for results in the other channels.

The basic idea is to use the technique of contour integration to express the frequency integral for each value of $\mathbf{k}$ in terms of the singularities of $G_R^{\mu\nu,\alpha\beta}(\omega, \mathbf{k})$ on the corresponding lower half complex-ω plane, see Fig. 1. Based on case studies within holography [25, 26, 28, 53, 54], free QFT [55] and kinetic theory [56], in general we expect singularities to come in two varieties: single poles or branch-points, and we allow for an infinite number of either type. On the same grounds, apart from the trivial free theory case when there is no equilibration (see Ref. [55]), we

also expect them to lie away from the origin for $\mathbf{k} \neq 0$. Note that singularities are symmetric with respect to the imaginary axis. At late times either type of singularity at a given value of $\omega = \omega_{\text{sing}}(k)$ will give rise to the contribution of the form

$$\delta \langle \hat{T}^{\mu\nu} \rangle(x) \sim e^{-i\,\omega_{\text{sing}}(k)\,x^0 + i\,\mathbf{k}\cdot\mathbf{x}}, \tag{3.3}$$

where the imaginary part of $\omega_{\text{sing}}(k)$ is responsible for dissipation (here $k = |\mathbf{k}|$) and we suppressed possible subleading power-like fall-off with time occurring for singularities being branch-points. The contribution given by Eq. (3.3) generically, see also below, gives rise to exponential decay with time. A possible real part of $\omega_{\text{sing}}(k)$ is then responsible for oscillations in time during the approach of $\langle \hat{T}^{\mu\nu} \rangle$ to equilibrium. *Each such contribution we call a mode – an excitation of equilibrium plasma.* Clearly, the same type of analysis applies to other than $\hat{T}^{\mu\nu}$ operators in an underlying microscopic model, but whenever possible[4] we will specialize to the $\hat{T}^{\mu\nu}$ case due to its direct importance in the context of heavy-ion collisions.

The equilibration time for each mode is set by the inverse of $\Im[\omega_{\text{sing}}(k)]$ and, clearly, the long-lived modes are those for which $\Im[\omega_{\text{sing}}(k)] \to 0$. In the absence of second order phase transition or spontaneous symmetry breaking which is the situation we specialize to in this review, the only long-lived modes appear for operators being conserved currents, see e.g. Ref. [57]. These modes are called *hydrodynamic* since, as we shall see in Sec. 6, they can be modelled by solutions of linearized hydrodynamic equations. For these special modes also the real part of the frequency approaches zero as momentum vanishes, see Sec. 6.5. In the absence of other than $\hat{T}^{\mu\nu}$ conserved charges, which is the situation considered in this review, there are only two kinds of hydrodynamic modes: one kind in the shear channel and one kind in the sound channel. All remaining modes are transient (short-lived) modes which become negligible after the longest timescale among $1/\Im[\omega_{\text{sing}}(k)]$ for the values of $\mathbf{k}$ giving nontrivial contribution to Eq. (3.2). Such modes are referred to as *nonhydrodynamic* or *transient modes*.

Although heuristic in flavour, the discussion above is actually quite general. The differences between microscopic models seem to manifest themselves in different singularity structures for the transient modes, as well as in the detailed way hydrodynamic modes approach the origin as momentum vanishes.

The most important notion introduced in this section is the idea of a mode defined as a contribution to $\langle T^{\mu\nu} \rangle$ from a particular singularity in ω of $G_R^{\mu\nu,\,\alpha\beta}(\omega, \mathbf{k})$ at a given value of $\omega = \omega_{\text{sing}}(k)$ and the distinction between two types: the long-lived modes and all the rest transient and model-dependent excitations. This distinction is the reason why a hydrodynamic effective description of late time non-equilibrium behaviour is possible.

---

[4]Note that the analysis of modes in free $\text{SU}(N_c)$ at finite temperature in Ref. [55], reviewed in the next Section, has been performed only for the simplest scalar operator.

Excitations for which the imaginary part of the frequency is small relative to the real part are often referred to as quasiparticles. It is important to stress at this point that unless we are explicitly talking about kinetic theory we will not assume that we are dealing with systems for which excitations of the equilibrium state are quasiparticles. The latter case is, however, quite important and we shall discuss some of its general aspects in the following Section.

Finally, one practical remark is the following. Let us assume that in the absence of any metric perturbation (source) we have obtained a solution to the relevant microscopic equations of motion, say a variant of relativistic kinetic theory or holography, of the form of Eq. (3.3). Then, the momentum-dependent frequency $\omega(k)$ corresponds to the singularity of the retarded two-point function of the energy-momentum tensor. One can see it via Eq. (3.2): the retarded two-point function of the energy-momentum tensor in the Fourier space is the ratio of the change in the expectation value of the energy-momentum tensor to the metric perturbation. At the outset we assumed the latter is zero, which gives the singular behaviour of a pole or branch-point type (a branch-cut associated with two branch-points can be viewed as a sequence of poles which condensed).

In the following, we proceed with an overview of modes of an equilibrium relativistic matter as described by free $SU(N_c)$ gauge theory (Sec. 3.2), RTA kinetic theory (Sec. 3.3.3) and strongly coupled QFTs captured by holography (Sec. 4.3). To the best of our knowledge, these are the only examples of systems in which such analysis has been performed at the moment of writing this review.

3.2 Free $SU(N_c)$ Yang-Mills theory

Motivated by development in holography that we describe in Sec. 4.3, Ref. [55] considered free $SU(N_c)$ Yang-Mills theory and calculated the retarded two-point function at finite temperature of the scalar glueball operator $\operatorname{tr} F_{\mu\nu}F^{\mu\nu}$, where $F_{\mu\nu}$ is the field strength of the $SU(N_c)$ gauge field[5]. The Fourier-transformed result takes the form

$$
G_R^{\operatorname{tr} F_{\mu\nu}F^{\mu\nu}}(\omega, \mathbf{k}) = -\frac{N_c^2}{\pi^2}\left(k^2 - \omega^2\right)^2 \left\{ \frac{1}{2} + \left(i\frac{\pi T}{2k} - \frac{\omega}{4k}\right) \log\frac{\omega+k}{\omega-k} + i\frac{\pi T}{k}\log\frac{\Gamma\left(\frac{-i(\omega+k)}{4\pi T}\right)}{\Gamma\left(\frac{-i(\omega-k)}{4\pi T}\right)} \right\}
$$

$$
+ \frac{N_c^2}{\pi^2}\left\{ \frac{2\pi^2 T^2}{3}\left(\omega^2 - k^2\right) + \frac{16\pi^4 T^4}{15} + \frac{k^2}{6}\left(\frac{7k^2}{5} - \omega^2\right) \right\}. \tag{3.4}
$$

Its singularity structure originating from the term $\log\frac{\Gamma\left(\frac{-i(\omega+k)}{4\pi T}\right)}{\Gamma\left(\frac{-i(\omega-k)}{4\pi T}\right)}$ is given by a series of branch-cuts extending between $\omega = -4\pi i T n - k$ and $\omega = -4\pi i T n + k$, where $n = 1, 2, \ldots$. As advocated in Sec. 3.1, these branch cuts are responsible for the exponential fall-off of $\delta\langle\operatorname{tr} F_{\mu\nu}F^{\mu\nu}\rangle$.

---

[5]In fact, this two-point function is the same as of the $\operatorname{tr} F_{\mu\nu}\tilde{F}^{\mu\nu}$ operator.

Furthermore, at vanishing momentum, $\mathbf{k} = 0$, branch cuts transform into single poles located at imaginary axis at $\omega = -4\pi\, i\, T\, n$. On top of that there is another branch-cut extending between $\omega = -k$ and $\omega = k$ that gives rise to oscillatory power law behaviour. All these features can be explicitly seen upon Fourier transforming Eq. (3.4) to real time $t = x^0 - y^0$:

$$G_R^{\operatorname{tr} F_{\mu\nu} F^{\mu\nu}}(t,\, \mathbf{k}) = \theta(t)\, \frac{N_c^2}{\pi}\, \frac{1}{k}\, \left(k^2 + \partial_t^2\right)^2 \left\{ T\, \frac{\sin k t}{t}\, \coth\left(2\pi T\, t\right) - \frac{\sin k t - k t\, \cos k t}{2\pi\, t^2} \right\}. \quad (3.5)$$

In the above expression, branch-points positions $\omega = -4\pi\, i\, T\, n \pm k$ give rise to the behaviour $\sin k t \coth 2\pi\, T\, t$ whereas the branch-cut itself leads to the subleading power-law fall-off of $1/t$. The other term, $\frac{\sin k t - k t\, \cos k t}{2\pi\, T\, t^2}$, originates from the branch-cut between $\omega = \pm k$. It is apparent in Eq. (3.5) that the latter effect is present also in the vacuum (i.e. for $T = 0$), whereas the former comes from the presence of a medium.

This analysis applies in the absence of any interactions and, as noted in the original Ref. [55], the exponential decay seen in correlators must come from the interference between different partial contributions to Eq. (3.5). At the moment of writing this review and to the best of authors' knowledge there are no quantitative weak-coupling results on the general structure of singularities of correlators upon inclusion of interactions. A toy-model of this situation is the RTA kinetic theory for which the correlators of the energy-momentum tensor and conserved current were recently computed in Ref. [56] and we discuss this important recent development in Sec. 3.3.4.

3.3 Kinetic theory

In this Section we introduce elements of relativistic kinetic theory, as a weak-coupling language appropriate for QCD at asymptotically high temperatures in which some of the problems of interests for this review, such as values of transport coefficients [58–62] or emergence of hydrodynamic behaviour [63–65], can be phrased and investigated. Touching upon these important developments in the context of the so-called effective kinetic theory [58], we will devote much of our attention to a much simpler yet rich in physics model of relativistic kinetic theory in the relaxation time approximation [66, 67].

3.3.1 Boltzmann kinetic equation

The fundamental object used in kinetic theory is the one-particle distribution function $f(x, p) = f(t, \mathbf{x}, \mathbf{p})$, giving the number of particles ΔN in the phase-space volume element $\Delta^3 x \Delta^3 p$ placed at the phase-space point $(\mathbf{x}, \mathbf{p})$ and the time t [68],

$$\Delta N = f(x, p)\, \Delta^3 x \Delta^3 p, \quad (3.6)$$

where the four-momentum argument of the distribution function is taken to be on-shell. The main task of the kinetic theory is to formulate the time evolution equation for $f(x,p)$. In the non-relativistic case $f(x,p)$ satisfies the famous Boltzmann equation derived in 1872. The knowledge of $f(x,p)$ allows us to calculate several important macroscopic quantities, in particular, the particle number four-current

$$n^\mu(x) = \int dP\, p^\mu f(x,p) \tag{3.7}$$

and the energy-momentum tensor

$$T^{\mu\nu}(x) = \int dP\, p^\mu p^\nu\, f(x,p). \tag{3.8}$$

It is time-dependence of the latter quantity that is of central importance in the context of hydrodynamics. In Eqs. (3.7) and (3.8) we have introduced the Lorentz invariant momentum measure

$$dP = \frac{d^3 p}{p^0}. \tag{3.9}$$

One may check that the phase space distribution function $f(x,p)$ transforms like a scalar under Lorentz transformations, hence, (3.7) and (3.8) transform indeed like a four-vector and a second rank tensor. The energy and momentum conservation laws have the form

$$\partial_\mu T^{\mu\nu}(x) = 0. \tag{3.10}$$

Expression (3.8) includes only the mass and the kinetic energy of particles. Note also that through the definition of the energy-momentum tensor given by Eq. (3.8), in kinetic theory one never encounters negative pressures.

For systems where the effects of collisions are negligible, the relativistic Boltzmann equation is reduced to the continuity equation expressing the conservation of the number of particles

$$p^\mu \partial_\mu f(x,p) = 0. \tag{3.11}$$

If the collisions are present, the kinetic equation is written in the form

$$p^\mu \partial_\mu f(x,p) = C(x,p), \tag{3.12}$$

where the collision term (integral) $C(x, p)$ on the right-hand side of (3.12) is

$$C(x, p) \;=\; \frac{1}{2} \int dP_1 dP' dP'_1 \left[f' f'_1 W(p', p'_1|p, p_1) - f\, f_1 W(p, p_1|p', p'_1) \right].$$
(3.13)

In Eq. (3.13) we use the notation

$$f' = f(x, p'), \; f'_1 = f(x, p'_1), \; f = f(x, p), \; f_1 = f(x, p_1).$$
(3.14)

In the similar way we define the measures dP_1, dP', and dP'_1. The transition rate W is defined by the formula

$$W(p, p_1|p', p'_1) \equiv F_i\, p'^0 p'^0_1 \frac{\Delta\sigma(p, p_1|p', p'_1)}{\Delta^3 p' \Delta^3 p'_1},$$
(3.15)

where F_i is the invariant flux

$$F_i = \sqrt{(p \cdot p_1)^2 - m^4}$$
(3.16)

and $\Delta\sigma(p, p_1|p', p'_1)$ is the differential cross section.

The form (3.12) is valid for identical particles obeying classical statistics. It can be easily generalised to the case where different types of particles scatter on each other. The generalisation to the quantum statistics case is obtained by the introduction of the so called Uehling-Uhlenbeck corrections to the collision integral. They have the form of the factors $1 - \epsilon f$, where $\epsilon = +1$ for bosons, $\epsilon = -1$ for fermions.

3.3.2 Effective kinetic theory

For a weakly-interacting QFT at high temperatures and densities, the particles gain effective masses and widths. In this case it is possible to construct the effective kinetic theory which uses the quasiparticle distribution function $f(x, p)$ [58, 60, 69]. The latter depends on an on-shell four-momentum p, but now the quasiparticle energy E is a function of the spatial momentum and an effective, thermal mass, $E = (\mathbf{p}^2 + m_{\text{th}}(q(x))^2)^{1/2}$. The effective mass depends on a space-time dependent auxiliary field $q(x)$ which, in turn, depends self-consistently on the distribution function

$$q(x) = \int dP\, f(x, p).$$
(3.17)

The modified quasiparticle Boltzmann equation can be written in the form

$$p^\mu \partial_\mu f(x,p) + m_{\text{th}} \partial^\nu m_{\text{th}} \partial_\nu^{(p)} f(x,p) = C(x,p). \tag{3.18}$$

Here $\partial_\nu^{(p)} = \partial/\partial_{p^\nu}$ denotes the derivative with respect to momentum and $C(x,p)$ describes now scattering of quasiparticles. Since quasiparticles are on the mass shell, the term $\partial_0^{(p)} f(x,p)$ vanishes and we see that the spatial gradient of the effective mass acts like an external force, changing the momentum of propagating quasiparticles.

The formalism of the effective kinetic theory allows for the calculations of kinetic coefficients although their form depends on the approximations made and number of processes included in the collision integral. In a SU(3) gauge theory, the high temperature shear viscosity has the leading-log form

$$\eta = \kappa \frac{T^3}{g^4 \ln g^{-1}}, \tag{3.19}$$

where g is the temperature dependent coupling constant and κ is a factor depending on the number of fermion species ($\kappa = 106.664$ for $N_f = 3$ [59]).

Note that the presence of small dimensionless coupling constant introduces a characteristic hierarchy of timescales for equilibration in weakly-coupled models. Using the EKT framework outside its regime of validity, i.e. for intermediate values of the coupling constant expected in heavy-ion collisions at RHIC and LHC energy, destroys this hierarchy [65] and, as we discuss in the following, leads to results very similar to the kinetic theory with simple collisional kernel in the relaxation time approximation and to strong-coupling physics of holography.

3.3.3 Relaxation time approximation

Due to the complicated form of the collision integral, in practical applications one very often uses a simplified version of the kinetic equation [66, 67]

$$p^\mu \partial_\mu f(x,p) = p \cdot U(x) \frac{f(x,p) - f_{\text{eq}}(x,p)}{\tau_{\text{rel}}}, \tag{3.20}$$

where $U^\mu(x)$ is the flow vector of matter (defined as the unique, normalized timelike eigenvector of the energy-momentum tensor $T^\mu{}_\nu(x)$, see Eq. (6.1)), τ_{rel} is the relaxation time, and $f_{\text{eq}}(x,p)$ is the equilibrium distribution function. Equation (3.20) has a simple physics interpretation – the non-equilibrium distribution function $f(x,p)$ approaches the equilibrium form $f_{\text{eq}}(x,p)$ at the rate defined by the relaxation time τ_{rel}. This is the reason why the theory defined by Eq. (3.20) is often referred to as to the relaxation time approximation (RTA).

The equilibrium distribution $f_{\text{eq}}(x,p)$ has the standard (Bose-Einstein or Fermi-Dirac) form

$$f_{\text{eq}}(x,p) = \frac{1}{(2\pi)^3} \left\{ \exp\left[-\frac{p \cdot U}{T(x)}\right] - \epsilon \right\}^{-1}. \tag{3.21}$$

where, again, $\epsilon = +1$ for bosons, $\epsilon = -1$ for fermions and the classical Boltzmann definition corresponds to the limit $\epsilon \to 0$

The function $T(x)$ defines local (effective) temperature of the system. The values of $T(x)$ are determined at each space-time point x from the condition that $f_{\text{eq}}(x,p)$ yields the same local energy density as $f(x,p)$. Note that this condition, together with the definition of U, make Eq. (3.20) highly nonlinear. Below we shall refer to these conditions as to the Landau matching conditions. Only if the system is very close to local equilibrium can T be treated as a thermodynamic quantity and used in thermodynamic identities.

The relaxation time τ_{rel} which appears in Eq. (3.20) may take different forms. For conformal systems without any conserved currents, τ_{rel} should scale inversely with the effective temperature of the system, namely

$$\tau_{\text{rel}} = \frac{\gamma}{T}, \tag{3.22}$$

where γ is a dimensionless constant. As discussed below in Sec. 5 this coefficient can be related to the shear viscosity in an effective hydrodynamic description of the system. Also, see Ref. [56], one can use this relation together with Eq. (3.19) to make the RTA kinetic theory a simple model of the EKT kinetic theory of QCD.

3.3.4 Modes of the conformal RTA kinetic theory

In order to determine structure of singularities of the retarded correlator of the energy-momentum tensor in kinetic theory, one has to generalise the Boltzmann equation to arbitrary curved background and use Eq. (3.1). As already anticipated in Sec. 3.1, we will adopt a slightly different strategy in order to reproduce the results of Ref. [56]. We work directly in Fourier space and focus entirely on the sound channel, i.e. perturbations of T, U^3 and f exhibiting harmonic dependence on x^0 and x^3: $e^{-i\omega x^0 + ikx^3}$. Looking for solutions of the flat space RTA Boltzmann equation in which δT and δU^3 fulfil Eq. (6.1) one obtains the following condition for ω as a function of k

$$2k\,\tau_{\text{rel}} \left\{ (k\,\tau_{\text{rel}})^2 + 3\,i\,\omega\,\tau_{\text{rel}} \right\} + i \left\{ (k\,\tau_{\text{rel}})^2 + 3\,i\,\omega\,\tau_{\text{rel}} + 3\,(\omega\,\tau_{\text{rel}})^2 \right\} \log \frac{\omega\,\tau_{\text{rel}} - k\,\tau_{\text{rel}} + i}{\omega\,\tau_{\text{rel}} + k\,\tau_{\text{rel}} + i} = 0. \tag{3.23}$$

Indeed, as one can check this is equivalent to the expression for singularities of the retarded two-point function of the energy-momentum tensor obtained in Ref. [56]. One immediately notices a branch cut-singularity given by $\log \frac{\omega\,\tau_{\text{rel}} - k\,\tau_{\text{rel}} + i}{\omega\,\tau_{\text{rel}} + k\,\tau_{\text{rel}} + i}$ with branch points at $\omega = -i\frac{1}{\tau_{\text{rel}}} \pm k$.

Note that in the absence of interactions in this model, i.e. in the limit of $\tau_{\rm rel} \to \infty$, this branch-cut coincides with the branch-cut surviving the $T \to 0$ limit of the free $SU(N_c)$ gauge theory calculation of Ref. [55] described in Sec. 3.2. One should then think of it as of an alteration of free propagation of underlying particles by interactions captured by the RTA collisional kernel. For massive particles, we expect branch-cut extending between $\log \frac{\omega\,\tau_{\rm rel} - \sqrt{k^2 + m^2}\,\tau_{\rm rel} + i}{\omega\,\tau_{\rm rel} + \sqrt{k^2 + m^2}\,\tau_{\rm rel} + i}$ and when $m\,\tau_\Pi \gg 1$ we obtain quasiparticle excitations. Note also that the singularity $\log \frac{\omega\,\tau_{\rm rel} - k\,\tau_{\rm rel} + i}{\omega\,\tau_{\rm rel} + k\,\tau_{\rm rel} + i}$ becomes a pole in the limit $\mathbf{k} \to 0$.
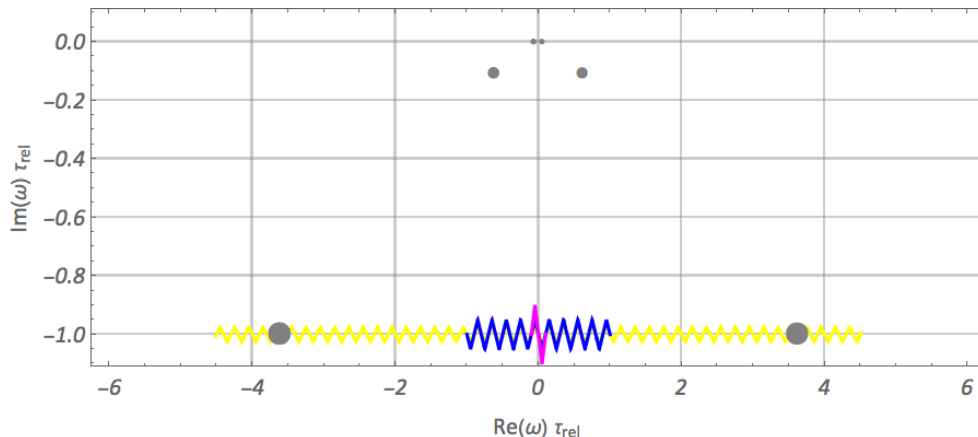
Figure 2: The structure of singularities in the complex frequency plane at fixed spatial momentum k of the retarded two-point function of $\hat{T}^{\mu\nu}$ in the sound channel in the RTA kinetic theory. Gray dots represent single poles corresponding to the sound wave mode at $k\,\tau_{\rm rel} = 0.1$ (the smallest dots), $k\,\tau_{\rm rel} = 1$ (medium dots) and at the verge of its existence at $k\,\tau_{\rm rel} = 4.531$ (the largest dots). Spiked lines represent branch cut singularities which connect the branch point at corresponding values of momenta: $k\,\tau_{\rm rel} = 0.1$ (magenta with the largest amplitude), $k\,\tau_{\rm rel} = 1$ (blue with medium amplitude) and $k\,\tau_{\rm rel} = 4.531$ (yellow with the smallest amplitude). See the main text for the discussion.

Regarding other excitations, it turns out there is only one in this setup and at low momenta it is a long-lived mode corresponding to hydrodynamic sound wave, see Fig. 2. More precisely, for each value of momentum between $k\,\tau_{\rm rel} = 0$ and $k\,\tau_{\rm rel} \approx 4.531$ there are two poles in the complex frequency symmetrically located with respect to the imaginary axis whose positions at low momenta approach the sound wave dispersion relation $\omega = \pm\frac{k}{\sqrt{3}} + O(k^2)$, see Sec. 6.5 for the hydrodynamic interpretation. This type of singularity, single pole, is also seen at strong coupling in holography, see Sec. 4.3. The key difference here is that for $k\,\tau_{\rm rel} > 4.531 \dots$ there is no solution to Eq. (3.23) and this mode ceases to exist. This is the value of momentum for which $\Im(\omega)$ approaches $-\frac{1}{\tau_{\rm rel}}$. For higher momenta, the momentum transfer in sound channel occurs solely through the transient mode represented by the branch-cut singularity in the function $\log \frac{\omega\,\tau_{\rm rel} - k\,\tau_{\rm rel} + i}{\omega\,\tau_{\rm rel} + k\,\tau_{\rm rel} + i}$.

21

Note that there seems to be no physical principle why more singularities in the two-point function of the energy-momentum tensor are not present and one should expect that for more complicated collisional kernels there would be a more intricate mode structure. At the moment of writing this review, this issue remains an important open problem.

3.4 String theory

A very influential approach to the issues studied in this review grew out of string theory. It is holography [70–72], also known as the AdS/CFT correspondence or the gauge-gravity duality, which geometrizes certain QFTs in the form of solutions of gravity with negative cosmological constant (and more generally string theory) in higher number of dimensions.

The archetypical example of such a QFT is a maximally supersymmetric conformal Yang-Mills theory in 3+1 dimensions, known as $\mathcal{N}=4$ super Yang-Mills (SYM) theory. It arises by replacing the quark sector of QCD by a specially crafted matter sector[6]. Furthermore, the rank of its $SU(N_c)$ gauge group and the coupling constant are parameters specifying the theory.

The nature of holography is such that when N_c is large and interactions are strong then a large class of observables, in particular many observables of interest in the context of heavy-ion collisions, can be obtained by solving classical gravity equations coupled to appropriate matter fields in one dimension higher. By now, it has been understood that there are vastly more examples of holography involving both conformal (as $\mathcal{N}=4$ SYM) and non-conformal QFTs. Such theories are called holographic and we will refer to them as hQFTs. When they are conformal, we called them holographic conformal field theories (hCFTs). In our review we will focus on the simplest case of hCFTs.

Due to its asymptotic freedom, it is clear that QCD does not fall into the class of QFTs for which holographic description is general relativity. Nevertheless, some of the properties of QGP above but not far above crossover temperature are in qualitative agreement with the properties of deconfined phases of hQFTs. The prime example here is the value of the shear viscosity to entropy density ratio, which obtained holographically qualitatively matches the one used for a successful phenomenological description of experimental data from RHIC and LHC. See in particular Ref. [2] for an extensive overview of holography applied to QCD. It should be perhaps noted that in the regime of weak coupling (and so outside the regime in which holography operates with general relativity), effective similarities at long wavelengths were also observed between deconfined phases of QCD and $\mathcal{N}=4$ SYM, see Ref. [74].

Regardless of whether there are some holographic results which directly apply to QCD due to universality of some sort, there is another sense in which holographic calculations have

---

[6]It consists of 6 scalar fields and 4 Weyl spinor fields in the adjoint representation of the gauge group, see e.g. Ref. [73] for a review

proved tremendously useful: they have provided a reliable means of observing how hydrodynamic behaviour appears in a non-equilibrium system in a fully ab initio manner. This has prompted a number of crucial developments in the field of relativistic hydrodynamics, which apply to any system, including QGP. Recent progress in this field is one of the focal points of our review.

4 Lessons from holography and the strong coupling picture

In this section we examine the lessons for relativistic hydrodynamics which follow from holographic calculations at the linearized level. We will however begin with an overview of the origins of this approach and the way it is currently used.

4.1 Gravitational description of strongly-coupled quantum field theories

The AdS/CFT correspondence [70–72] is ultimately due to the fact that closed strings (which describe gravity) and open strings (which describe Yang-Mills degrees of freedom) are made of the same "stuff". This leads to a representation (in a sense a reformulation) of string theory using supersymmetric Yang-Mills theory. In the 't Hooft limit the observables of this Yang-Mills theory in flat four-dimensional Minkowski space become expressible in terms of classical gravity in five dimensions. This gravitational representation (called holographic due to the additional, fifth dimension) involves a negative cosmological constant, which implies that the asymptotic behaviour of the geometry is not flat Minkowski space, but rather anti-de Sitter space (at least locally).

All the results used in this review were obtained in the context of $\mathcal{N} = 4$ SYM, which is the original setting of the AdS/CFT correspondence (often referred to by the more general term – holography), intuited by Maldacena by considerations of the dynamics of coincident D3-branes in type IIB string theory. It is not known how to extend this relationship to cover a theory like QCD (which, in particular, is not conformal and has no supersymmetry). The promise of such a generalisation is so great however, that despite the lack of a firm grounding in string theory, much effort has gone into guessing what such a description might look like. In this spirit, we will try to give a picture of holography which focuses on the aspects which one may expect to be relevant in such a wider context. At the same time we wish to stress that this section aims at explaining some of the intuitions behind the advances in relativistic hydrodynamics which are the subject of this review. For a reader interested mainly in those advances, the intuitions behind them may not be of prime importance, so such readers may browse this section lightly or even skip it entirely without much detriment.

In holography, the gravitational description of hQFTs of relevance for QCD is captured by solutions of equations of motion originating from the following higher dimensional gravitational

action

$$S = \frac{1}{2l_P^3} \int d^5x \sqrt{-g} \left\{ R - 2 \times \left(-\frac{6}{L^2} \right) + \dots \right\}, \tag{4.1}$$

where R is the Ricci scalar of a five-dimensional geometry, $-6/L^2$ stands for negative cosmological constant and the ellipsis contain boundary terms as well as possible five-dimensional matter fields obeying two-derivative equations of motion. The most symmetric solution of these equations of motion is anti-de Sitter (AdS) space given by

$$ds^2 = g_{ab} \, dx^a dx^b = \frac{L^2}{u^2} \left\{ du^2 + h_{\mu\nu}(u, x) dx^\mu dx^\nu \right\}, \tag{4.2}$$

with $h_{\mu\nu}(u, x)$ given by the Minkowski space metric $\eta_{\mu\nu}$ and all matter fields set equal to zero. Other solutions involve non-trivial profiles of $h_{\mu\nu}(u, x)$ as well as nontrivial matter fields. Generically, one most often neglects higher derivative terms that could potentially appear in Eq. (4.1), e.g. R^2, since when treated exactly they give rise to unphysical effects and when treated as small perturbations they do not change qualitative features of results derived from Eq. (4.1). It is interesting to note that the issue of higher derivative terms here is mathematically very similar to the task of making sense of the truncated gradient expansion of hydrodynamics, as discussed in Sec. 7. Furthermore, it could be the case that higher derivative terms treated as leading order corrections may be trustworthy even when large. In the context of relativistic hydrodynamics this turned out to be the case, as discussed in Sec. 5.

It is important to make a distinction between features of Eq. (4.1) that characterise a given hQFT and those that characterise a particular state within this hQFT. When it comes to the former, the parameter that controls the scaling of observables with the number of microscopic degrees of freedom is the ratio of the curvature scale of AdS, L, and the five-dimensional Planck scale, l_P, that is related to the so-called central charge c [7] through the formula

$$\frac{L^3}{l_P^3} = \frac{c}{\pi^2}. \tag{4.3}$$

For $\mathcal{N} = 4$ SYM with N_c colours the central charge is

$$c = \frac{N_c^2}{4} \tag{4.4}$$

---

[7]In CFTs in even spacetime dimensions central charges are coefficients appearing at independent contributions to the energy-momentum tensor two-point function in the vacuum or, equivalently, independent contributions to the conformal anomaly $\langle \hat{T}^\mu_\mu \rangle \neq 0$ when a CFT is placed on a generic curved background. For theories in four spacetime dimensions there are two such central charges, denoted by a and c. However, in the case when the action (4.1) in the holographic description contains only two-derivative terms, the central charges are equal and it is then customary to use the letter c to denote both of them.

and in most of the results discussed in what follows we use this value of c. Of course, in order to trust the physical description in terms of classical gravity, one must have $L \gg l_P$, which as it turns out translates, see Eqs. (4.3) and (4.4), to $N_c \gg 1$, i.e. the 't Hooft planar limit [75]. The other parameter is the interaction strength between microscopic constituents and it turns out that for infinite interaction strength, i.e. 't Hooft coupling constant $g_{\mathrm{YM}}^2 N_c \equiv \lambda \gg 1$, this parameter does not appear in the two-derivative part of Eq. (4.1). This observation has already an important phenomenological bearing because it shows that none of the features of processes at infinite coupling captured by Eq. (4.1) will be coupling-enhanced.

Another set of parameters characterizing an underlying theory lies in the choice of infinitely many matter fields in Eq. (4.1) and associated infinitely many dimensionless (with respect to L) parameters in front of their kinetic and interaction terms. In the case of $\mathcal{N} = 4$ SYM these terms as well as their coefficients are determined by type IIB string theory, but in the spirit of this section they may be regarded in a phenomenological spirit as something to be chosen at will. Ideally one would like to hava "top-down" understanding of any such terms, but at this stage requiring such an understanding may be too restrictive for progress to be made.

Finally, since the AdS geometry acts effectively as a box[8] with a boundary at $u = 0$, c.f. Eq. (4.2), for each field one needs to prescribe a boundary condition at $u = 0$. These boundary conditions have interpretation of sources for single trace gauge-invariant local operators in an underlying hQFT and complete the specification of the latter.

As for the parameters which specify the states, these are all the other parameters appearing in solutions of equations of motion derived from Eq. (4.1) that cannot be removed by diffeomorphisms involving u and x coordinates. Such transformations need to vanish at $u = 0$, since otherwise they would become physical by altering a given set of boundary conditions (i.e. the definition of an underlying hQFT). Let us stress here that the same geometry, i.e. the same state in an underlying QFT, can be described using different coordinates, all of which are clearly on the same footing. Note however that these coordinate systems might cover different parts of the geometry and might break down (in the sense of components of the metric or its inverse diverging) even when that geometry itself is perfectly regular.

In vast majority of cases studied in this review, we will be concerned with solutions of Einstein's equations with negative cosmological constant,

$$R_{ab} - \frac{1}{2} R \, g_{ab} + \left(-\frac{6}{L^2} \right) g_{ab} = 0, \tag{4.5}$$

that is with a consistent truncation of the equations of motion coming from Eq. (4.1) when

---

[8]By analyzing propagation of light rays in metric given by Eq. (4.2) with $h_{\mu\nu}(u, x) = \eta_{\mu\nu}$ one concludes that geodesics can reach the plane of $u = 0$ in a finite time. As a result, their further propagation depends on a boundary condition imposed at $u = 0$. Similar holds for fields propagating on the AdS geometry.

the sources associated with all the other (than the five-dimensional metric) fields vanish. These solutions have interpretation of states in strongly-coupled CFTs for which the only local operator with a nontrivial expectation value is the energy-momentum tensor. These equations possess few analytic solutions and tackling the problem of time-dependent processes in strongly-coupled QFTs in general requires solving them on a computer using elaborate numerical methods.

Using the parametrization of the five-dimensional metric from Eq. (4.2), the expectation value of the energy-momentum tensor of an underlying strongly-coupled CFT can be obtained from the near-boundary ($u = 0$) behaviour of $h_{\mu\nu}(u, x)$ as

$$h_{\mu\nu}(u, x) = \eta_{\mu\nu} + \frac{\pi^2}{2\,c} \langle \hat{T}_{\mu\nu} \rangle \, u^4 + \dots , \tag{4.6}$$

where the expression is provided for a CFT in a Minkowski space and all the suppressed contributions are proportional to $\frac{\pi^2}{2c} \langle \hat{T}_{\mu\nu} \rangle$, as well as its powers and derivatives. CFT states of interest will be then characterized by $\frac{\pi^2}{2c} \langle \hat{T}_{\mu\nu} \rangle$ as a function of x and one can obtain them by constructing appropriate solutions of Eq. (4.5) using Eq. (4.6). It is also interesting to note that a given form of $\frac{\pi^2}{2c} \langle \hat{T}_{\mu\nu} \rangle$ as a function of x characterizes simultaneously many holographic CFTs, out of which $\mathcal{N} = 4$ SYM correspond to setting the value of c in Eq. (4.4).

This analysis makes it also apparent that an empty AdS space represents the vacuum state of a hCFTs characterized by vanishing $\langle \hat{T}_{\mu\nu} \rangle$ together with expectation values of all the other local operators. A generalization of Eq. (4.6) to a hCFT in an arbitrarily curved albeit fixed background $h_{\mu\nu}(x)$ is straightforward albeit tedious and starts by replacing the Minkowski metric $\eta_{\mu\nu}$ in Eq. (4.6) by $h_{\mu\nu}(x)$. The details of this can be found in Ref. [76]. The considerations presented here also make it apparent why x act as coordinates in an underlying hQFT. For the reasons outlined above, one often encounters in literature the statement that a hQFT "lives on the boundary" (at $u = 0$) which is simply supposed to mean that boundary conditions at $u = 0$ define a given hQFT. Furthermore, the interior of higher dimensional geometry, Eq. (4.2) is often referred to as to bulk. Note that the radial coordinate u has an interpretation of the inverse of an energy scale in a hCFT, since for the vacuum AdS solution the change of a physical distance in a dual CFT, $\Delta x \to \gamma \, \Delta x$ can be compensated by the change of u, $u \to \gamma \, u$. Note further that the bulk geometry and other fields contain only information about one-point functions of local operators. Higher-point functions are not specified by the geometry alone and provide a set of independent observables.

The last point to discuss is that solutions of Eq. (4.5) describe the simplest, yet very rich sector of dynamics of a class of the most symmetric (because conformal) hQFTs. There are many possible and well-studied generalizations. Perhaps the most interesting possibility from the phenomenological standpoint is to break the conformal symmetry, which can be achieved

by introducing a nonzero constant boundary condition for one of the scalar fields suppressed in Eq. (4.1) which represents a source for a relevant operator. We do not review such setups in detail. Another interesting possibility which we do not consider either is to allow for the U(1) conserved current to acquire a nonzero expectation value by coupling gravity from Eq. (4.5) to a gauge field sector. These two generalizations bring up the following important point. Whereas considering vacuum Einstein's equations with negative cosmological constant alone, Eq. (4.5), is a consistent truncation of equations of motion following from the actions (4.1) containing a priori infinitely many bulk fields (as determined by string theory), it is not always clear if a reduction to a small set of fields including gravity and other bulk matter makes sense. This problem has led to the so-called bottom-up perspective in which one postulates an action coupling gravity to a desired set of fields in a way we want and deriving the consequences of such a bulk matter sector for a putative hQFT.

Finally, as we anticipated earlier, adding a finite number of higher curvature terms in vast majority of cases is inconsistent with them contributing significantly to solutions. Such terms are there (certainly from a string theory perspective) and certainly become important outside the strict $N_c = \infty$, $\lambda = \infty$ limit, but we do not have a controllable way to account for them. This is why it is useful and illuminating to consider as a toy-model adding the so-called Gauss-Bonnet term to the Einstein-Hilbert part of the action (4.1),

$$ S_{GB} = \frac{1}{2l_P^3} \int d^5 x \sqrt{-g} \, \frac{\lambda_{GB}}{2} L^2 \left\{ R^2 - 4 R_{ab} R^{ab} + R_{abcd} R^{abcd} \right\}, \tag{4.7} $$

for which the equations of motion for the bulk metric g_{ab} turn out to be of a two-derivative type and avoid aforementioned problems [77]. By changing the real dimensionless parameter λ_{GB} in Eq. (4.7) one can try to model the effects of relaxing the strict limit of $N_c = \infty$, $\lambda = \infty$ on both equilibrium and non-equilibrium properties in hQFTs, see, e.g., Refs. [54, 78–81]. A naive consistency of gravitational picture requires $\lambda_{GB} \in (-\infty, \frac{1}{4}]$. An important caveat though is that other considerations demonstrate that gravity with cosmological constant and only the Gauss-Bonnet term cannot be consistent with the full self-consistency of a hQFT [82], which means that we can fully trust Eq. (4.7) only for $|\lambda_{GB}| \ll 1$. Let us also stress that supplementing the Einstein-Hilbert action with negative cosmological constant, Eq. (4.1), with the Gauss-Bonnet term, Eq. (4.7), does not affect the expectation values of any operators other than $\hat{T}^{\mu\nu}$.

In the rest of this section we will survey the simplest solutions of Eq. (4.5) with a view to make contact with the material from Sec. 3.1. Regarding other holographic results in this review, in Sec. 5.2 we will discuss $\langle \hat{T}^{\mu\nu} \rangle$ obtained from holography in a fully nonlinear manner for the simplest model of heavy-ion collisions – one-dimensionally expanding plasma system of a Bjorken type. In Sec. 7.2 we discuss the so-called fluid-gravity duality which accounts in the

bulk for the hydrodynamic gradient expansion in hQFTs. In Sec. 9 we overview holographic calculation of the gradient expansion at large orders for the Bjorken flow (late-time expansion) and make contact with the results of Sec. 4.3.

4.2 Black branes and equilibrium states

Collective equilibrium states of hQFTs are represented on the gravity side by static black hole solutions [83]. Because solutions corresponding to equilibrium state of CFTs in flat space have planar horizons, they are referred to in the literature as black branes. Equilibrium states are characterized by conserved charges (or associated thermodynamics potentials, depending on the choice of ensemble) and in the case of interest, strongly-coupled CFTs' setups described by Eq. (4.5), the relevant quantity is the energy density or the temperature T. Because of the underlying conformal symmetry there is no other dimensionful parameter associated with the thermal state.

The relevant solution, known under the name of the AdS-Schwarzschild black brane takes the following form

$$ds^2 = \frac{L^2}{u^2} \left\{ du^2 - \frac{\left(1 - \frac{u^4}{u_0^4}\right)^2}{1 + \frac{u^4}{u_0^4}} \left(dx^0\right)^2 + \left(1 + \frac{u^4}{u_0^4}\right) d\mathbf{x}^2 \right\} \tag{4.8}$$

with static horizon located at $u = u_0$. In holography, horizon thermodynamics is a reflection of the underlying thermodynamics of a strongly-coupled hCFT. The Hawking temperature [84] of the AdS-Schwarzschild, equal to $\frac{\sqrt{2}}{\pi u_0}$, is the temperature T of the strongly-coupled hCFT's thermal state, whereas the Bekenstein-Hawking entropy [85,86] (here: density) of the black hole (here: brane), equal to

$$\mathcal{S} = \frac{\text{area density}}{4G_N} = \frac{\pi^2}{2} N_c^2 T^3,$$

is simply the entropy density of the hCFT (here $\mathcal{N} = 4$ SYM in the holographic regime). Comparing this result, valid for $\lambda \to \infty$, with thermodynamic entropy evaluated at vanishing coupling λ (i.e. for an ideal gas of quarks and other degrees of freedom appearing $\mathcal{N} = 4$ SYM Lagrangian), Ref. [87] pointed out that they differ by only 25%. On the gravity side, this follows from the aforementioned observation that the coupling constant λ does not enter the holographic calculations in two-derivative gravity at all. Furthermore, a small change in thermodynamic properties of quark-gluon plasma from weak-coupling to the strong-coupling regime (albeit away from the crossover) was also seen in lattice studies of QCD, see e.g Ref. [88].

For completeness, it will be also useful to display the AdS-Schwarzschild geometry given by

Eq. (4.8) in coordinates that are regular at the horizon,

$$ds^2 = \frac{L^2}{u^2} \left\{ -2\, dx^0\, du - \left(1 - \pi^4 T^4 u^4 \right) \left(dx^0 \right)^2 + d\mathbf{x}^2 \right\}, \tag{4.9}$$

where one should note that despite using the same names, x^0 and u coordinates are now different (in the sense that the same values correspond to different bulk points) than the ones in Eq. (4.8).

The key feature of the AdS-Schwarzschild black brane solution is the presence of the horizon, which acts as a surface of no return for all physical signals. To make this statement clear: in the approximation in which it does not backreact to the AdS-Schwarzschild geometry, once a wave-packet passes the hypersurface of $u = u_0$, it cannot influence whatever is happening between $u = 0$ and $u = u_0$. This notion extends also outside equilibrium with the horizon evolution obeying the second law of thermodynamics [89, 90]. One can thus say that it is the presence of the horizon that is the holographic manifestation of dissipation (entropy production) in QFTs.

4.3 Excitations of strongly-coupled plasmas as black branes' quasinormal modes

The simplest non-equilibrium phenomenon to study holographically is the dynamics of linearized perturbations on top of the AdS-Schwarzschild black brane. Because the background solution (4.9) is translational invariant in both x^0 and $\mathbf{x}$, it is natural to seek for solutions in terms of Fourier modes,

$$Z(u, x^0, \mathbf{x}) = \int d\omega\, d^3k\, e^{-i\,\omega\,x^0 + i\,\mathbf{k}\cdot\mathbf{x}}\, Z(u, \omega, \mathbf{k}), \tag{4.10}$$

where we make use of the fact that in the case of interest perturbations can be recast into a set of decoupled functions.

In order to make contact with the linear response theory introduced in Sec. 3.1, see Eqs. (3.1) and (3.2), we are interested in the bulk metric perturbations, δg_{ab} (or, after fixing the bulk coordinates freedom as in Eq. (4.2), $\delta h_{\mu\nu}$), solving Eqs. (4.5) linearized on top of the AdS-Schwarzschild metric. The reason for it is that via Eq. (4.6) they correspond to perturbations of the expectation value of the energy-momentum tensor on top of its equilibrium value and can be generated by perturbing the metric in which an underlying hCFT lives.

The decomposition of the retarded two-point function of the energy-momentum tensor (and the resulting change in the expectation value of the energy-momentum tensor) into shear, sound and scalar channels has, as it must, its direct counterpart on the gravity side. Focusing on the sound channel and assuming the momentum $\mathbf{k}$ is aligned along the x^3-direction, the relevant bulk metric perturbations, see Eq. (4.2), are the following: δh_{00}, δh_{03}, δh_{33} and the sum of
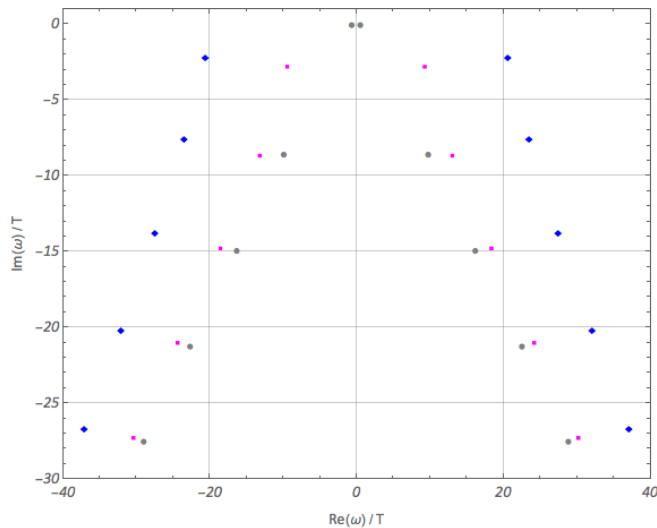
Figure 3: The structure of the lowest lying singularities in the complex frequency plane at fixed spatial momentum k of the retarded two-point function of $\hat{T}^{\mu\nu}$ in the sound channel in hCFTs for $k = 0.1\,T$ (dots), $k = T$ (squares) and $k = 10\,T$ (diamonds). One can clearly see that singularities are single poles (QNMs) and all of them apart from one retain fast decay time of the order of $1/T$. The remaining singularity can be made arbitrary long-lived by considering low-enough momentum, see also Fig. 4, and, as we discuss in Sec. 6.5, is a manifestation of the hydrodynamic behaviour.

δh_{11} and δh_{22}. They can be combined into single bulk variable $\tilde{Z}(u, \omega, \mathbf{k})$ which obeys a second order ordinary differential equation in u. Its behaviour at $u = 0$ is precisely such as dictated by Eq. (4.6) and following the general discussion about the definition of modes within the linear response theory from Sec. 3.1, we will be interested in turning off the source, i.e. the situation in which $Z(u, \omega, \mathbf{k}) = \mathcal{O}(u^4)$. The solution depends on two integration constants and this requirement fixes one to zero. Given that $\tilde{Z}$ can be freely rescaled, demanding that the horizon acts as a surface of no return imposes a condition on frequencies ω, which turn out for each value of k to have infinitely many discrete complex solutions. In the black hole physics language, these solutions are called quasinormal modes (QNMs) and are responsible for the approach of horizon to equilibrium when nonlinear effects become negligible, see e.g. [91] for a comprehensive review.

As a result, we see that the singularities of the retarded two-point function of the energy-momentum tensor of the strongly-coupled hCFT plasma at fixed $\mathbf{k}$ are single poles located at the QNMs' frequencies $\omega(k)$ of the AdS-Schwarzschild black brane. The same holds in the scalar and shear channels and, more generally, occurs for any other operator in strongly-coupled plasma and extends to situations in the absence of conformal symmetry. There are several comments in order. First, the QNMs frequencies are symmetric with respect to the imaginary axis and

typically contain both the real and imaginary part. Second, the only scale in the problem is the temperature T and QNMs frequencies of strongly-coupled hCFTs are necessarily linear in T. Hence, apart from the observation that the singularities of the retarded two-point function of the energy-momentum tensor are single poles, the only nontrivial feature is their distribution on the complex frequency plane as a function of k measured in the units of T. Regarding the former, Fig. 3 displays the position of the lowest five QNMs' frequencies in the sound channel for three different values of k/T. One can infer from this plot that the frequencies are continuous functions of momentum k and as a result, what one then calls a mode is the set of all excitations associated with a given $\omega(k)$. Furthermore, one sees that for all QNMs apart from one their amplitude decreases by an order of magnitude over at most a time scale of $1/T$. The number of oscillations of each QNMs over this decay time is of the order of unity. This feature of QNMs needs to be drastically contrasted with the quasiparticle behaviour, occurring in weakly-coupled systems, in which there are many long-lived excitations. In the present case of the sound channel, there is only one long-lived excitation, which is the least-damped mode at low momenta. This special excitation is to be interpreted in Sec. 6.5 as the hydrodynamic sound wave – one of the two independent solutions of the equations of hydrodynamics linearized on top of the static plasma, which explains the name of the channel. The same situation occurs in the shear channel in which there is also one hydrodynamic mode appearing, the shear wave, and all the remaining QNMs are exponentially damped over $1/T$. In the so-called scalar channel, all the modes are fast decaying. More generally, the presence of such long-lived, slowly evolving excitations can be inferred from the conservation of the energy-momentum tensor $\hat{T}^{\mu\nu}$, see Ref. [92]. Finally, let us also remark that qualitative changes in the spectrum of QNMs can occur by considering more complicated holographic equations of motion than Eqs. (4.5). A particularly interesting case to consider is supplementing Einstein-Hilbert action with negative cosmological constant with the Gauss-Bonnet term (4.7), as recently considered in Refs. [54, 81]. As can be seen in Fig. 5, this theory is characterized by new excitations which in certain regions of parameter space dominate late-time response response and can even exhibit quasiparticle features.

5 Bjorken flow ab initio and hydrodynamization

In this Section we review ab initio studies of microscopic models revealing transition to hydrodynamic behaviour starting from highly non-equilibrium initial stations. We focus on the simplest available setup by assuming that systems under consideration are conformally-invariant, as well as transversely homogeneous and invariant under longitudinal Lorentz boosts. In the context of hydrodynamics, one frequently speaks of boost-invariant, or Bjorken flow [93].
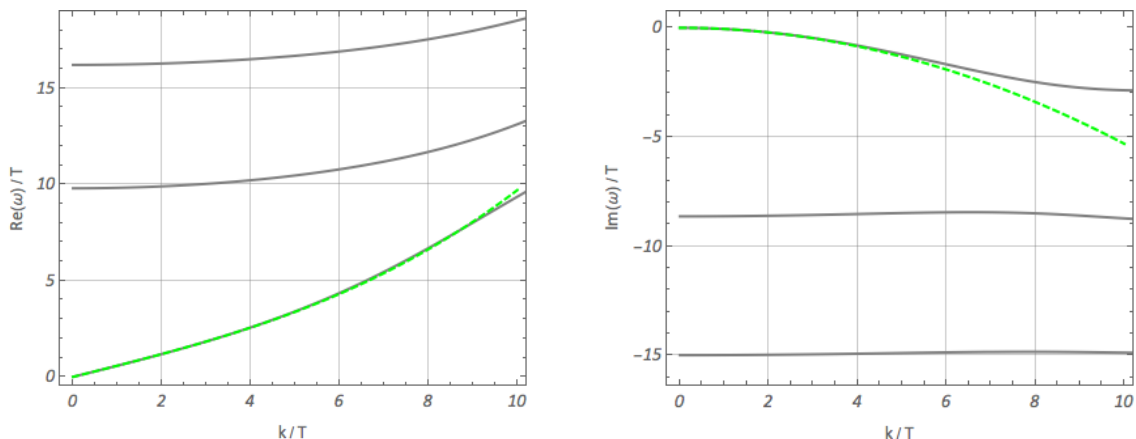
Figure 4: Momentum-dependence of the lowest three QNMs in the sound channel. One clearly sees one long-lived excitation at low momentum whose frequency matches the dispersion relation (dashed green curve) for the hydrodynamic sound wave evaluated up to second order in gradient expansion. Furthermore, one can also notice a rather mild momentum-dependence of the transient modes at low enough momentum. This observation is one of the starting points for the HJSW theory discussed in Sec. 7.5.

5.1 Boost invariance and the large proper-time expansion

Boost invariance is a natural symmetry of systems produced at extremely high energies. Suppose that in the initial state we deal with two colliding objects that approach each other with the rapidities[9] y and $-y$. In a Lorentz boosted reference frame, these two objects have rapidities $y - y_f$ and $-y - y_f$, where y_f is the rapidity of the new Lorentz reference frame with respect to the original one. As long as $y_f \ll y$, the initial and final states look approximately the same in the two reference frames, which is the origin of boost invariance. Strictly speaking, boost invariance is reached only in the limit $y \to \infty$. In practice, one deals with a very large y and a finite range of boosts y_f, for which the system may be regarded as approximately boost invariant. For exactly boost-invariant systems, the rapidity distribution of produced particles, dN/dy, is a (rapidity independent) constant. For systems which are approximately boost invariant, one expects that the rapidity distribution exhibits a finite range plateau.

In practice it is often convenient to introduce the proper time τ and spacetime rapidity Y as new coordinates replacing lab-frame time, t, and the spacial coordinate along the beam axis, z, see Eqs. (C.1), (C.2) and (C.3).[10] The statement of boost invariance then boils down to saying that dependence of scalar quantities on the four Minkowski coordinates is reduced to dependence

---

[9]See Appendix C for the definition of rapidity.

[10]One should in general distinguish between the rapidity of a particle (measure of its longitudinal velocity) and spacetime rapidity (spacetime coordinate).
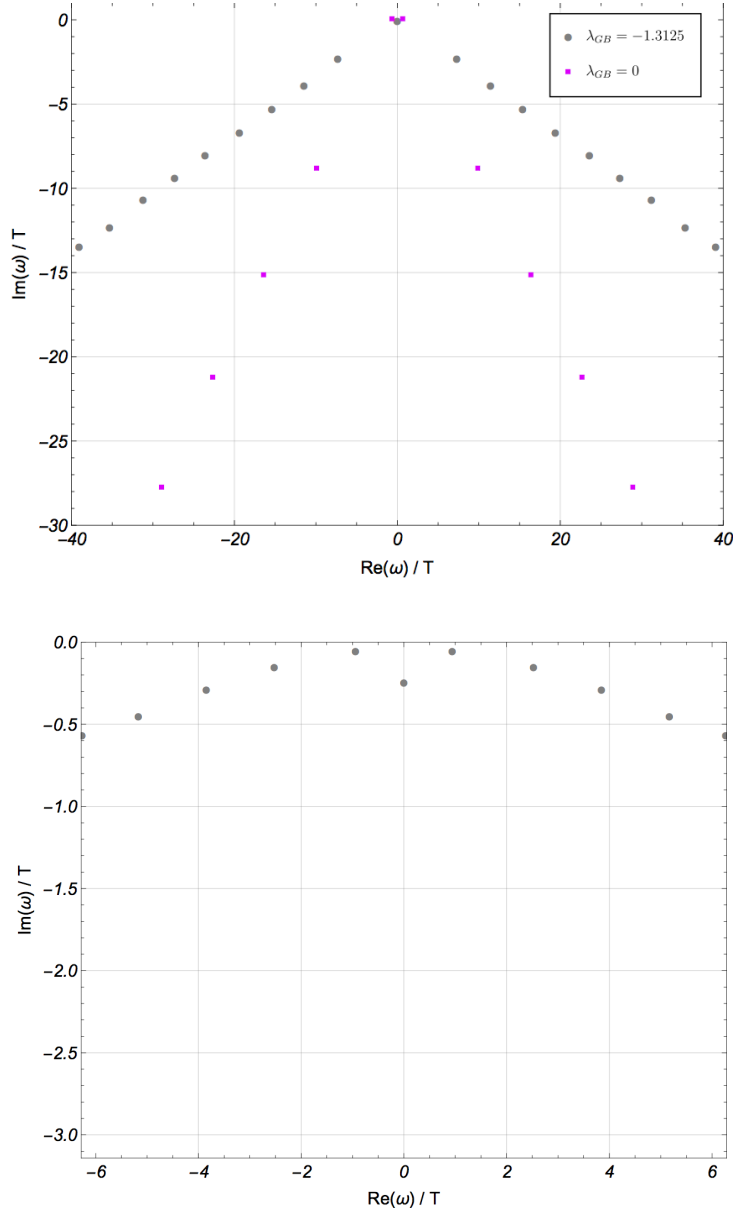
Figure 5: Modes in sound channel in Gauss-Bonnet gravity at $k \approx 0.63\,T$ for two different values of the Gauss-Bonnet coupling: $\lambda_{GB} = -1.3125$ (top) and $\lambda_{GB} = -24.75$ (bottom). One sees a qualitative change in the structure of modes as compared to the Einstein gravity case ($\lambda_{GB} = 0$). In particular at non-zero values of λ_{GB} new modes appear and at fixed momentum one can make them dominate late time dynamics instead of the long-lived $\lambda_{GB} = 0$ mode, as happens in both plots. Furthermore, in the bottom plot one sees new modes approaching the real axis (becoming long-lived), reminiscent of quasiparticles. There is a numerical evidence that poles condense and form a branch-cut as $\lambda_{GB} \to -\infty$, which would result in a picture somewhat similar to free $\mathrm{SU}(N_c)$ gauge theory discussed in Sec. 3.2. The plot is based on data and methods from Refs. [54, 81].

on the proper time τ alone.

The expectation value of the boost-invariant energy-momentum tensor in a local rest frame takes the form

$$T^\mu_{\ \nu} = \mathrm{diag}(\mathcal{E}, \mathcal{P}_L, \mathcal{P}_T, \mathcal{P}_T)^\mu_{\ \nu} , \tag{5.1}$$

where the eigenvalues – the energy density $\mathcal{E}$ and the longitudinal and transverse pressures $\mathcal{P}_L$ and $\mathcal{P}_T$ – are functions of the proper time τ alone. Furthermore, in a conformal theory, the conditions of tracelessness and conservation lead to the relations [94]

$$\mathcal{P}_L = -\mathcal{E} - \tau \dot{\mathcal{E}} , \quad \mathcal{P}_T = \mathcal{E} + \frac{1}{2}\tau \dot{\mathcal{E}}. \tag{5.2}$$

The departure of these quantities from the equilibrium pressure at the same energy density

$$\mathcal{P} \equiv \frac{\mathcal{E}}{3}, \tag{5.3}$$

is a measure of how far a given state is from local equilibrium. It is therefore natural to study the approach to local equilibrium by examining the behaviour of the normalized pressure anisotropy

$$R \equiv \frac{\mathcal{P}_T - \mathcal{P}_L}{\mathcal{P}}. \tag{5.4}$$

This will be done in the following Sections both for holography and RTA kinetic theory.

Conformal invariance also implies that energy density scales with the fourth power of temperature, that is,

$$\mathcal{E} \sim T^4 , \tag{5.5}$$

with some dimensionless constant σ. For example, for the equilibrium $\mathcal{N} = 4$ theory at strong coupling one finds [83]

$$\mathcal{E} = \frac{3}{8}\pi^2 N_c^2\, T^4, \tag{5.6}$$

see also Sec. 4.2. Similarly as in the case of the RTA kinetic theory discussed in Sec. 3.3.3, the quantity T in (5.5) should be interpreted as an effective temperature, which is the measure of the local, possibly non-equilibrium in the sense of non-vanishing R defined in Eq. (5.4), energy density $\mathcal{E}$. In what follows we denote the effective temperature by T, since this introduces no ambiguity. [11]

---

[11]Note that it may not be possible to do this for more general flows [95, 96].

In a boost invariant configuration all the physics is encoded in the dependence of the energy density (or, equivalently, the effective temperature) on τ. This is a dramatic simplification compared to the general case, but it retains the key physical feature of power law relaxation to equilibrium, characteristic of hydrodynamics. This is clearly the prime reason why we decided to focus on this particular flow.

In conformal theories, such as those considered in this Section, the late-time behaviour of the temperature is strongly restricted by symmetry. In all the microscopic models considered in the present Section, the late-time behaviour turns out to be captured by the following formal formulae

$$T(\tau) = \frac{\Lambda}{(\Lambda\tau)^{1/3}} \left(1 + \sum_{k=1}^{\infty} \frac{t_k}{(\Lambda\tau)^{2k/3}} \right), \tag{5.7}$$

where Λ is a dimensionful parameter which depends on the initial conditions. Indeed, it is the only trace of initial conditions to be found in the late-time behaviour of the system.

The existence of such late-time solutions in microscopic theories is of fundamental importance, since it describes the manner in which the system approaches local equilibrium at late times.[12]. These late-time states will differ in temperature at a given finite value of proper time; this dependence on the initial conditions is captured by the dimensionful constant Λ. When the system behaves to a good accuracy as described by a truncated expansion of Eq. (5.7), we say that it has reached the hydrodynamic stage of it evolution. The reason for this nomenclature is that the leading behaviour seen in Eq. (5.7) appears in perfect fluid hydrodynamics of Bjorken flow [93] and subleading power-law corrections capture dissipative hydrodynamic effects such as shear viscosity, see Sec. 7.4.

It is interesting and useful to examine more closely how one can technically establish, given a numerically calculated temperature history, that the hydrodynamic stage has been reached. To this end it is very convenient to formulate a criterion [13] which is independent of the parameter Λ, whose value is different for each solution. First let us define the dimensionless variable

$$w = \tau\, T(\tau), \tag{5.8}$$

which can be thought of as the proper time in units of inverse effective temperature; it has in fact a much more profound significance, which is revealed in Sec. 7.1. The key idea is to consider not the temperature as a function of proper time, but rather a dimensionless observable such as

---

[12]Note this is a one-dimensionally expanding systems, which in the limit of infinite proper time completely dilutes.

the pressure anisotropy Eq. (5.4) as a function of the dimensionless evolution parameter w. In a conformal theory, as the hydrodynamic regime is reached such a function is guaranteed to tend to a universal form, independent of the initial, non-equilibrium state. This is because (as seen in Eq. (5.7)) in the hydrodynamic regime the only trace of the initial state is the scale Λ, but this dimensionful quantity cannot appear in $R(w)$ at late times.

In most papers on this subject the discussion was formulated in terms of the the dimensionless function (not to be confused with the distribution function of kinetic theory!)

$$f \equiv \frac{\tau}{w}\frac{dw}{d\tau}\,. \tag{5.9}$$

Using Eq. (5.2) one can check that this quantity is trivially related to the pressure anisotropy:

$$f = \frac{2}{3} + \frac{1}{18}\,R\,. \tag{5.10}$$

Since in the context of Bjorken flow the pressure anisotropy R is a natural observable with a clear physical significance, here we focus on this quantity.

In terms of the dimensionless variable w the large proper-time expansion of R takes the form

$$R(w) = \sum_{n=1}^{\infty} r_n\,w^{-n}, \tag{5.11}$$

i.e., it is a series in negative integer powers of w. This fact follows directly from Eq. (5.10) and Eq. (5.7) and, as we discuss in Sec. 9, holds up to corrections that are exponentially suppressed at large times (large w). The coefficients r_n appearing in Eq. (5.11) are pure numbers, i.e., they are independent of the parameter Λ which distinguishes different histories of the system. The large-w expansion (5.11) is therefore a universal solution, determined only by the microscopic parameters of the system under study.

5.2   Strong coupling analysis using holography

In the context of holography, the imposition of boost invariance reduces the gravitational problem to one involving just two coordinates: the "radial" coordinate u and a time coordinate identified with the proper-time τ on the boundary. This has made it possible to carry out explicit calculations on the gravity side of holography from its very early days and translate the results into the language of quantum field theory in four-dimensional Minkowski space.

At first, analytic calculation were performed in an expansion in inverse powers of the proper-time. These calculations, reviewed below in Sec. 5.2.1, reproduced first as the leading order late-time behaviour the Bjorken description of boost-invariant flow in the framework

of perfect-fluid hydrodynamics (see Sec. D). Viscous as well as higher order corrections were subsequently computed, placing the hydrodynamic description on the very firm ground of *ab initio* calculations in a strongly coupled Yang-Mills theory. This was subsequently supplemented by numerical calculations of early time evolution using methods of numerical general relativity – these developments are reviewed in Sec. 5.2.2 below.

5.2.1 Large proper-time expansion

Einstein's equations (4.5) determining the bulk geometry possess an approximate analytic (semi-analytic at high orders) solution in the form of a power series in inverse powers of τ first found in Ref. [94] and later developed in Refs. [18, 97, 97–101]. We discuss what is perhaps a more streamlined version of this framework in Sec. 9.2.1.

Using the methodology of Sec. 4, see Eq. (4.6), one can read off the expectation value of hCFT's energy-momentum tensor from the asymptotic behaviour of these solutions near the boundary. Proceeding in this manner terms up to third order have been calculated analytically [97, 99, 101]. These results determine the energy density of hCFTs as a function of proper time. Expressed in terms of the effective temperature the result reads

$$T(\tau) = \frac{\Lambda}{(\Lambda\,\tau)^{1/3}}\left\{1 - \frac{1}{6\pi\,(\Lambda\,\tau)^{2/3}} + \frac{-1+\log 2}{36\pi^2\,(\Lambda\,\tau)^{4/3}} + \frac{-21+2\pi^2+51\log 2-24(\log 2)^2}{1944\pi^3\,(\Lambda\,\tau)^2}\right\}. \quad (5.12)$$

The form of this expansion matches Eq. (5.7). It can be translated into the large-w expansion of $R(w)$. At very late times the pressure anisotropy approaches zero, which one interprets as reaching local equilibrium. The approach is governed by Eq. (5.11), with the leading coefficients given by

$$r_1 = \frac{2}{\pi}, \quad r_2 = \frac{2-2\log 2}{3\pi^2}, \quad r_3 = \frac{15-2\pi^2-45\log 2+24\log^2 2}{54\pi^3}. \quad (5.13)$$

As discussed earlier in Sec. 5.1, these coefficients are dimensionless and independent of the scale Λ appearing in Eq. (5.7). The truncation of Eq. (5.11) keeping only the three leading terms with the above values of the expansion coefficients will be denoted by $R_H(w)$.

Up to this point, we have only discussed hydrodynamic behaviour at the microscopic level, but have not begun to develop the effective description of this regime. However, anticipating the developments discussed below in Sec. 6, we wish to point out that the leading coefficient, r_1, is a multiple of the shear viscosity to entropy ratio,

$$r_1 = 8\,\frac{\eta}{\mathcal{S}}, \quad (5.14)$$

so the value quoted in Eq. (5.13) reproduces the result $\eta/\mathcal{S} = 1/4\pi$ obtained in holographic

models involving two-derivative gravity actions.

To summarise: the importance of Eq. (5.12) lies in the fact that it represents an *ab initio* calculation in a specific microscopic theory, which is consistent with the form expected on the basis of hydrodynamics. This point will be explored in greater detail in Sec. 7, where we will also discuss the significance of the coefficients appearing in the series Eq. (5.12). Note also that the large-time expansion in Sec. 5.12, or more directly its counterpart in the language of $R(w)$, is a manifestation of the fluid-gravity duality [102] which we discuss in Sec. 7.2.

5.2.2 Hydrodynamization: emergence of hydrodynamic behaviour

It was to be expected that starting from any initial state the system should evolve in such a way that at late times it will be described by Eq. (5.7) for some value of the constant Λ. The quantitative study of this issue in a holographic setting translates into solving a set of nonlinear partial differential equations with two independent variables. This task cannot be fulfilled analytically, but numerical calculations can be set up in a relatively straightforward way. They involve three stages:

1. finding initial metrics which satisfy constraints implicit in the Einstein equations (4.5);

2. evolving the geometry using a suitable numerical scheme, see e.g. Refs. [103–105];

3. calculating the expectation value of the energy-momentum tensor in hCFT using Eq. (4.6).

The first numerical holographic calculations in this and similar contexts were presented in Refs. [11,12,106]. Our presentation here follows slightly later developments of Refs. [13,103,107] since, first, in these studies expanding boost-invariant matter relaxes unforced to hydrodynamics and, second, by analysing a large number of different initial non-equilibrium state they allowed to isolate regularities with more certainty.

The outcome of these efforts can be summarised by saying that it has been verified directly in numerical simulations that the behaviour described by Eq. (5.12) emerges at late times for all initial states which were studied. The cleanest way to see it will be through the use of the pressure anisotropy R as a function of dimensionless clock variable w.

One should mention at this point, that it was shown in [108] that for small proper times only even powers of τ can appear in a power series expansion of the energy density:

$$\mathcal{E}(\tau) = \sum_{n=0}^{\infty} \mathcal{E}_n \tau^{2n}, \tag{5.15}$$

but there is no known constraint on what the leading power should be. Both groups [13,103] and [107] assumed that the energy density approaches a nonzero constant value $\mathcal{E}_0 \neq 0$ at
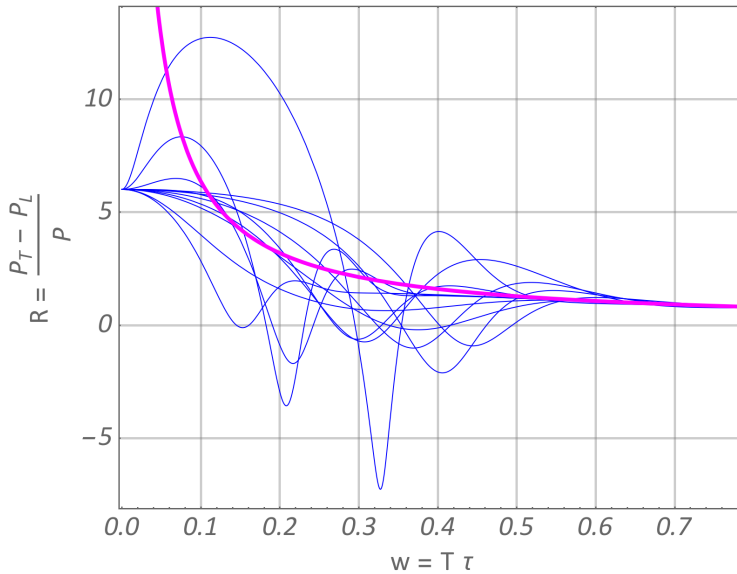
Figure 6: The pressure anisotropy for a small sample of solutions, represented by the blue curves. The red curve is the first order truncation of $R_H(w)$. As will become more apparent in Fig. 7, blue curves join the red curve when the anisotropy in the system is very sizable, much more than anticipated before. The figure is based on numerical data taken from Ref. [107].

$\tau = 0$ where the initial conditions were set. Note that from Eq. (5.4) it follows that $R = 6$ at $w = 0$ and this value can be indeed seen in Fig. 6. The same value of the initial pressure anisotropy is obtained within the CGC framework, see Ref. [109], and necessarily involves negative longitudinal pressure $\mathcal{P}_L = -\mathcal{P}_T$. More generally for $\mathcal{E}(\tau) \sim \tau^{2n}$ at small τ one obtains $R(w = 0) = 6 + 9\,n$, see Ref. [110] for results motivated by Ref. [111] which assume $n = 1$.

A given numerical solution for the energy density $\mathcal{E}(\tau)$ starts out far from equilibrium, but the damping of transient modes ensures, see Sec. 4.3, that after a sufficiently long time only hydrodynamic modes remain. Given the result of a numerical simulation for $\mathcal{E}(\tau)$ one can check whether the hydrodynamic regime has been reached by comparing the pressure anisotropy $R(w)$ calculated from the simulation data with the hydrodynamic form given by the truncated large-w expansion $R_H(w)$. Despite significant differences at early times, all numerical solutions studied in [13, 103, 107] exhibit this behaviour: over 600 initial conditions have been evolved and in all cases it was found that hydrodynamics become a good description at some $w < 1$. This can be seen qualitatively in a plot of the pressure anisotropy in Fig. 6, where a small set of histories is plotted.

In more quantitative terms, for a given solution $\mathcal{E}(\tau)$ one can evaluate the resulting pressure anisotropy $R(w)$, and then calculate the difference between this and the asymptotic form given

by a truncation of Eq. (5.11) with leading coefficients taken from Eq. (5.13). This difference converges to zero, and one can define the hydrodynamization "time" w_H as the value beyond which the difference is smaller than some threshold. The distribution of hydrodynamization times w_H obtained in [107] on the basis of 600 histories is clustered around $w = 0.6$, which is consistent with the evidence found earlier in Ref. [13].

The essential physical message, seen already in Fig. 6, is that the truncated large-w expansion $R_H(w)$ typically becomes a good approximation at a time when the pressure anisotropy is still substantial, of the order of 50% of what would be the equilibrium pressure. For this reason it has been proposed that instead of speaking of thermalization which requires approximate local equilibrium, in particular approximate local isotropy, one should use a term such as hydrodynamization to describe this effect.

5.3   Kinetic theory in the RTA

The calculations reviewed above present a compelling picture of the emergence of universal behaviour at late times when the coupling is strong. It is also possible to carry out analogous calculations in the weak coupling framework of kinetic theory.

As explained in Sec. 3.3.3, one can simplify the potentially very complex collision kernel appearing in the Boltzmann equation by replacing it with a simplified expression, linearized around the the equilibrium distribution which we assume of the Boltzmann form (neglecting quantum statistics for simplicity). Assuming the expansion along the x^3-axis and introducing the boost-invariant variables [112, 113]

$$u = p_L\, x^3 - E\, x^0, \quad v = Ex^0 - p_L\, x^3, \tag{5.16}$$

the equilibrium distribution takes the form

$$f_0(\tau, u, p_T) = \frac{1}{(2\pi)^3} \exp\left[-\frac{\sqrt{u^2 + p_T^2\tau^2}}{\tau\, T(\tau)}\right], \tag{5.17}$$

where the quantity $T(\tau)$ appearing here is identified with the effective temperature and determined self-consistently by imposing the Landau-matching condition discussed below.

The boost-invariant RTA Boltzmann equation reads [114–116]

$$\tau_{\text{rel}} \frac{\partial f(\tau, u, p_T)}{\partial \tau} = f_0(\tau, u, p_T) - f(\tau, u, p_T). \tag{5.18}$$

To ensure conformal symmetry we take the relaxation time to be of the form (3.22). The dependence of the temperature on the proper time is determined dynamically by imposing the

Landau matching condition

$$\mathcal{E}(\tau) = \frac{6}{\pi^2} T^4(\tau), \tag{5.19}$$

where

$$\mathcal{E}(\tau) = 4 \int d^4p \, \delta\left(p^2\right) \theta(p^0) \frac{v^2}{\tau^2} f(\tau, u, p_T) = 2 \int dP \, \frac{v^2}{\tau^2} f(\tau, u, p_T) \tag{5.20}$$

is the energy density (the factor 2 accounts for the spin degeneracy). Note again that despite apparent linearity of the Boltzmann equation (5.18), the Landau matching condition (5.19) renders the problem of determining the distribution function f strongly nonlinear.

5.3.1 Large proper-time expansion

To determine the coefficients r_n in Eq. (5.11) we can proceed in a number of ways. What is perhaps the most streamlined formulation providing access to the large-n behaviour of r_n is presented in Sec. 9.2.2. The least efficient, but conceptually simplest way is to compute an iterative solution of the Boltzmann equation (5.18), which can be done by setting up the iteration:

$$f_{n+1}(\tau, u, p_T) = -\tau_{\text{rel}} \frac{\partial f_n(\tau, u, p_T)}{\partial \tau}, \quad n \geq 0, \tag{5.21}$$

with f_0 given by Eq. (5.17). This is the Chapman-Enskog iteration discussed in the same context in Ref. [117]; the generated series of approximations is precisely the large proper-time expansion. At each order one obtains an explicit expression for the distribution function at that order of approximation, but one still needs to impose the Landau matching condition (5.19), which determines the proper-time dependence of the temperature $T(\tau)$ up to that order.

At order zero the Landau condition (5.19) identifies the function T appearing in Eq. (5.17) with the effective temperature appearing in Eq. (5.19). Imposing Eq. (5.19) at first subleading order leads to the equation

$$3\tau \dot{T} + T = 0, \tag{5.22}$$

whose late-time solution is

$$T = \frac{\Lambda}{(\Lambda\tau)^{1/3}} + \dots \tag{5.23}$$

The integration constant appearing in this solution was denoted by Λ in order to allude to the solution (5.7).

At order K in place of Eq. (5.22) one finds a differential equation of order K. These equations can be solved at large values of the proper time τ and posess solutions of the form given in Eq. (5.7), where the coefficients t_k appearing there must be determined by imposing the Landau matching condition (5.19). It is important to note that matching at order $K > 1$ determines the coefficient t_{K-1} of Eq. (5.7). The coefficients t_k for $k \geq K$ are not reliably determined by matching at order K, since they will receive corrections from matching at orders $> K$.

Once the late-time solution is determined to some order, one can calculate the expansion coefficients of the pressure anisotropy (5.4) in powers of the dimensionless variable w (as described in Sec. 5.1). The leading coefficients read

$$ r_1 = 8/5\,\gamma, \quad r_2 = 32/105\,\gamma^2, \quad r_3 = -416/525\,\gamma^3. \tag{5.24} $$

As already noted in Eq. (5.14), when matched to viscous hydrodynamics, the first coefficient is directly proportional to the shear viscosity to entropy ratio. The first relation in (5.24) then translates to

$$ \bar{\eta} = \frac{\eta}{\mathcal{S}} = \frac{\gamma}{5}, \tag{5.25} $$

This reveals the dual physical significance of the parameter γ. On the one hand it determines the relaxation time, but on the other it reflects the viscosity of the fluid once hydrodynamic behaviour emerges. This is an important physical property of the RTA: it correlates the microscopic relaxation time and the viscosity at the level of the effective, hydrodynamic description.

5.3.2 Emergence of hydrodynamic behaviour

The numerical solution of the Boltzmann equation Eq. (5.18) has been extensively discussed in Ref. [115,116] following earlier work by Baym [114]. This is done by reformulating the calculation of the energy density as the following integral equation for the function $T(\tau)$,

$$ T^4(\tau) = D(\tau, \tau_0) \frac{\pi^2 \mathcal{E}^0(\tau)}{6} + \int_{\tau_0}^{\tau} d\tau' \left(\frac{T(\tau')}{\gamma} D(\tau, \tau') \right) \times \left(T^4(\tau')\, H\left(\frac{\tau'}{\tau}\right) \right). \tag{5.26} $$

where we assumed the relaxation time τ_{rel} of a conformal theory, see Eq. (3.22), $D(\tau_2, \tau_1) = e^{-\frac{1}{\gamma}\int_{\tau_1}^{\tau_2} d\tau'' T(\tau'')}$ and $H(s) = \frac{s^2}{2} + \frac{\arctan\sqrt{\frac{1}{s^2}-1}}{2\sqrt{\frac{1}{s^2}-1}}$. The information about initial distribution function is encoded in $\mathcal{E}^0(\tau)$ given by Eq. (5.20), but[13] evaluated at time τ. Eq. (5.26) can be solved efficiently by fixed-point iteration. Knowing $T(\tau)$ one can find the remaining components of the

---

[13]Note explicit and implicit time-dependence in the measure and integrand in Eq. (5.20). There only the choice $\tau = \tau_0$ gives the initial energy density.

energy-momentum tensor and get the quantity of interest, i.e. $R(w)$. It should be also noted that one can rewrite Eq. (5.26) directly in terms of $R(w)$ by, e.g., taking a derivative of both sides with respect to τ and using Eq. (5.10). This can be advantageous for some purposes, e.g. when comparing different solutions at late times when high numerical accuracy is required to resolve subtle transient effects.

A formal transition to hydrodynamics in a model of QGP given by the RTA kinetic theory has been recently studied, in the analogous way to that used from strongly-coupled hQFTs, in Ref. [118]. This work, motivated by earlier results in Ref. [65], discusses qualitative similarities of the hydrodynamization process in the EKT kinetic theory extrapolated to intermediate coupling, RTA kinetic theory and strongly-coupled theories. In particular, one can see very explicitly how generic initial conditions lead to the late-time behaviour embodied by the universal late-time solution described in the previous Section. Below, we discuss those findings, together with earlier results obtained in the EKT setting of Refs. [63, 64].

5.4 Hydrodynamization as a generic feature

As originally noticed in Ref. [65], at the level of boost-invariant flow the patterns of thermalization discovered in strongly coupled hCFTs and the kinetic theory models discussed in the previous Section are not vastly different. The key observation here is that the leading late-time behaviour is always $1/w$, and different theories are distinguished only by the coefficient. This means that if we consider the evolution of the anisotropy R as a function of a rescaled variable $\tilde{w} \equiv w/2r_1$, the leading late-time behaviour of R is universally given by

$$R_H(\tilde{w}) = \frac{2}{\pi\tilde{w}} + \mathcal{O}(\frac{1}{\tilde{w}^2}).$$

The choice of rescaling is somewhat arbitrary, but once the coefficient r_1 is scaled away, the leading behaviour is completely universal. This means that if we compensate for the possibly very different values of $\eta/\mathcal{S}$ by using the rescaled variable $\tilde{w}$, the approach to equilibrium should be the same at sufficiently large $\tilde{w}$. This can be checked by comparing the results of gravity calculations for hCFTs with the results for models based on kinetic theory [118].

Figure 7 shows a comparison of the time evolution of the system evolved in the EKT from [64], RTA using the methodology of [114, 116], and numerical AdS/CFT calculation of [13, 103, 107]. For the EKT and RTA simulations we used the initial condition used in [64], whereas for the AdS/CFT simulation we took a typical initial conditions from [107]. The EKT curve correspond to evolution with $\lambda = 10$ corresponding to $\eta/\mathcal{S} \approx 0.642$, while the holographic result has $\eta/\mathcal{S} = 1/4\pi$. The RTA curves come from calculations with with γ fixed to reproduce the value of $\eta/\mathcal{S}$ of either model. As seen in the figure, the evolution in all cases is similar, but distinct. Quite
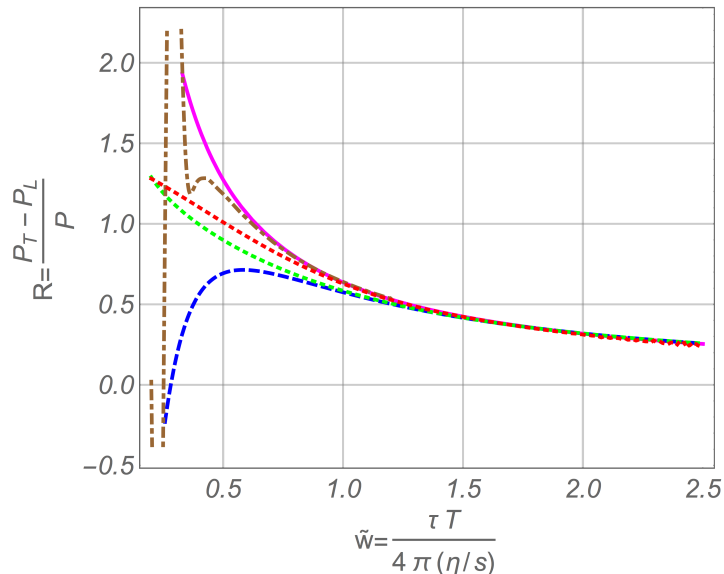
Figure 7: The magenta plot represents first order hydrodynamics, the brown dot-dashed line is the holographic result, and the red, dotted line is from EKT. The remaining lines are numerical solutions of the RTA model starting from the same initial distribution, but with different values of $\eta/\mathcal{S}$. The blue, dashed curve corresponds to $\eta/\mathcal{S} = 1/4\pi$, while the green, dotted curve corresponds $\eta/\mathcal{S} = 0.624$ (matching the data behind the red dotted line). The plot is adapted from Ref. [118].

remarkably, in all models, with vastly differing microphysics, the evolution converges to first order viscous hydrodynamics roughly at same $\tilde{w} \approx 1$ with large pressure anisotropy $R \approx 0.6 - 0.8$. To summarize: the quantitative differences between weakly-coupled scenarios extrapolated to intermediate couplings and genuinely strongly-coupled scenarios arise largely from the numerical values of the hydrodynamization time measured in units of inverse temperature, $w = \tau T$. In the strong coupling scenario, $w \approx 0.7$ at the hydrodynamic threshold. In phenomenological analysis of heavy ion experiments hydrodynamic codes are initialized typically at $w \approx 0.5$, which corresponds roughly to a time $\tau = 0.5$ fm after the collision, with the temperature $T = 350$ MeV at the centre of the fireball at RHIC (see e.g. [119]). In weak coupling framework this can be much larger in consequence of much larger shear viscosity (which, in the RTA, implies a correspondingly longer relaxation time).

6 Fundamentals of relativistic hydrodynamics

The microscopic calculations presented in the previous Section point to universal behaviour at late times, which we associate with the long-lived subset of modes of equilibrium matter discussed in Secs. 3 and 4. The developments reviewed in Sec. 5 assumed boost-invariance,

but the picture which emerges from them fits in perfectly with the microscopic expectations which do not rely on any symmetry assumptions. There we argued that the time evolution of non-equilibrium states in interacting systems can be seen as comprising of two stages. The first is a transient stage during which non-hydrodynamic modes decay exponentially fast on some scale determined by the microscopic theory. The second stage is governed by long-lived hydrodynamic modes, which dominate the dynamics already at times when the system is still far from local thermal equilibrium (hydrodynamization). This picture has been observed in a striking way in studies based on holography (reviewed in Sec. 5.2) as well as in models based on kinetic theory (reviewed in Sec. 5.3). It is natural to try to formulate an effective theory which captures the late time dynamics in terms of variables, which are phenomenologically relevant and useful. Since the emergence of hydrodynamic behaviour is a feature seen in diverse microscopic studies, one can formulate this effective description without assuming any specifics of the underlying microscopic dynamics (such as, for example, the existence of quasiparticle excitations).

The universal character of late time behaviour comes from a significant reduction in the number of degrees of freedom characterizing the expectation value of the energy-momentum tensor. The minimum number of independent components of this matrix is four, since it needs to describe at least the fluctuations of the four conserved quantities associated with spacetime translation symmetries. These hydrodynamic fields could be taken to be the energy density T^{00} and momentum densities T^{0i}. Instead of these, in order to conform to standard practice in hydrodynamics, we will instead use the 4-velocity local flow variable U defined as the boost velocity from some fixed frame of reference to the local rest frame in which the momentum densities vanish, and the energy density $\mathcal{E}$ in the local rest frame. A covariant way of introducing these quantities *at the microscopic level* is through the equation

$$\langle T^{\mu}_{\ \nu} \rangle U^{\nu} = -\mathcal{E} U^{\mu} \tag{6.1}$$

provided the vector U^{μ} is timelike. The goal of the hydrodynamics is to formulate an effective description of $\langle T^{\mu\nu} \rangle$ in terms of classical fields which are analogous to and mimic the quantities $\mathcal{E}, U^{\mu}$ defined by Eq. (6.1). The precise way in which this description, reviewed in the present Section, can be compared to and reconciled with the microscopic theory is the subject of Sec. 7.

6.1 Dynamical variables and evolution equations: the perfect fluid

By a hydrodynamic description one means a theoretical framework that uses a small set of *fluid variables* interpreted as the local energy density $\mathcal{E}(x)$ and local hydrodynamic flow vector $U^{\mu}(x)$, which is normalized as $U^2 = -1$.

The point of departure is the assumption that we are dealing with a system which reaches

global thermodynamic equilibrium at late times. At this stage one can be agnostic about the fundamental physics governing this system: it could be composed of well defined quasiparticles, but it need not be.

The equilibrium energy-momentum tensor in the rest-frame is given by

$$T_{\text{EQ}}^{\mu\nu} = \text{diag}\left(\mathcal{E}_{\text{EQ}}, \mathcal{P}(\mathcal{E}_{\text{EQ}}), \mathcal{P}(\mathcal{E}_{\text{EQ}}), \mathcal{P}(\mathcal{E}_{\text{EQ}})\right), \tag{6.2}$$

where we assume that the equation of state is known, so that the pressure $\mathcal{P}$ is a given function of the energy density $\mathcal{E}_{\text{EQ}}$. It is worth stressing, that $T_{\text{EQ}}^{\mu\nu}$ is a classical object which we should identify with the expectation value of the energy-momentum tensor operator in the underlying quantum theory.

The components of the equilibrium energy-momentum tensor (6.2) can be written in an arbitrary boosted frame of reference as

$$T_{\text{EQ}}^{\mu\nu} = \mathcal{E}_{\text{EQ}}U^{\mu}U^{\nu} + \mathcal{P}(\mathcal{E}_{\text{EQ}})\Delta^{\mu\nu}, \tag{6.3}$$

where U^{μ} is a constant boost velocity, and $\Delta^{\mu\nu}$ is the operator that projects on the space orthogonal to U^{μ}, namely

$$\Delta^{\mu\nu} = g^{\mu\nu} + U^{\mu}U^{\nu}. \tag{6.4}$$

Of course, the four-vector U^{μ} can equally well be regarded as a constant fluid four-velocity.

The energy-momentum tensor of a perfect fluid is obtained by allowing the variables $\mathcal{E}$ and U^{μ} to depend on the spacetime point x. In this way one obtains

$$T_{\text{eq}}^{\mu\nu} = \mathcal{E}(x)U^{\mu}(x)U^{\nu}(x) + \mathcal{P}(\mathcal{E}(x))\Delta^{\mu\nu}(x). \tag{6.5}$$

In this equation, and in those which follow, the subscript "eq" refers to local thermal equilibrium.

It is often convenient to introduce local effective temperature $T(x)$ by the condition that the equilibrium energy density at this temperature agrees with the non-equilibrium value of the energy density, namely

$$\mathcal{E}_{\text{EQ}}(T(x)) = \mathcal{E}_{\text{eq}}(x) = \mathcal{E}(x). \tag{6.6}$$

One can then express the perfect fluid energy-momentum tensor in terms of the fluid variables $T(x)$ and $U^{\mu}(x)$. Note that the relativistic perfect fluid energy-momentum tensor (6.5) is the most general symmetric tensor which can be expressed in terms of these variables without using derivatives. We also note that the effective temperature $T(x)$ in this case can be interpreted as a genuine thermodynamic quantity satisfying locally thermodynamic identities.

46

The dynamics of the perfect fluid theory is provided by the conservation equations of the energy-momentum tensor

$$\partial_\mu T^{\mu\nu}_{\text{eq}} = 0. \tag{6.7}$$

These are four equations for the four independent hydrodynamic fields, that form a self-consistent hydrodynamic theory.

6.2 Viscosity and the Navier Stokes equations

The essential physical element which is missing in the approach based on Eqs. (6.5) and (6.7) is dissipation. The perfect fluid evolution equations equations imply the covariant conservation of the 4-vector

$$s^\mu = \mathcal{S} \, U^\mu \tag{6.8}$$

which is called the entropy current. This equation implies that thermodynamic entropy is constant under hydrodynamic flows. This is not a feature expected of real-world flows, except in idealized situations. Since Eq. (6.8) is in fact just a rewriting of the projection of the conservation equation Eq. (6.7) onto U^μ (and using local thermodynamic relations, see e.g. Ref. [4]), a natural step is to consider modifications of the energy-momentum tensor so as to obtain a non-vanishing divergence of the entropy current Eq. (6.8) (possibly corrected by higher order terms). The requirement that this divergence be nonnegative has been used as a guide in formulating hydrodynamic equations (see e.g. Ref. [120]) and has a beautiful holographic interpretation [34, 36, 37, 101, 102, 121]. Note that requiring that the divergence of the entropy be nonnegative typically imposes constraints on parameters appearing in the hydrodynamic energy-momentum tensor, see Refs. [22, 120, 122] for a very comprehensive analysis of this issue.

To account for dissipation, we have to introduce correction terms to $T^{\mu\nu}_{\text{eq}}$ and write the complete energy-momentum tensor components $T^{\mu\nu}$ as

$$T^{\mu\nu} = T^{\mu\nu}_{\text{eq}} + \Pi^{\mu\nu}. \tag{6.9}$$

Here one can impose the condition $\Pi^{\mu\nu} U_\nu = 0$, which corresponds to the Landau definition of the hydrodynamic flow U^μ [1] specified by the formula

$$T^\mu_{\ \nu} U^\nu = -\mathcal{E} \, U^\mu. \tag{6.10}$$

This formula is the counterpart of Eq. (6.1) at the level of hydrodynamics.

It proves useful to further decompose $\Pi^{\mu\nu}$ into two components,

$$\Pi^{\mu\nu} = \pi^{\mu\nu} + \Pi\,\Delta^{\mu\nu}, \tag{6.11}$$

which introduces the bulk viscous pressure Π (the trace part of $\Pi^{\mu\nu}$) and the shear stress tensor $\pi^{\mu\nu}$ which is symmetric, $\pi^{\mu\nu} = \pi^{\nu\mu}$, traceless, $\pi^\mu{}_\mu = 0$, and orthogonal to U^μ, $\pi^{\mu\nu}U_\nu = 0$.

Equation (6.9) encodes ten independent components of $T^{\mu\nu}$ in terms of the effective temperature, three independent components of U^μ, five independent components of $\pi^{\mu\nu}$, and the bulk viscous pressure Π. We note that the latter vanishes for conformal systems, for which the entire energy-momentum tensor is traceless.

We still have the four conservation equations at our disposal,

$$\partial_\mu T^{\mu\nu} = 0, \tag{6.12}$$

but to obtain a closed system of equations one needs additional information. The most straightforward option is to express $\Pi^{\mu\nu}$ in terms of the hydrodynamic variables and their gradients. Since the perfect-fluid energy-momentum tensor contains no gradients, it is natural to try to build up the theory as a series of corrections in gradients. The simplest possibility is to include terms with only a single gradient, which leads to the relativistic Navier-Stokes theory [1], in which the bulk pressure and shear stress tensor are given by the gradients of the flow vector

$$\Pi = -\zeta\,\partial_\mu U^\mu, \quad \pi^{\mu\nu} = -\eta\,\sigma^{\mu\nu}. \tag{6.13}$$

Here ζ and η are the bulk and shear viscosity coefficients, respectively, and $\sigma^{\mu\nu}$ is the shear flow tensor defined as

$$\sigma^{\mu\nu} = 2\,\Delta^{\mu\nu}_{\alpha\beta}\,\partial^\alpha U^\beta, \tag{6.14}$$

where the projection operator $\Delta^{\mu\nu}_{\alpha\beta}$ has the form

$$\Delta^{\mu\nu}_{\alpha\beta} = \frac{1}{2}\left(\Delta^\mu{}_\alpha \Delta^\nu{}_\beta + \Delta^\mu{}_\beta \Delta^\nu{}_\alpha\right) - \frac{1}{3}\Delta^{\mu\nu}\Delta_{\alpha\beta}. \tag{6.15}$$

Equations (6.13) should be used in the conservation equations, (6.12), that can be split into the parallel and orthogonal parts with respect to the flow vector U^μ, namely

$$D\mathcal{E} + (\mathcal{E} + \mathcal{P} + \Pi)\theta + \frac{1}{2}\pi^{\mu\nu}\sigma_{\mu\nu} = 0 \tag{6.16}$$

and

$$(\mathcal{E} + \mathcal{P} + \Pi)DU^\mu = -\Delta^{\mu\nu}\partial_\nu(\mathcal{P} + \Pi) - \Delta^\mu{}_\nu\partial_\alpha\pi^{\alpha\nu}. \qquad (6.17)$$

6.3 The problem of causality

Unlike nonrelativistic Navier-Stokes theory, its direct relativistic generalisation [1] is not consistent, because it is not causal [15, 123, 124]. Specifically, while the evolution equations obtained by taking the shear stress tensor as in Eq. (6.13) are covariant, they have solutions which propagate with arbitrarily high velocities.

The easiest way to see the problem is to consider the hydrodynamic equations linearized around the equilibrium configuration $T = \text{const}, U^\mu = \text{const}$. Looking for solutions of these linearized equations on finds dispersion relations which determine the velocity of propagation $v \sim k$, where k is the modulus of the wave vector. This shows that at small distances causality is violated. It has been argued (see e.g. Ref. [125]) that this fact is not relevant, since one in any case would not trust hydrodynamics on small scales. However, as stressed (for example) in Refs. [4, 124], this acuasality leads to instabilities in numerical simulations for generic initial conditions.

Adding extra terms with higher gradients on the right-hand side of (6.13) does not help to solve the problem with causality. The only known way to avoid it is to relax the assumption that Π and $\pi^{\mu\nu}$ are expressed locally in terms of the hydrodynamic variables T, U^μ, and (a finite number of) their spacetime derivatives [126]. This means that the shear stress tensor is treated as an independent hydrodynamic field for which evolution equations must be provided. Thus, the conservation equations alone are no longer enough to determine the dynamics of $T^{\mu\nu}$ and one needs to postulate additional dynamic equations, or derive them (possibly by some heuristic means). The outcome, a closed set of hydrodynamic equations, will clearly involve additional degrees of freedom beyond those already present in the theory of the perfect fluid. To write down such equations additional assumptions or information will be required, beyond what is embodied by conservation laws.

6.4 Approaches to finding evolution equations

A well-known and widely applied approach to the task of positing a set of closed equations for the hydrodynamic fields is the Müller-Israel-Stewart (MIS) theory [126–128], in its modern incarnation described in Ref. [10, 129] (BRSSS). This approach parametrises dominant contributions classified by symmetries and the number of gradients. It does not make any special assumptions about the microscopic dynamics, which accounts for its generality. A major advantage of this

approach is that the resulting equations are causal at least for some domain in the space of transport coefficients.

If we commit to a specific microscopic model, we gain the option of deriving (at least in a heuristic way) a set of hydrodynamic equations which can provide a better physical picture than a generic approach such as the MIS/BRSSS theory. An important testbed for this idea is provided by kinetic theory with an idealized collision kernel, see Sec. 3.3.3. In this case a number of complementary approaches exist, which we now briefly review.

One important approach developed on the context of kinetic theory makes use of the *hydrodynamic expansion* of Ref. [130–132]: this is the process of constructing dynamical hydrodynamic equations by making an expansion order by order in the Knudsen and inverse Reynolds numbers. The hydrodynamic expansion is performed around the local equilibrium state that corresponds to the perfect-fluid limit $T_{\text{eq}}^{\mu\nu}$. The Knudsen number is the ratio of the molecular mean free path length to a representative physical length scale. On the other hand, the inverse Reynolds number describes deviations of the energy-momentum components from their local equilibrium values — they are typically expressed by the ratios $\sqrt{\pi^{\mu\nu}\pi_{\mu\nu}}/P$ and Π/P. The hydrodynamic expansion serves as a tool to systematically derive hydrodynamic equations from kinetic theory.

Another approach to the task of formulating a closed set of hydrodynamic equations for models of kinetic theory is known under the name of anisotropic hydrodynamics [133, 134] (for a recent review see [135]). This name originated in the desire of finding hydrodynamic equations suited to describing early stages of evolution of QGP produced in heavy-ion collisions. Equations of anisotropic hydrodynamics were formulated in such a way as to capture some features of highly anisotropic initial states, but also to ensure that at late times their predictions should be consistent with MIS/BRSSS. In modern formulations, the equations of anisotropic hydrodynamics are suitable for studying arbitrary flows.

6.5 Müller-Israel-Stewart (MIS) theory

The simplest example of a theory of relativistic hydrodynamics where no causality violations appear (at least at the linearized level) is MIS theory, which adds a single purely damped non-hydrodynamic degree of freedom. This is done by replacing the Navier-Stokes form of the shear-stress tensor (see Eq. (6.13)) by an independent field satifying a relaxation equation of the form [126–128]

$$(\tau_\pi U^\alpha \partial_\alpha + 1)\,\pi^{\mu\nu} = -\eta\,\sigma^{\mu\nu}, \tag{6.18}$$

where τ_π is a new parameter called the relaxation time. Equation (6.18) guarantees that at late times the shear stress will tend to the Navier-Stokes form Eq. (6.13) – this point will be made

much more explicit below (in Sec. 7). At the same time, it introduces new modes of propagation and alters the dispersion relations in a way which renders the propagation velocity finite.

The relaxation equation described in Ref. [128] include some additional terms with additional transport coefficients. In fact, a number of variants of the MIS equations have been written down and applied to QGP evolution – these will be reviewed in Sec. 8. For simplicity of presentation we will focus on the case of conformal hydrodynamics, which is also interesting for comparison with the results of holographic calculations. For a conformal theory in Minkowski spacetime the energy-momentum tensor must be traceless, which requires a conformal equation of state, vanishing of the bulk viscous pressure and tracelessness of the shear-stress tensor. These features much be preserved under time evolution, which requires augmenting Eq. (6.18) by additional terms. The simplest way to present the resulting equation is to realize that the additional terms complete the spacetime derivative in Eq. (6.18) to a Weyl-covariant derivative denoted by $\mathcal{D}$:

$$\left(\tau_\pi U^\alpha \mathcal{D}_\alpha + 1\right) \pi^{\mu\nu} = -\eta \sigma^{\mu\nu}. \tag{6.19}$$

The explicit form of the derivative $\mathcal{D}$ is given in Sec. E. Its main feature is that it preserves the tracelessness and transversality of the shear stress tensor under time evolution. We will refer to equation (6.19) as the conformal MIS equation.

Modes of this theory have been worked out in Ref. [10] (see also Ref. [4]). Note that this analysis is not sensitive to the presence of the additional terms present in BRSSS theory (discussed below in Sec. 7.4). As discussed in Sec. 3.1 and assuming momentum aligned with the x^3-direction, one obtains three channels (we just list independent components):

- scalar channel: non-vanishing $\delta\pi^{12}$;

- shear channel: non-vanishing δu^a and $\delta\pi^{3a}$ with $a = 1, 2$;

- sound channel: non-vanishing δT, δu^3, $\delta\pi^{33}$.

For example, in the sound channel one obtains the following equation for modes:

$$\omega^3 + \frac{i}{\tau_\pi}\omega^2 - \frac{k^2}{3}\left(1 + 4\frac{\eta/\mathcal{S}}{T\,\tau_\pi}\right)\omega - \frac{ik^2}{3\tau_\pi} = 0. \tag{6.20}$$

For small k one finds a pair of hydrodynamic modes (whose frequency tends to zero with k)

$$\omega_\mathrm{H}^{(\pm)} = \pm\frac{k}{\sqrt{3}} - \frac{2i}{3\,T}\frac{\eta}{\mathcal{S}}\,k^2 + \dots \tag{6.21}$$

and a single transient mode

$$\omega_{\text{NH}} = -i \left(\frac{1}{\tau_\pi} - \frac{4}{3} \frac{\eta}{T} \frac{\eta}{S} k^2 \right) + \dots \tag{6.22}$$

The dominant mode at long wavelengths is the one whose imaginary part is the least negative, so at large distances the hydrodynamic modes dominate.

Using the dispersion relation Eq. (6.20) we can calculate the speed of propagation of linear perturbations. The result is

$$v = \frac{1}{\sqrt{3}} \sqrt{1 + 4 \frac{\eta/S}{T \tau_\pi}}, \tag{6.23}$$

This formula implies that as long as the relaxation time is sufficiently large,

$$T \tau_\pi > 2\eta/S, \tag{6.24}$$

there is no transluminal signal propagation. This is clearly not the case if one tries to eliminate the relaxation time by taking it to vanish.

6.6 The non-hydrodynamic sector as a regulator

The presence of transient modes is essential for the consistency of the hydrodynamic description in the relativistic case. The success of relativistic hydrodynamics in describing the dynamics of QGP can be ascribed to the exponential decay of these modes, which leads to the fast emergence of quasiuniversal, attractor behaviour of this system [19, 136]. This will be discussed in detail in Sec. 7.4; here we wish to focus on another aspect: the inequality Eq. (6.24) suggests that the non-hydrodynamic sector of relativistic hydrodynamics should be thought of as a regulator, ensuring that the speed of propagation does not exceed the speed of light.

This regulator cannot be removed, but its effects may or may not be practically significant in the regime of interest. It is important to understand when these effects may be ignored, otherwise one may be studying the physics of the regulator rather than universal hydrodynamic behaviour. This is certainly the case at very early times. It may also be an issue in the case of small systems [137, 138], where it may happen that the non-hydrodynamic modes do not have time to decay and hydrodynamic simulations become sensitive to the choice of the non-hydrodynamic sector – that is, to the choice of regulator.[14]

One can try to make this a little more quantitative by writing down explicitly the condition for

---

[14]One can think of the regulator sector as an analogue of the notion of a "UV-completion", which arose in the context of effective field theories.

the non-hydrodynamic mode to be subdominant using Eq. (6.20). This leads to the condition [138]

$$RT > 2\pi\sqrt{2(T\tau_\pi)(\eta/\mathcal{S})} \ . \tag{6.25}$$

where R is the spacial extent of the system. The violation of this bound, crude as it is, is an indication that the regulator sector cannot be ignored. The interesting point is that for reasonable values of the parameters this bound translates into a rather weak condition on the final charged particle multiplicity

$$\left(\frac{dN}{dY}\right)_{MIN} \approx 3 \ . \tag{6.26}$$

which is consistent with another (but related) line of reasoning developed in Ref. [137]. This conclusion makes it less surprising that relativistic hydrodynamics is successful not only in describing heavy ion collisions, but also for tha case of pA, or even pp collisions.

If the bound Eq. (6.25) is violated, it may be necessary to compare different regulators. Examples of hydrodynamic theories with a qualitatively different non-hydrodynamic sector were discussed in Ref. [20] and will be reviewed in Sec. 7.5 below.

7 Hydrodynamics as an effective theory – insights from holography

As stressed in Sec. 6.1, once dissipative effects are incorporated within a hydrodynamic framework, one loses the universality of perfect fluid theory, and many different sets of hydrodynamic equations are possible. This raises the question of how they are to be compared, and how they can be reconciled with computations carried out directly in the microscopic theory. In this Section we argue that a useful way to proceed is to compare the gradient expansion of a microscopic theory with the gradient expansion generated from hydrodynamic models. This way one can try to mimic the hydrodynamic behaviour of the microscopic theory in a systematic, quantitative way. Throughout this Section we assume conformal invariance, apart from Sec. 7.3. The reasons for this are twofold. From the point of view of holography this allows us to focus on its most complete and best understood instance. The second reason is simplicity: the assumption of conformality restricts the number of terms appearing in hydrodynamic equations in a significant way.

7.1 The gradient expansion as an infinite series

We have seen is Sec. 6 that causal theories of relativistic hydrodynamics are constructed in such a way as to reproduce at late times the approach to equilibrium captured by the Navier-Stokes terms. Indeed, solving Eq. (6.19) by iteration starting from the Navier-Stokes term one obtains

a formal solution in the form of an infinite series graded by the numer of spacetime gradients

$$\pi^{\mu\nu} = -\eta\sigma^{\mu\nu} + \tau_\pi U^\alpha \partial_\alpha \left(\eta\sigma^{\mu\nu}\right) + \dots \tag{7.1}$$

For the case of BRSSS theory this expansion will be discussed at length in Sec. 7.4. The point we wish to make here is that the gradient expansion of the energy-momentum tensor in causal theories of hydrodynamics contains an infinite number of terms. These expansions arise as a generic late-time solution. Given the set of evolution equations for the shear stress tensor, we can always find such a solution explicitly by writing down the most general gradient series consistent with Lorentz symmetry (and any other constraints, such as perhaps conformal invariance), and determine the scalar coefficient functions by using the evolution equation order by order in gradients. This leads to a formal, infinite series expansion in powers of gradients of the fluid variables $T(x)$ and $U^\mu(x)$:

$$T^{\mu\nu} = T^{\mu\nu}_{\text{eq}} + \text{powers of gradients of } T \text{ and } U^\mu. \tag{7.2}$$

By comparing such formal solutions, one may quantify differences between different hydrodynamic theories [139]. It is important to note at this point, that at each order in the number of gradients there is a finite number of terms which can appear in Eq. (7.2). These terms are of course subject to the constraints of Lorentz covariance, and possibly other symmetries, such as conformal symmetry. The terms which can appear in Eq. (7.2) have been classified up to second [10, 120] and third [140] orders in gradients.

Crucially, an infinite expansion of the form of Eq. (7.2) also arises in microscopic theories. We have already seen this implicitly in Sec. 5 for the special case of Bjorken flow, where we in fact referred to the large-w expansion as the gradient expansion. We can now fully justify using this term: once we recognize that for Bjorken flow, see e.g. Eq. (D.1),

$$\partial_\mu U^\mu = \frac{1}{\tau}$$

we can see that w is the only dimensionless quantity of order one in the gradient expansion which is consistent with boost invariance:

$$\frac{1}{T} \partial_\mu U^\mu = \frac{1}{w}.$$

This shows that the large-w expansion is in fact precisely the gradient expansion for the special case when boost-invariance is imposed. This also shows that the gradient expansion is a partial resummation of the large proper-time expansion of Bjorken flow.

This example shows explicitly that the gradient expansion of the energy-momentum tensor expectation value in a microscopic theory contains an infinite series of terms. Comparing such a microscopic calculation to the gradient solution of a given hydrodynamic model provides a definite and unique way to relate the parameters of the hydrodynamic theory to those of an underlying theory. From this perspective we might say that phenomenological theories of hydrodynamics can be viewed as theoretical devices constructed in such a way as to reproduce the gradient expansion of a given microscopic theory to some order in gradients.

7.2 Matching MIS to holography and BRSSS theory

A beautiful illustration of these ideas is fluid-gravity duality [102]: the relationship between the near-equilibrium behaviour of hCFT plasma, or more generally hQFT plasma, and a generalisation of MIS theory. This is in fact a direct extension of the large proper-time expansion to general flows. The basic insight appears already Ref. [94], which observed that the leading hydrodynamic effect corresponds to a "slow" dependence of the black-brane horizon on the proper time see also Sec. 9.2.1. In a general setting this suggests looking for solutions in which the horizon position in the bulk of spacetime is allowed to depend on the boundary spacetime position x. The key insight of Ref. [102] was to consider a boost and dilation of the black brane solution given by Eq. (4.9) and to allow the boost and dilation parameters to depend on x in a smooth way. This naturally leads to a solution of the Einstein equations which takes the form of an expansion in the gradients of the x-dependent parameters of the solution. Remarkably, at each order of this gradient expansion, the constraint equations among Einstein's equations (4.5) take the form of conservation laws for the boundary energy-momentum tensor, which has the form of a gradient expansion in the boost and dilation parameters. The holographic dictionary, see Eq (4.6), therefore leads to a form of the expectation value of the energy-momentum tensor in a hCFT which has the form of a gradient expansion in local temperature (the dilation parameter) and 4-velocity (the boost parameters). The result of this holographic calculation is consistent with what one a priori could have expected based only on the symmetries of the problem. Indeed, all the terms which can appear in such calculations in relativistic conformal hydrodynamics have been classified [10]:

$$
\begin{aligned}
\pi^{\mu\nu} &= -\eta\sigma^{\mu\nu} + \eta\tau_\pi \mathcal{D}\sigma^{\mu\nu} + \kappa\left(R^{\langle\mu\nu\rangle} - 2U_\alpha R^{\alpha\langle\mu\nu\rangle\beta}U_\beta\right) \\
&+ \lambda_1 \sigma^{\langle\mu}{}_\lambda \sigma^{\nu\rangle\lambda} + \lambda_2 \sigma^{\langle\mu}{}_\lambda \Omega^{\nu\rangle\lambda} + \lambda_3 \Omega^{\langle\mu}{}_\lambda \Omega^{\nu\rangle\lambda} + \dots ,
\end{aligned} \tag{7.3}
$$

where η, τ_π, κ, λ_1, λ_2 and λ_3 are scalar functions of the effective temperature, the ellipsis denotes terms with 3 and more derivatives of fluid velocity, temperature and background metric and

$\mathcal{D}\sigma^{\mu\nu}$ stands for

$$\mathcal{D}\sigma^{\mu\nu} = \langle D\sigma^{\mu\nu}\rangle + \frac{1}{d-1}\sigma^{\mu\nu}(\partial_\alpha u^\alpha). \tag{7.4}$$

The form of Eq. (7.3) is a consequence of Lorentz and conformal symmetries, as well as a choice of integration constants which is equivalent to a choice of frame in hydrodynamics (see e.g. Ref. [141]).

In conformal theories, the only equilibrium scale is set by the temperature and the non-trivial theory-dependent content of thermodynamic quantities and transport coefficients η, τ_π, κ, λ_1, λ_2 and λ_3 sits in their dimensionless combinations with appropriate powers of the local temperature (or, equivalently, the entropy density s):

$$
\begin{aligned}
\eta &= C_\eta\, \mathcal{S}, & \tau_\pi &= \frac{C_{\tau_\pi}}{T}, & \kappa &= C_\kappa \frac{\eta}{T} \\
\lambda_1 &= C_{\lambda_1}\frac{\eta}{T}, & \lambda_2 &= C_{\lambda_2}\frac{\eta}{T}, & \lambda_3 &= C_{\lambda_3}\frac{\eta}{T},
\end{aligned}
\tag{7.5}
$$

The relevant dimensionless constants for $\mathcal{N} = 4$ SYM in the holographic regime read Ref. [102]:

$$
\begin{aligned}
C_\eta &= \frac{1}{4\pi}, & C_\kappa &= \frac{1}{\pi}, & C_{\tau_\pi} &= \frac{2-\log(2)}{2\pi}, \\
C_{\lambda_1} &= \frac{1}{2\pi}, & C_{\lambda_2} &= -\frac{\ln 2}{\pi}, & C_{\lambda_3} &= 0.
\end{aligned}
\tag{7.6}
$$

Assuming that one wants to model the late-time dynamics of, say $\mathcal{N} = 4$ SYM, using the conformal MIS equation, it would be natural to match the gradient expansion of the latter with Eq. (7.3) to a desired order in derivatives, e.g. to the second order. However, the gradient expansion of the conformal MIS equation (6.18) reads (up to second order in gradients)

$$\pi^{\mu\nu} = -\eta\sigma^{\mu\nu} + \eta\,\tau_\pi\,\mathcal{D}\sigma^{\mu\nu}. \tag{7.7}$$

Comparing the above to Eq. (7.3), we thus see that the expression (7.7) is not complete at second order, since it does not allow to account for all possible gradient structures which can appear. Indeed, as seen in Eq. (7.6), one cannot reproduce the result of the holographic calculation of Ref. [102] at second order in gradients by using MIS theory. The solution is to include more terms on the RHS of Eq. (6.18). The point made in Ref. [10] was that one needs modify the MIS relaxation equation (6.18) in such a way that it generates all second order terms admitted by symmetries with tunable coefficients. If that is ensured, then one is guaranteed to match any microscopic calculation up to second order.

Specifically, Baier et al. noted [10] that if one replaces $\sigma^{\mu\nu}$ by $-\pi^{\mu\nu}/\eta$ in some terms of

Eq. (7.3), one can rewrite that equation in a form which resembles Eq. (6.18):

$$\left(\tau_\pi U^\alpha \mathcal{D}_\alpha + 1\right)\pi^{\mu\nu} = -\eta\sigma^{\mu\nu} + \kappa\left(R^{\langle\mu\nu\rangle} - 2U_\alpha R^{\alpha\langle\mu\nu\rangle\beta}U_\beta\right) +$$
$$+ \lambda_1\pi^{\langle\mu}{}_\lambda\sigma^{\nu\rangle\lambda} + \lambda_2\pi^{\langle\mu}{}_\lambda\Omega^{\nu\rangle\lambda} + \lambda_3\Omega^{\langle\mu}{}_\lambda\Omega^{\nu\rangle\lambda} \tag{7.8}$$

The replacement of $\sigma^{\mu\nu}$ by $-\pi^{\mu\nu}/\eta$ which lead to Eq. (7.8) is allowed at first order in gradients due to Eq. (6.13). The resulting equation clearly generates the desired expansion Eq. (7.3) plus an infinite number of higher order terms with coefficients expressed in terms of the scalar functions already present in Eq. (7.3) and their spacetime derivatives. This particular way of turning the gradient expansion result of a microscopic calculation into an effective hydrodynamic evolution equation is not unique, but it guarantees matching up to second order in the gradient expansion. Other possibilities exist which coincide with the above up to second order, but differ at higher orders. At the level of the gradient expansion this may not be a significant issue, but the properties of the differential equations will be different and some may be more suitable than others for numerical evaluation and phenomenological applications.

Finally, let us comment briefly on the physics of shear viscosity in hQFTs. It has been understood very early on, see Ref. [142], that whenever a gravitational setup does not contain terms higher order in curvature, the ratio of shear viscosity to entropy density takes the universal value given by Eq. (7.6). This occurs for conformal and non-conformal hQFTs in any spacetime dimension, also when on the gravity side other than bulk metric fields are excited. This observation, together with other indications, has led to the famous conjecture that $1/4\pi$ is the lowest value of shear viscosity permitted in physics [49]. We know now due to Ref. [80] that this conjectured KSS bound is certainly violated in certain hCFTs whose gravity dual contains the Gauss-Bonnet term (4.7). In these cases, the shear viscosity is given by the exact[15] expression, see Ref. [79],

$$\frac{\eta}{\mathcal{S}} = \frac{1}{4\pi}\left(1 - 4\,\lambda_{GB}\right) \tag{7.9}$$

and Ref. [80] found a very specific class of hCFTs for which gravity duals are consistent and characterized by a very small positive λ_{GB}. The emerging picture is that viscosity in consistent holographic QFTs is very close to the famous result, but can be a tiny bit lower. How much lower than $1/4\pi$ $\eta/\mathcal{S}$ can get in a controllable setting and if any viscosity to entropy density bound actually exists do not really seem to be clear at the moment of writing this review.

---

[15]Since viscosity cannot get negative (otherwise one has an instability in the system), Eq. (7.9) explains why one should certainly not consider $\lambda_{GB} > \frac{1}{4}$.

7.3 Hydrodynamics without conformal symmetry

The point of departure for the arguments leading to the BRSSS evolution equation Eq. (7.8) was the observation expressed in Eq. (7.3), which encapsulates the information about the symmetries of the underlying microscopic theory, specifically Lorentz and conformal invariance. Conformal invariance offers significant constraints which greatly reduce the number of terms which can appear in Eq. (7.3) if only Lorentz covariance is imposed. Furthermore, for QGP the assumption of conformal symmetry is a reasonable one at temperatures above the chiral transition. However, this symmetry is an approximation which clearly has to be abandoned at lower temperatures, and Eq. (7.3) has to be replaced by a more general expansion. The terms which can appear after imposing Lorentz covariance alone have been classified Ref. [120]. Since there is a significant number of allowed terms (2 at first order and 15 at second order – compared to 1 and 5 respectively in the conformal case), it is hard, and probably impractical to try to include them all in a generalized MIS relaxation equation. The approach which has been adopted in practice has been to include only a subset of the terms allowed by symmetries. Indeed, in various practical applications of MIS theory to relativistic heavy ion collisions no single form of the relaxation equations has universally been adopted, with different authors using different sets of terms. The choice of this subset is sometimes motivated by consistency with microscopic models, especially in the framework of kinetic theory. Indeed, as reviewed in some detail in Sec. 8, there are rather sophisticated methods of motivating particular forms of the relaxation equations.

The hydrodynamic evolution equations may be viewed as a parametrisation of a stage of non-equilibrium dynamics which encapsulates conservation laws and the constraints of Lorentz symmetry. They are valid under very general conditions, regardless of whether quasiparticle excitations are present. In their gerneral form they guarantee matching the gradient expansion of any microscopic theory. At the same time, they can be used in a purely phenomenological manner, allowing a description of a rich spectrum of behaviours in terms of a finite number of transport coefficients. Since calculations of the transport coefficients directly from QCD are not available, practitioners often resort to intuitive choices of all the possible terms on the RHS of the shear stress tensor relaxation equation. One of the most popular versions of the MIS approach, which has been used frequently in phenomenological applications and is sometimes identified with the Israel-Stewart approach, is a system of two equations for the shear stress tensor and the bulk pressure [143–147],

$$D\pi^{\langle\mu\nu\rangle} + \frac{\pi^{\mu\nu}}{\tau_\pi} = -\beta_\pi \sigma^{\mu\nu} - \frac{\beta_\pi T}{2}\pi^{\mu\nu}\partial_\lambda\left(\frac{U^\lambda}{\beta_\pi T}\right), \tag{7.10}$$

$$D\Pi + \frac{\Pi}{\tau_\Pi} = -\beta_\Pi \theta - \frac{\beta_\Pi}{2}\Pi\,\partial_\lambda\left(\frac{U^\lambda}{\beta_\Pi T}\right), \tag{7.11}$$

where $D = U^\alpha \partial_\alpha$. The shear viscosity of the system, η, is given by the product of the shear relaxation time, τ_π, and the coefficient β_π, $\eta = \tau_\pi \beta_\pi$. Similarly, for the bulk viscosity we have $\zeta = \tau_\pi \beta_\Pi$.

It is interesting to consider Eq. (7.10) for the case of conformal systems, for which the bulk pressure and the bulk viscosity vanish, so the second equation is fulfilled trivially. Moreover, $\beta_\pi = 4\mathcal{P}/5$ and $\mathcal{E} = 3\mathcal{P}$. Calculating the gradients in the last term on the right-hand side of Eq. (7.10) and using the perfect-fluid equations for the expansion scalar θ we find

$$D\pi^{\langle \mu\nu \rangle} + \frac{\pi^{\mu\nu}}{\tau_\pi} \quad = \quad -\beta_\pi \sigma^{\mu\nu} - \frac{4}{3}\pi^{\mu\nu}\theta. \tag{7.12}$$

By comparing this equation with the MIS expression, see Eq. (6.18), we find that Eq. (7.12) includes one more term in the gradient expansion. However, there are still a number of possible second-order terms missing in Eq. (7.12). Moreover, Eq. (7.12) includes some terms which are of third order in gradients. Thus, even for conformal systems Eq. (7.12) is not of the same form as the BRSSS equations, even though their gradients expansions match up to second order.

Even though one may justify the specific form of hydrodynamic equations such as (7.10)–(7.11) on the basis of a microscopic model, they may be (and often are) used on their own, with values of the kinetic coefficients taken from other considerations. For example, a popular choice at the moment is to use the value of $\bar{\eta}$ suggested by holography, $\bar{\eta} = 1/(4\pi)$, or its multiple. Similarly, the equation of state is not necessarily taken as that of an ideal gas as in all CFTs but may follow from another type of calculations. In this case, one usually uses the QCD equation of state obtained from the lattice simulations [45] (if the systems at zero baryon chemical potential are considered). Recently, several attempts have been made to consistently include the QCD equation of state in the kinetic theory by using an effective, temperature dependent mass and introducing consistently the mean fields [148, 149]. Needless to say, Eqs. (7.10)–(7.11) with some parameterisation of the kinetic coefficients can be used in order to determine them directly from the experiment [150, 151].

7.4 Bjorken flow in BRSSS theory

It is very instructive to consider a restriction of the BRSSS equation Eq. (7.8) to Bjorken flow. The reason for this is that while the resulting equations are relatively simple, they provide a very explicit model where higher orders of the gradient expansion may be easily calculated and their significance can be directly explored. It can also usefully be regarded as a model of full, nonlinear dynamics where the interplay between hydrodynamic and non-hydrodynamic modes is in full view [19, 152]. This attitude is natural if one views theories of MIS type as "UV completions" of a purely hydrodynamic theory such as Navier-Stokes.

In the case of Bjorken flow described in Sec. 5.1, the BRSSS equations (7.8) reduce to the following, simple form

$$\tau \dot{\mathcal{E}} = -\frac{4}{3} \mathcal{E} + \phi \,,$$

$$\tau_\pi \dot{\phi} = \frac{4 \eta}{3 \tau} - \frac{\lambda_1 \phi^2}{2 \eta^2} - \frac{4 \tau_\pi \phi}{3\tau} - \phi \,,$$

(7.13)

where the dot denotes a proper time derivative and $\phi \equiv -\pi_y^y$, is the single independent component of the shear stress tensor [10].

Combining Eq. (7.13) with Eq. (7.5) one can derive a single second order equation for the energy density, or equivalently the temperature [19]:

$$C_{\tau_\pi} \tau \ddot{T} + \frac{3}{2}\tau \left(\frac{C_{\lambda_1} \tau}{C_\eta} + \frac{2 C_{\tau_\pi}}{T} \right) \dot{T}^2 + \left(\frac{\tau \left(C_\eta + C_{\lambda_1} \right) T}{C_\eta} + \frac{11 C_{\tau_\pi}}{3} \right) \dot{T}$$
$$+ \frac{(2 C_\eta + C_{\lambda_1}) T^2}{6 C_\eta} - \frac{4 \left(C_\eta - C_{\tau_\pi} \right) T}{9} = 0.$$

(7.14)

To proceed further it is convenient to rewrite Eq. (7.14) in first order form. Introducing the dimensionless time variable w, see Eq. (5.8), and using Eq. (5.10) the evolution equation Eq. (7.14) (including the the terms proportional to C_{λ_1}) rewritten for the pressure anisotropy R takes the simple form

$$C_{\tau_\pi} w \left(1 + \frac{1}{12} R \right) R' + \left(\frac{1}{3} C_{\tau_\pi} + \frac{1}{8} \frac{C_{\lambda_1}}{C_\eta} w \right) R^2 + \frac{3}{2} w R - 12 C_\eta = 0,$$

(7.15)

where the prime denotes a derivative with respect to w. Equations (5.8), (5.10) and (7.15) are equivalent to Eq. (7.14) as long as the function $w(\tau)$ is invertible.

At large values of w (late times) we expect universal hydrodynamic behaviour. Eq. (7.15) indeed possesses a unique stable solution which can be presented as a series in powers of $1/w$

$$R(w) = 8 C_\eta \frac{1}{w} + \frac{16}{3} C_\eta \left(C_{\tau_\pi} - C_{\lambda_1} \right) \frac{1}{w^2} + O\left(\frac{1}{w^3} \right).$$

(7.16)

This is precisely of the form of the gradient expansion Eq. (5.11) discussed earlier at the microscopic level in Sec. 5.

It is easy to see that linear perturbations around this formal solution decay at late times exponentially on a time scale set by τ_π:

$$\delta R(w) \sim e^{-\frac{3}{2 C_{\tau_\pi}} w} w^{\frac{C_\eta - 2 C_{\lambda_1}}{C_{\tau_\pi}}} \left\{ 1 + O\left(\frac{1}{w} \right) \right\}.$$

(7.17)

This is in fact the short-lived mode introduced by the MIS prescription. In the language of the gravity dual to $\mathcal{N} = 4$ SYM, see Sec. 4.3, this would be an analogue of a transient QNM whose frequency is purely imaginary [18,20]. The factor $3/2$ difference in the frequency (decay rate) when the mode is considered on expanding background is attributed to the fact that the frequency at every instant of proper time τ depends on what then the local temperature is, see Refs. [18, 20, 153] for an extensive discussion of this point. The integral $\int_{\tau_0}^{\tau} d\tau' \, T(\tau')$ evaluated for the leading late time term from Eq. (5.7) gives $3/2 \, w$, which explains the exponent in Eq. (7.17). Extending this analysis to the first subleading term explains the possibility of power-law modification. The logic presented here applies to all conformal models and will become particularly important in Sec. 9.

These observations show that the term $\tau_\pi \, \mathcal{D}\pi^{\mu\nu}$ from which the C_{τ_π} coefficient originates plays simultaneously two a priori *different* roles in the BRSSS and related frameworks:

- it captures the purely hydrodynamic effect described by the second-order term $\tau_\pi \, \mathcal{D}\sigma^{\mu\nu}$;

- it controls the decay rate of a putative purely imaginary transient mode.

If the microscopic theory contains such a purely decaying excitation as the least damped non-hydrodynamic effect, this provides us with two (in general incompatible) possibilities: matching C_{τ_π} to the second order hydrodynamic transport coefficient or relating it to the decay rate of a transient mode. If the least damped non-hydrodynamic mode in the microscopic theory is not purely decaying, then MIS theory can only be useful once the effects of the transient mode dies away.

The presence of the exponentially decaying mode (7.17) suggests that at least for sufficiently large values of w Eq. (7.15) possesses an attractor solution which the gradient expansion is trying to approximate. As we will see in Sec. 9 the gradient expansion has to be interpreted appropriately for this to be successful.

The existence of the hydrodynamic attractor in Eq. (7.15) is supported by examining the behaviour of generic numerical solutions of Eq. (3.6), with initial conditions set at various values of w. Examining the behaviour of R for w close to zero analytically, one finds two solutions, one of which is stable

$$R(w) = 6\sqrt{\frac{C_\eta}{C_{\tau_\pi}}} + O(w). \tag{7.18}$$

By setting the initial value of R at small w which is arbitrarily close to Eq. (7.18), the attractor can be determined numerically with the result shown in Fig. 8.

Note also, that one can determine the attractor by using a scheme similar to the slow-roll expansion used in inflationary cosmology, see e.g. Ref. [154], in which case one at first solves
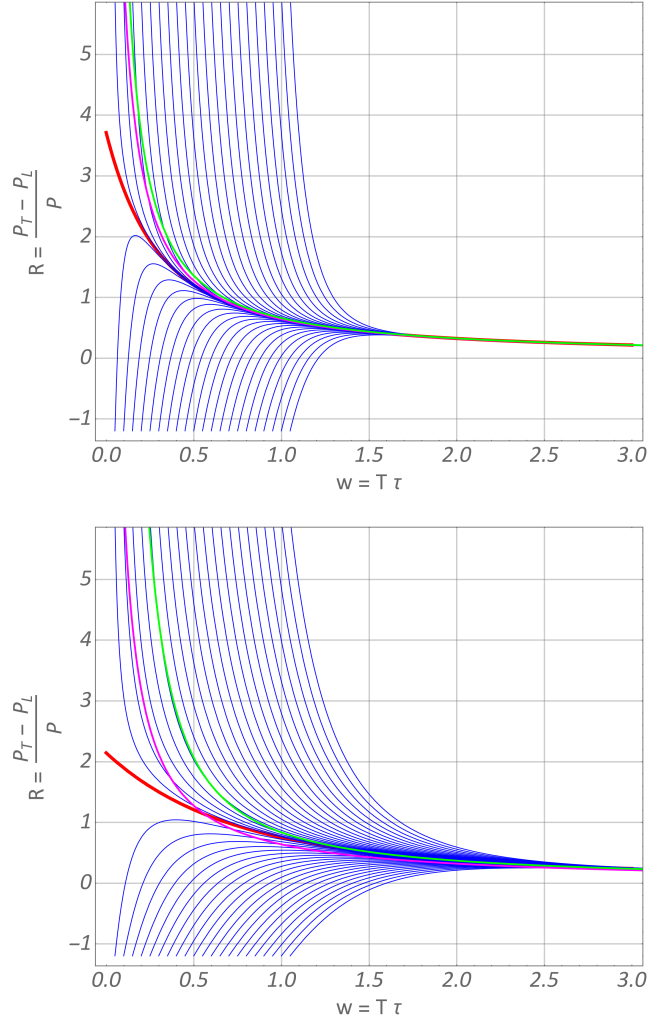
Figure 8: Numerical solutions of Eq. (7.15) for various initial conditions are represented by blue line. They asymptote to the numerically determined attractor solution given by the red line. The magenta, dashed and green, dotted lines are approximations to the attractor given by the hydrodynamic gradient expansion truncated at first and second order in derivatives respectively. The upper plot was made using parameter values appropriate for $\mathcal{N} = 4$ SYM, while the lower plot has the relaxation time increased by a factor of 3.

Eq. (7.15) by neglecting the R' term and then one accounts for it iteratively [19]. At leading order this gives

$$R(w) = \frac{6C_\eta \left(\sqrt{64C_\eta C_{\tau_\pi} + 24C_{\lambda_1} w + 9w^2} - 3w \right)}{8C_\eta C_{\tau_\pi} + 3C_{\lambda_1} w}. \qquad (7.19)$$

The resulting series provides then an alternative to the standard hydrodynamic gradient expansion, in particular it does not break down at $w = 0$.

As seen in Fig. 8, a generic solution rapidly decays to the attractor. Furthermore, the attractor appears to persist even at very small values of w, where the truncated gradient expansion cannot be reliable but slow-roll approach works well. Perhaps unsurprisingly, truncating Eq. (7.16) at first or second order gives results distinctly different from the attractor at very small w, but the difference becomes negligible at larger values of w. The magnitude of the difference depends on the values of the transport coefficients. Assuming $\mathcal{N} = 4$ SYM parameter values, we see that adopting just the viscous hydrodynamics constitutive relations provides a remarkably good approximation to the attractor for a wide range of w. In particular, this holds with an error smaller than 10% for $w > 0.5$.

It is tempting to propose that the hydrodynamic attractor constitutes the definition of hydrodynamic behaviour: it is the universal solution to which the system tends as transient non-hydrodynamic modes decay. Recent results of Ref. [136] indicate the presence of an attractor solution for boost-invariant expansion in the RTA kinetic theory and in holography, which significantly strengthens the case for this idea. At the moment of writing this review, it remains to be seen how this putative attractor would manifest itself when the conformal symmetry is broken or for more complicated flows.

7.5   Beyond BRSSS: HJSW and transient oscillatory behaviour

BRSSS theory includes the minimal regulator sector necessary to ensure causality. However, given some information about the non-hydrodynamic sector of a specific microscopic theory of model one may try to mimic it at the level of an effective hydrodynamic theory. Heuristic arguments given in Ref. [20], and earlier in Ref. [17, 155], suggest modifying the dynamics of the shear-stress tensor, which in MIS theory and similar frameworks is governed by relaxation equations such as Eq. (6.18). This is of interest if one aims to describe phenomena where the non-hydrodynamic sector is not subdominant, such as for example early time dynamics or the behaviour of small systems. One may hope that by including a more faithful representation of the non-hydrodynamic sector at least some transient effects of non-hydrodynamic modes can be captured. For some observables (such as the final multiplicities) this may not be quantitatively important. However for observables sensitive to the pre-equilibrium stages of evolution (such

as photon [156, 157] or dilepton emission [158, 159]) capturing the early time dynamics may be valuable.

The goal of this Section is to review an attempt to capture the dynamics of the least damped non-hydrodynamic modes of $\mathcal{N} = 4$ SYM plasma based on studies of AdS Schwarzschild black-brane QNMs and to incorporate them in an extension of the hydrodynamic framework. The basic observation is that in $\mathcal{N} = 4$ SYM and most other holographic strongly-coupled QFTs the least damped transient modes are oscillatory. The idea is then to generalize the BRSSS framework to try to capture not only the effects of viscosity, but also some of the effects of the least-damped oscillatory transient excitation. It is not obvious that this idea can be successful: if the least damped non-hydrodynamic modes are not clearly separated from others, then one has to accept that the hydrodynamic description can only be useful after the non-hydrodynamic sector has decayed.

The simplest way to incorporate additional non-equilibrium degrees of freedom into a causal (and hyperbolic) description is to set

$$\pi^{\mu\nu} = \pi^{\mu\nu}_{MIS} + \tilde{\pi}^{\mu\nu}$$

with $\pi^{\mu\nu}_{MIS}$ satisfying Eq. (6.19) and $\tilde{\pi}^{\mu\nu}$ obeying a second order equation designed to reproduce the damped-oscillatory behaviour of transient QNMs:

$$(\frac{1}{T}\mathcal{D})^2\,\tilde{\pi}_{\mu\nu} + 2\,\Omega_I\,\frac{1}{T}\,\mathcal{D}\,\tilde{\pi}_{\mu\nu} + |\Omega|^2\,\tilde{\pi}_{\mu\nu} = 0, \tag{7.20}$$

where $|\Omega|^2 \equiv \Omega_I^2 + \Omega_R^2$. This is formally the equation of motion of a damped harmonic oscillator. To match the least-damped QNMs of $\mathcal{N} = 4$ SYM plasma one needs to choose the parameter Ω appropriately. For example, in the case of interest, i.e. the energy-momentum tensor operator, at vanishing momentum $\mathbf{k}$ one has in all channels the following leading transient QNMs frequency [53, 160]:

$$\frac{1}{T}\,\omega\Big|_{k=0} = \pm\Omega_R - i\,\Omega_I \approx \pm 9.800 - i\,8.629. \tag{7.21}$$

Although the frequency of this mode (and, in fact, of any other mode) depends on momentum $\mathbf{k}$, as explicit results discussed in Sec. 4.3 and displayed in Fig. 4, this dependence is weak for a whole range of momenta around zero. Neglecting this dependence is thus a justified approximation. Furthermore, the use of Weyl-covariant derivatives here ensures that the evolved shear-stress tensor remains transverse and traceless. These two traceless and transverse quantities, $\tilde{\Pi}^{\mu\nu}_{MIS}$ and $\tilde{\Pi}^{\mu\nu}$, are coupled together by the conservation law of the energy-momentum tensor.

The resulting theory satisfies the same causality and stability properties as the MIS formula-

tion. At the linearized level, in addition to the standard hydrodynamic modes it contains the damped modes which resembles the transient QNM seen in holography. However, in addition we still the purely decaying MIS mode, which is spurious from the perspective of reproducing the pattern seen in holographic plasma.

An alternative which disposes of the MIS mode altogether is to abandon the relaxation equation such as Eq. (6.18) entirely and adopt the following second order equation for the shear-stress tensor:

$$\left\{ \left(\frac{1}{T} \mathcal{D} \right)^2 + 2\,\Omega_I \, \frac{1}{T}\,\mathcal{D} + |\Omega|^2 \right\} \pi^{\mu\nu} = \eta \, |\Omega|^2 \, \sigma^{\mu\nu} - c_\sigma \, \frac{1}{T}\,\mathcal{D}\,(\eta\,\sigma^{\mu\nu}) + \ldots \qquad (7.22)$$

where the ellipsis denotes contributions of second and higher order in gradients. Of all possible second order terms only one term has been kept, with a coefficient c_σ. The key property of Eq. (7.22) is that linearization around an equilibrium background leads to a system of partial differential equations which is hyperbolic and causal for $0 \leq c_\sigma \leq 2\pi$. Requiring stability imposes further conditions on all parameters appearing in Eq. (7.22); unfortunately the values of $\eta/\mathcal{S}$ and $\Omega_{R,I}$ characteristic of $\mathcal{N} = 4$ SYM are outside the region of causality and stability. While these unstable modes appear far outside the range of applicability of the long wavelength description, for numerical calculations this is an issue. We will refer to the model based on Eq. (7.22) as the HJSW model.

Both schemes discussed above make no attempt to match the gradient expansion to second order: they only ensure that the first order matches. The rationale for this is that while viscosity is a critically important physical effect seen in QGP dynamics, the second order terms appearing in MIS theory and its generalizations such as BRSSS are more important for consistency and less for modelling actual physical processes.

Regardless of which of the two alternative dynamical descriptions one chooses, for practical applications to QGP dynamics one needs to develop an effective heuristic for setting initial conditions for the non-hydrodynamic modes. One of the possible approaches might be to extract these initial conditions from the early post-collision state following from the numerical simulations of [161] or [162].

The appearance of the second derivative in HJSW theory given by Eq. (7.22) leads to non-hydrodynamic modes which are not purely decaying, in contrast with what we saw in MIS (or BRSSS) theory. Indeed, the linearization of equations (6.12) and (7.22) around flat space reveals a pair of non-hydrodynamic modes with complex frequencies Ω and $\bar{\Omega}$.

As in the case of BRSSS it is very interesting to study Bjorken flow in this theory. Imposing boost-invariance, the hydrodynamic equations reduce to a third order ordinary differential equation for the temperature. Introducing new variables as in Eqs. (5.8) and (5.10) one can

rewrite it as a second order differential equation for the function $R(w)$:

$$a_1\, R'' + a_2\, R'^2 + a_3\, R' + 12\, R^3 + a_4\, R^2 + a_5\, R + a_6 = 0, \qquad (7.23)$$

where

$$
\begin{aligned}
a_1 &= w^2\, (R+12)^2, \\
a_2 &= w^2\, (R+12), \\
a_3 &= 12\, w\, (R+12)\, (R+3\, w\, \Omega_I), \\
a_4 &= 48\, (3\, w\, \Omega_I - 1), \\
a_5 &= 108\, \left(4\, C_\eta\, C_{\tau_\pi} + 3\, w^2\, \Omega^2\right), \\
a_6 &= -864\, C_\eta\, \left(2\, C_{\tau_\pi} + 3\, w\, \Omega^2\right).
\end{aligned}
\qquad (7.24)
$$

This is the analog of Eq. (6.18) of MIS theory. At large w, the corresponding hydrodynamic gradient expansion takes the form

$$R(w) = 8\, C_\eta\, \frac{1}{w} + \frac{16\, C_\eta\, (C_{\tau_\pi} + 2\, \Omega_I)}{3\, |\Omega|^2}\, \frac{1}{w^2} + \dots \qquad (7.25)$$

As expected, the first term, which encodes the shear viscosity, coincides with what one obtains in BRSSS theory, see Eq. (7.16), whereas the higher order terms are necessarily different.

At early times one finds a unique real power series solution of the form

$$R(w) = 4 + \frac{54\, C_\eta\, |\Omega|^2 - 48\, \Omega_I}{20 + 9\, C_\eta\, C_{\tau_\pi}}\, w + \dots \qquad (7.26)$$

By examining numerical solutions of Eq. (7.23) it is clear that (similarly to the case of MIS theory) this is the small w behaviour of an attractor solution valid in the entire range of w.

Since Eq. (7.23) is of second order, one must specify both R and R' at the initial value of w. As seen in Fig. 9, setting initial conditions at various values of w shows that the numerical solutions converge to the attractor. However, unlike in the MIS case, the numerical solutions do not decay monotonically, but oscillate around the attractor. Note that because the phase space is three-dimensional, a plot like Fig. 9 is a two-dimensional section of a proper phase-space picture.

The ultimate check of the theories reviewed in this Section is to compare the evolution of R as governed by them with the microscopic holographic computation for, e.g., the Bjorken flow. This requires setting the parameters to appropriate values, i.e. $\eta/\mathcal{S} = 1/4\pi$ and $\Omega_{R,I}$ as in Eq. (7.21). A sample comparison is presented in Fig. 10, which shows that the MIS approach
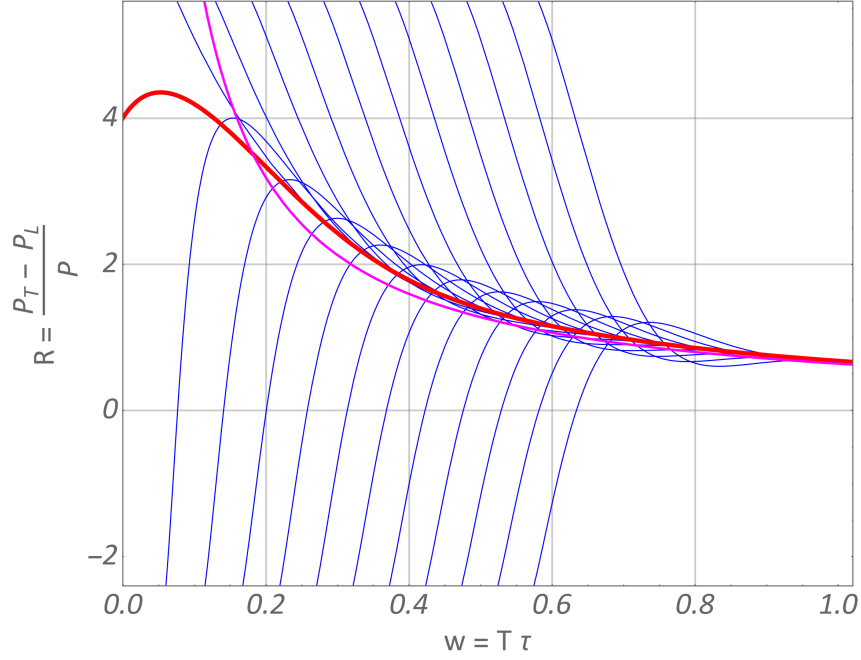
Figure 9: Numerical solutions of Eq. (7.23) are shown in blue; they converge (non-monotonically) to the numerically determined attractor (red). The magenta curve is the first order truncation of the gradient expansion.
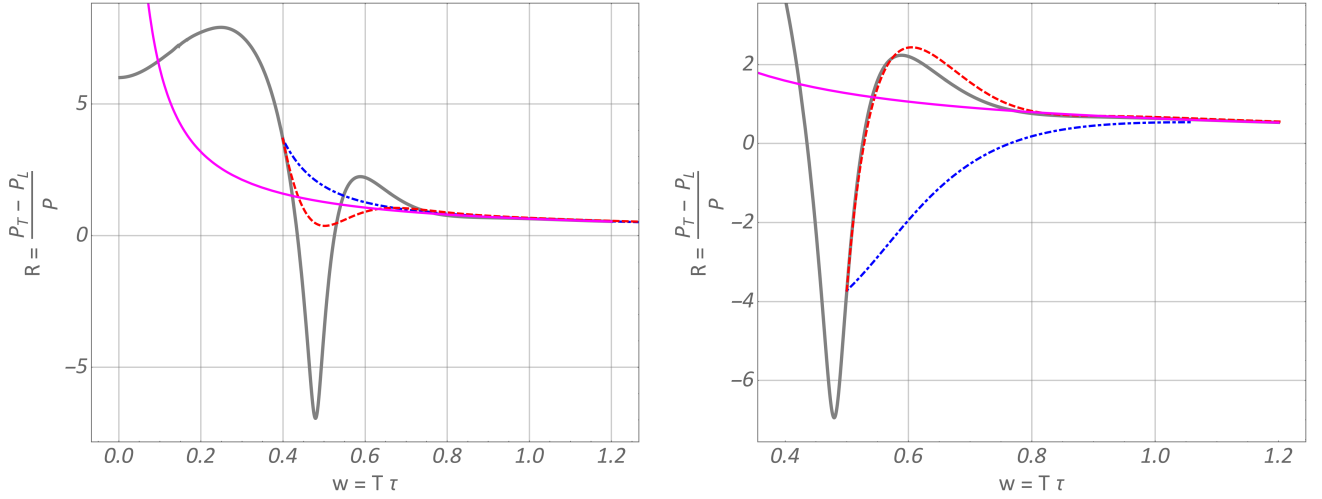
Figure 10: Comparing BRSSS ans HJSW: the blue dash-dotted curves are solutions of BRSSS theory while the red dashed curves are solutions of the HJSW equations. The grey curves represent numerical solutions obtained using holography. For reference, the prediction of first order hydrodynamics is displayed as the magenta curve. The plots show the results of setting initial conditions at $\tau T = 0.4$ (left), 0.5 (right). We see that the HJSW curve captures the oscillation missed by BRSSS.

captures the late time tail very well, as do the second order equations reviewed here. However, at earlier times Eq. (7.23) provides a much more accurate picture.

8 Hydrodynamics as an effective theory – insights from kinetic theory

The approach embodied in the BRSSS formulation of relativistic hydrodynamics is elegant from the theoretical perspective and completely general. Given a specific microscopic model it may however be possible to find a non-generic hydrodynamic description, which is crafted to reproduce that particular model. A significant body of work exists whose goal was to find such hydrodynamic descriptions of kinetic theory models. From the perspective of heavy-ion collisions such an approach is limited by our insufficient knowledge of an appropriate collision kernel for QCD and non-perturbative phenomena, but nevertheless this approach is an invaluable theoretical laboratory for studying relativistic hydrodynamics.

8.1 The gradient expansion in kinetic theory

In full analogy with the cases discussed in Secs. 7.2 and 7.3, the connection between kinetic theory models and effective hydrodynamic descriptions can be made by comparing gradient expansions. Indeed, the Boltzmann equation can be solved iteratively in a gradient expansion in a way similar to what was discussed in Sec. 5.3.1. The infinite series obtained this way is called the Chapman-Enskog expansion [16]. Depending on the collision kernel, the generated series will contain a subset (not necessarily proper) of all possible Lorentz covariant terms with specific coefficients. This can then be used to match generalised MIS equations such as Eq. (7.10) or Eq. (7.11). This matching determines the hydrodynamic transport coefficients much in the same way as in the case of holography in Sec. 7.2. If this is done for Eq. (3.20), one finds at first order that the shear viscosity coefficient η is connected with the relaxation time and entropy density $\mathcal{S}$. For classical statistics, one finds [67, 164]

$$\tau_{\text{rel}} = \frac{5\eta}{T\mathcal{S}} = \frac{5\bar{\eta}}{T}. \tag{8.1}$$

Here we have introduced the notation $\bar{\eta} = \eta/\mathcal{S}$ for the ratio of the shear viscosity and entropy density.

---

[16]Strictly speaking, the Chapman-Enskog method is introduced formally as an expansion in the Knudsen number, which is the ratio of the characteristic microscopic and macroscopic scales describing the system — see Ref. [132] where the case of a general collision term is discussed in this context. For the RTA kinetic equation, the Chapman-Enskog-like expansion has been introduced in Refs. [117, 163], which is based directly on the gradient expansion.

Equation (8.1) connects the relaxation time with the ratio $\eta/\mathcal{S}$. Thus, in this case, larger values of $\eta/\mathcal{S}$ lead to larger values of the relaxation time and, consequently, longer timescales for the decay of non-hydrodynamic modes (delayed hydrodynamization). This relation is a consequence of there being only a single parameter in the RTA collision kernel. We note however that results quantitatively consistent with Eq. (8.1) have been recently obtained in Ref. [62] in the context of scalar ϕ^4 theory.

Thus, starting from the gradient expansion of kinetic theory we can determine the transport coefficients appearing in the hydrodynamic equations, i.e., their dependence on temperature, chemical potential and the particle mass. In addition, the equation of state which follows from kinetic theory is known and corresponds typically to a gas of weakly interacting particles.

It is worth stressing – and is the subject of this section – that the approach outlined above is not the one most often used in practice in the context of kinetic theory. The standard approach is to write down a set of moments of the distribution function and impose an additional constraint in such a way as to obtain a closed differential equation of the MIS form. Various ways of carrying this out in practice are described below.

8.2 DNMR

The approach by Denicol, Niemi, Molnar and Rischke (DNMR) represents a general derivation of relativistic fluid dynamics from the underlying Boltzmann equation, with an arbitrary collision kernel, using the method of moments [130, 132, 165]. The authors derive first a general expansion of the distribution function $\delta f = f - f_{\text{eq}}$ in terms its irreducible moments. Then, the exact equations of motion for these moments are derived. It turns out, that there is an infinite number of such equations and, in general, one has to solve this infinite set of coupled differential equations in order to determine the time evolution of the system. The reduction of the number of equations is possible, however, if the terms are classified according to a systematic power-counting scheme in the Knudsen and inverse Reynolds numbers. As long as one keeps terms of second order (in both parameters) the equations of motion can be closed and expressed in terms of only 14 dynamical variables.

The simultaneous expansion in the Knudsen and inverse Reynolds numbers can be treated as a kind of *hydrodynamic expansion* that allows for a systematic derivation of hydrodynamic equations from the underlying kinetic theory. We wish to stress, however, the need to make a clear distinction between the gradient expansion discussed in this review and the hydrodynamic expansions treated as a means of deriving hydrodynamic equations. As we have showed so far, various methods exist for writing down hydrodynamic equations; once some set of hydrodynamic equations is found, one can look for their formal solutions in the form of a gradient expansion of the energy-momentum tensor as in Eq. (7.2). In particular, the gradient expansion can be
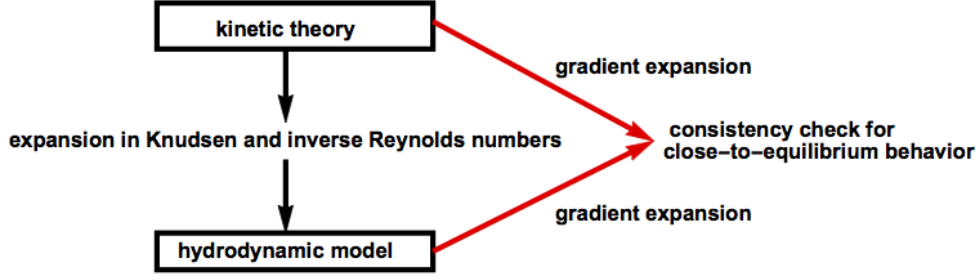
Figure 11: Schematic view of the hydrodynamics expansion that serves to obtain the hydrodynamic equations from the underlying kinetic theory by simultaneous expansion in the Knudsen and inverse Reynolds numbers. At the same time the gradient expansion can be used to check the agreement of the two approaches for close-to-equilibrium dynamics.

applied to both the underlying microscopic theory and the hydrodynamic model that serves as its approximation, in order to check the overall consistency between the two approaches, see Fig. 11.

For the case of the RTA kinetic equation, the DNMR formalism yields the following two equations for the bulk pressure and shear stress tensor

$$D\pi^{<\mu\nu>} + \frac{\pi^{\mu\nu}}{\tau_\pi} = -\beta_\pi \sigma^{\mu\nu} - 2\pi_\gamma^{<\mu}\omega^{\nu>\gamma} - \delta_{\pi\pi}\pi^{\mu\nu}\theta + \frac{1}{2}\tau_{\pi\pi}\pi_\gamma^{<\mu}\sigma^{\nu>\gamma} + \frac{1}{2}\lambda_{\pi\Pi}\Pi\sigma^{\mu\nu} \qquad (8.2)$$

and

$$D\Pi + \frac{\Pi}{\tau_\Pi} = -\beta_\Pi \theta - \delta_{\Pi\Pi}\Pi\theta - \frac{1}{2}\lambda_{\Pi\pi}\pi^{\mu\nu}\sigma_{\mu\nu}, \qquad (8.3)$$

where $\omega^{\mu\nu} = (1/2)(\nabla_\perp^\mu U^\nu - \nabla_\perp^\nu U^\mu)$ is the vorticity tensor ($\nabla_\perp^\mu = \Delta^{\mu\nu}\partial_\nu$). In the conformal limit the second equation is automatically fulfilled, while the coefficients appearing in the first equation are: $\delta_{\pi\pi} = 4/3$ and $\tau_{\pi\pi} = 10/7$. In the general, non-conformal case, it is interesting to observe that Eqs. (8.2) and (8.3) are directly coupled through the last terms appearing on their right-hand sides. The importance of such a shear-bulk coupling has been emphasised in [166].

8.3 Jaiswal's third order theory

In the case where the collision term in the kinetic equation is given by the relaxation-time form, see Eq. (3.20), the second and third order theory of viscous hydrodynamics has been worked recently out by Jaiswal, using the Chapman-Enskog-like expansion for the distribution function close to equilibrium [163, 167]. Separating the space-time gradient appearing in (3.20) into the

longitudinal and transverse part

$$\partial_\mu = g_{\mu\nu}\partial^\nu = (\Delta_{\mu\nu} - U_\mu U_\nu)\partial^\nu = \nabla_\mu^\perp - U_\mu D, \tag{8.4}$$

we can write

$$D\delta f = -\frac{\delta f}{\tau_{\text{rel}}} - Df_{\text{eq}} + \frac{1}{p \cdot U}p^\mu \nabla_\mu^\perp f, \tag{8.5}$$

where $\delta f = f - f_{\text{eq}}$ is the difference between the non-equilibrium distribution function and the reference equilibrium one. Similarly as in Eq. (5.21) we write $\delta f = f_0 + f_1 + f_2 + \cdots$, where the leading term f_0 is identified with the equilibrium distribution, $f_0 = f_{\text{eq}}$, and the next terms are obtained by consecutive differentiations of the previous terms, namely

$$f_1 = \frac{\tau_{\text{rel}}}{p \cdot U}p^\mu \partial_\mu f_0, \quad f_2 = \frac{\tau_{\text{rel}}}{p \cdot U}p^\mu \partial_\mu f_1, \quad \cdots \ . \tag{8.6}$$

As first shown in Ref. [165], the formula (8.5) can be used to find the exact equations satisfied by the shear and bulk pressures. For the shear sector in RTA one finds

$$D\pi^{<\mu\nu>} + \frac{\pi^{\mu\nu}}{\tau_{\text{rel}}} = -\Delta_{\alpha\beta}^{\mu\nu}\int dP\, p^\alpha p^\beta \left(Df_0 - \frac{1}{p \cdot U}p^\mu \nabla_\mu^\perp f\right). \tag{8.7}$$

In order that Eq. (8.7) is second-order in gradients, the distribution function on the right-hand side of (8.7) should be computed only up to the first-order in gradients, $f = f_0 + f_1$. In this way, for massless particles one derives the equation

$$D\pi^{<\mu\nu>} + \frac{\pi^{\mu\nu}}{\tau_{\text{rel}}} = -\beta_\pi \sigma^{\mu\nu} - 2\pi_\gamma^{<\mu}\omega^{\nu>\gamma} + \frac{5}{7}\pi_\gamma^{<\mu}\sigma^{\nu>\gamma} - \frac{4}{3}\pi^{\mu\nu}\theta. \tag{8.8}$$

In the transition from (8.7) to (8.8) one uses the first order relation $\pi^{\mu\nu} = -\eta\sigma^{\mu\nu}$ in order to remove the relaxation times on the right-hand side of (8.8). By comparing Eqs. (7.12) and (8.8) one finds that the last equation includes two more terms on the right-hand side, indicating that (7.12) is incomplete.

The strategy to find the third order equation is similar. In this case, the right-hand side of (8.7) is computed including the second-order terms, $f = f_0 + f_1 + f_2$, and Eq. (8.8) is used to replace $\sigma^{\mu\nu}$. For details of this procedure we refer to [163, 168]. It is worth noting, that comparing the gradient expansion generated by these third-order equations [139] with the gradient expansion obtained directly from kinetic theory in the RTA [118] one finds, as expected, that the third order contributions indeed match (see also Sec. 8.6).

71

8.4 Anisotropic hydrodynamics

We have discussed above, that standard viscous hydrodynamics is usually constructed as the expansion of the underlying microscopic kinetic theory in the Knudsen and inverse Reynolds numbers around the local equilibrium state [132]. This type of expansion may be questioned in the situation where space-time gradients and/or deviations from the local equilibrium are large. The goal of the anisotropic hydrodynamics program [133–135] is to create a framework of dissipative hydrodynamics that is better suited to deal with such cases and accurately describes several features such as: the early time dynamics of the QGP created in heavy-ion collisions, dynamics near the transverse edges of the nuclear overlap region, and temperature-dependent and possibly large shear viscosity to entropy density ratio $\bar{\eta}$.

8.4.1 Reorganized hydrodynamic expansion

In the standard approach to viscous hydrodynamics, the energy-momentum tensor components $T^{\mu\nu}$ may be treated as functions of T, U^μ, $\pi^{\mu\nu}$, and Π, which we write schematically as

$$
\begin{aligned}
T^{\mu\nu} &= T^{\mu\nu}\left(T, U^\mu, \pi^{\mu\nu}, \Pi\right) \\
&= T^{\mu\nu}_{\text{eq}}(T, U) + \pi^{\mu\nu} + \Pi\Delta^{\mu\nu} \\
&\equiv T^{\mu\nu}_{\text{eq}} + \delta T^{\mu\nu}.
\end{aligned}
\tag{8.9}
$$

The hydrodynamic equations that determine the dynamics of $T^{\mu\nu}$ contain various terms that may be characterised by the power of space-time gradients and/or the power of the dissipative terms (strictly speaking one considers the powers of the ratios $\sqrt{\pi^{\mu\nu}\pi_{\mu\nu}}/\mathcal{P}$ and $\Pi/\mathcal{P}$ which are known as the inverse Reynolds numbers). For example, in the first order of viscous hydrodynamics one deals with $\pi^{\mu\nu}$ and Π and also with the gradients of T and U^μ, see Eqs. (6.13). In the second order, the products of $\pi^{\mu\nu}$ and Π appear, as well as the gradients of $\pi^{\mu\nu}$ and Π. Such approach may be continued to higher orders but, in practical applications, one stops at the third order (see our discussion in Sec. 8.3).

Anisotropic hydrodynamics can be treated as a method to reorganize this kind of expansion within the framework of the kinetic theory. One uses the classical concept of the phase space distribution function $f(x, p)$ and expresses different physical quantities as the moments of $f(x, p)$ (in the three-momentum space).

Within AHYDRO one separates the description of dissipative effects into two parts. The first part is characterised by the new fluid variables $\xi^{\mu\nu}$ and ϕ, see Refs. [169–174]. They may account for large possible values of the shear stress tensor and bulk viscosity and should be treated in a non-perturbative manner, similarly to T and U^μ. The second part is characterised by the tensors $\tilde{\pi}^{\mu\nu}$ and $\tilde{\Pi}$ that are

treated similarly as $\pi^{\mu\nu}$ and Π in the standard case [175–178]. Thus, we write

$$
\begin{aligned}
T^{\mu\nu} &= T^{\mu\nu}\left(T, U^{\mu}, \xi^{\mu\nu}, \phi, \tilde{\pi}^{\mu\nu}, \tilde{\Pi}\right) \\
&= T_{\mathrm{a}}^{\mu\nu}(T, U^{\mu}, \xi^{\mu\nu}, \phi) + \tilde{\pi}^{\mu\nu} + \tilde{\Pi}\Delta^{\mu\nu} \\
&\equiv T_{\mathrm{a}}^{\mu\nu} + \delta\tilde{T}^{\mu\nu}.
\end{aligned}
\tag{8.10}
$$

At this point it is important to emphasize several issues:

- Introducing the fluid variables $\xi^{\mu\nu}$ and ϕ simultaneously with $\tilde{\pi}^{\mu\nu}$ and $\tilde{\Pi}$ implies that the "dissipative" degrees of freedom are "doubled" and we need more than typical ten hydrodynamic equations to determine dynamics of $T^{\mu\nu}$. This can be easily accomplished within kinetic theory approach by including, for example, a corresponding number of the moments of the kinetic equation. The choice of the moments is, however, not well defined. One takes into account usually the lowest possible moments [175], since they are most sensitive to the low momentum sector which is expected to be well described by hydrodynamics-like models. We come back to the discussion of this ambiguity below.

- The anisotropy tensor $\xi^{\mu\nu}$ has analogous geometric properties as the shear stress tensor $\pi^{\mu\nu}$, i.e., it is symmetric, transverse to U^{μ} and traceless [172–174]. This means that it has in general five independent components. However, in practical applications one often uses simplified versions of $\xi^{\mu\nu}$ that contain one or two independent parameters. In such cases only these degrees of freedom may be "doubled". We note that the use of simplified forms of $\xi^{\mu\nu}$ is very often a consequence of the system's symmetries such as boost invariance, homogeneity in the transverse plane or cylindrical symmetry. The tensor $\tilde{\pi}^{\mu\nu}$ is also symmetric, transverse to U^{μ} and traceless. Consequently, using the Landau frame, one can determine the effective temperature of the system T and the flow U^{μ} by the equation

$$
\mathcal{E}_{\mathrm{EQ}}(T(x)) U^{\mu}(x) = -T_{\mathrm{a}}^{\mu\nu}(x)U_{\nu}(x).
\tag{8.11}
$$

Since the substantial part of the viscous effects is included through the use of $\xi^{\mu\nu}$ and ϕ, one expects that the terms $\tilde{\pi}^{\mu\nu}$ and $\tilde{\Pi}$ are small compared to the equilibrium pressure $\mathcal{P}$. The expansion in the ratios $\sqrt{\tilde{\pi}^{\mu\nu}\tilde{\pi}_{\mu\nu}}/\mathcal{P}$ and $\tilde{\Pi}/\mathcal{P}$ is discussed in this context as an expansion in the modified inverse Reynolds numbers [175–178].

- Using the kinetic theory approach, Eq. (8.10) is reproduced with the distribution function that has a structure

$$
f(x, p) = f_{\mathrm{a}}(x, p) + \delta\tilde{f}(x, p).
\tag{8.12}
$$

Here $f_{\mathrm{a}}(x, p)$ is the anisotropic distribution function in the momentum space. It can be regarded as an extension of the equilibrium distribution $f_{\mathrm{eq}}(x, p)$, which depends not only on T and

U^μ but also on $\xi^{\mu\nu}$ and ϕ. In the limit $\xi^{\mu\nu} \to 0, \phi \to 0$ one finds that $f_{\rm a}(x,p) \to f_{\rm eq}(x,p)$. Several special forms of $f_{\rm a}(x,p)$ will be discussed below. In the *leading order of anisotropic hydrodynamics*, we neglect the corrections $\delta\tilde{T}^{\mu\nu}$ in (8.10) and $\delta\tilde{f}(x,p)$ in (8.12). Then, the complete energy-momentum tensor is given by the formula

$$T^{\mu\nu} = T_{\rm a}^{\mu\nu} = k \int dP \ p^\mu p^\nu f_{\rm a}(x,p), \tag{8.13}$$

where we have added a degeneracy factor k to account for internal degrees of freedom. In this case, the components of $T_{\rm a}^{\mu\nu}$ depend, in general, on ten independent parameters contained in the set: T, U^μ, $\xi^{\mu\nu}$ and ϕ. The equations of anisotropic hydrodynamics specify the dynamics of $T_{\rm a}^{\mu\nu}$. They include four equations that follow directly from the energy-momentum conservation law and additional six equations that should be derived from kinetic theory.

- Doubling of dissipative degrees of freedom can be avoided if the use of a certain parameter in the set $(\xi^{\mu\nu}, \phi)$ is accompanied with the elimination of some parameter in the set $(\tilde{\pi}^{\mu\nu}, \tilde{\Pi})$. For example, using the bulk parameter ϕ we may assume that $\tilde{\Pi} = 0$. The extreme strategy in this context is to assume that the parameters $\xi^{\mu\nu}$ and ϕ are chosen in such a way that

$$T^{\mu\nu} = T_{\rm a}^{\mu\nu}. \tag{8.14}$$

This formula represents the *anisotropic matching principle* introduced by Tinti [174]. We note that (8.14) looks exactly like (8.13), however, these two equations are obtained with different assumptions: instead of neglecting the term $\delta\tilde{f}(x,p)$ in (8.12) one assumes that $\delta\tilde{f}(x,p)$ might be finite but it does not contribute to $T^{\mu\nu}$.

We can now define the gradient expansion for the leading-order anisotropic hydrodynamics. Given $T(x)$ and $U^\mu(x)$ we construct $f_{\rm eq}(x,p)$ and $T_{\rm eq}^{\mu\nu}$ and write

$$T^{\mu\nu} = T_{\rm eq}^{\mu\nu} + \delta T^{\mu\nu} = T_{\rm eq}^{\mu\nu} + \left(T_{\rm a}^{\mu\nu} - T_{\rm eq}^{\mu\nu}\right). \tag{8.15}$$

This formula suggests to use the gradient expansion of anisotropic hydrodynamics in the form

$$T^{\mu\nu} = T_{\rm eq}^{\mu\nu} + \text{powers of gradients of } T, U^\mu, \xi^{\mu\nu} \text{and } \phi. \tag{8.16}$$

Compared to (7.2), the expansion (8.16) includes in addition the gradients of $\xi^{\mu\nu}$ and ϕ. On the other hand, similarly to (7.2), the expansion (8.16) should be done around the perfect-fluid solution that is determined solely by the conservation law.

8.4.2 Phenomenological vs. kinetic-theory formulation

The original concepts of anisotropic hydrodynamics were introduced in Refs. [133,134], see also [179,180]. The approach of Ref. [133] was based on the energy-momentum conservation law and used an ansatz for

the entropy source term which defined the off-equilibrium dynamics. On the other hand, the approach of Ref. [134] was based on the kinetic theory, and employed the zeroth and first moments of the RTA Boltzmann kinetic equation [66]. It was demonstrated in [181] that these two approaches are equivalent as the first moment of the Boltzmann equation yields the energy-momentum conservation law, while the zeroth moment can be interpreted as a special form of the entropy source.

The two original approaches describe boost invariant, transversally homogeneous systems and refer to the (quasi)particle picture, where the phase-space distribution function is given by the Romatschke-Strickland (RS) form [182]. In the covariant formulation, the latter takes the form

$$f_{\rm RS} = \frac{1}{(2\pi)^3} \exp\left(-\frac{1}{\Lambda} \sqrt{(p \cdot U)^2 + \xi \, (p \cdot Z)^2} \right), \tag{8.17}$$

where Λ is the transverse-momentum scale, ξ is the anisotropy parameter, while U and Z are the two four-vectors that define a simple boost-invariant geometry, $U = (t/\tau, 0, 0, z/\tau)$ and $Z = (z/\tau, 0, 0, t/\tau)$ with $\tau = \sqrt{t^2 - z^2}$ being the longitudinal proper time. The distribution function (8.17) leads to the following form of the energy-momentum tensor

$$T^{\mu\nu} = \mathcal{E} U^\mu U^\nu + \mathcal{P}_T \, \Delta^{\mu\nu} + (\mathcal{P}_L - \mathcal{P}_T) Z^\mu Z^\nu. \tag{8.18}$$

Within the kinetic-theory formulation, if we restrict ourselves to conformal, boost-invariant and cylindrically symmetric systems, the form of the hydrodynamic flow is fixed and the AHYDRO equations are reduced to two coupled ordinary differential equations for the anisotropy parameter ξ and the transverse-momentum scale Λ [134]. They read

$$\frac{1}{1+\xi}\frac{d\xi}{d\tau} = \frac{2}{\tau} - 4\,\Gamma\,\mathcal{R}(\xi)\,\frac{\mathcal{R}^{3/4}(\xi)\sqrt{1+\xi}-1}{2\mathcal{R}(\xi)+3(1+\xi)\mathcal{R}'(\xi)}, \tag{8.19}$$

$$\frac{1}{1+\xi}\frac{1}{\Lambda}\frac{d\Lambda}{d\tau} = \Gamma\,\mathcal{R}'(\xi)\,\frac{\mathcal{R}^{3/4}(\xi)\sqrt{1+\xi}-1}{2\mathcal{R}(\xi)+3(1+\xi)\mathcal{R}'(\xi)}. \tag{8.20}$$

Here the parameter Γ is proportional to the inverse relaxation time and $\mathcal{R}'(\xi) = d\mathcal{R}(\xi)/d\xi$. If we demand that Eqs. (8.19) and (8.20) describe the system with the same shear viscosity as that obtained directly from the RTA kinetic theory based on Eq. (5.18) we should use the relation [116]

$$\frac{1}{\Gamma} = \frac{\tau_{\rm rel}}{2}. \tag{8.21}$$

The function $\mathcal{R}(\xi)$, appearing in Eqs. (8.19) and (8.20), is defined as [134]

$$\mathcal{R}(\xi) = \frac{1}{2}\left(\frac{1}{1+\xi} + \frac{\arctan\sqrt{\xi}}{\sqrt{\xi}} \right). \tag{8.22}$$

In the analogous way we introduce

$$\mathcal{R}_T(\xi) = \frac{3}{2\xi}\left(\frac{1 + (\xi^2 - 1)\mathcal{R}(\xi)}{\xi + 1}\right)\tag{8.23}$$

and

$$\mathcal{R}_L(\xi) = \frac{3}{\xi}\left(\frac{(\xi + 1)\mathcal{R}(\xi) - 1}{\xi + 1}\right).\tag{8.24}$$

The functions $\mathcal{R}(\xi)$, $\mathcal{R}_T(\xi)$, and $\mathcal{R}_L(\xi)$ are used to relate the non equilibrium energy density and the two pressures, depending on ξ and Λ, to the equilibrium (isotropic) quantities computed at the temperature Λ, namely

$$\mathcal{E}(\xi, \Lambda) = \mathcal{R}(\xi)\mathcal{E}_{\text{iso}}(\Lambda),\tag{8.25}$$
$$\mathcal{P}_T(\xi, \Lambda) = \mathcal{R}_T(\xi)\mathcal{P}_{\text{iso}}(\Lambda),\tag{8.26}$$
$$\mathcal{P}_L(\xi, \Lambda) = \mathcal{R}_L(\xi)\mathcal{P}_{\text{iso}}(\Lambda).\tag{8.27}$$

If the anisotropy parameter vanishes, the scale parameter Λ coincides with the effective temperature T, while the two pressures become identical and equal to one third of the energy density. Since $3\mathcal{R} - 2\mathcal{R}_T - \mathcal{R}_L = 0$ and $\mathcal{E}_{\text{iso}} = 3\mathcal{P}_{\text{iso}}$, we also find $\mathcal{E} - 2\mathcal{P}_T - \mathcal{P}_L = 0$, as required for conformal systems.

8.4.3 Perturbative vs. non-perturbative approach

Subsequent developments of anisotropic hydrodynamics were based exclusively on the kinetic theory and they may be classified either as perturbative or as non-perturbative schemes.

- In the perturbative approach [175, 177, 178] one assumes that the distribution function has the form $f = f_{\text{RS}} + \delta f$, where f_{RS} is the leading order described by the RS form, which accounts for the difference between the longitudinal and transverse pressures, while δf describes a correction. In this case, advanced methods of traditional viscous hydrodynamics are used to restrict the form of δf and to derive hydrodynamic equations. In this way non-trivial dynamics may be included in the transverse plane and, more generally, in the full (3+1)D case.

- In the non-perturbative approach one starts with the decomposition $f = f_{\text{a}} + \delta f$, where f_{a} is the leading order distribution function given by the generalised RS form. In this case, all effects due to anisotropy are included in the leading order, while the correction term δf is typically neglected. The generalised RS form includes more parameters than the original RS ansatz, namely one uses the expression

$$f_{\text{a}} = f_{\text{iso}}\left(\frac{\sqrt{p^\mu \Xi_{\mu\nu} p^\nu}}{\lambda}\right),\tag{8.28}$$

where λ is the transverse momentum scale, $\Xi_{\mu\nu}$ is the anisotropy tensor and f_{iso} denotes the

isotropic distribution (in practice the equilibrium Boltzmann, Bose-Einstein or Fermi-Dirac distribution).

The structure of the generalised RS distribution together with the corresponding hydrodynamic equations have been gradually worked out for: (1+1)D conformal case [170] (with two independent anisotropy parameters), (1+1)D non-conformal case [171] (with two anisotropy parameters and one bulk parameter), and full (3+1)D case [172, 173] (five anisotropy parameters included in the tensor $\xi^{\mu\nu}$ and one bulk parameter ϕ). In the latter case, one uses the following parameterisation

$$\Xi^{\mu\nu} = U^\mu U^\nu + \xi^{\mu\nu} + \Delta^{\mu\nu}\phi,$$
$$U_\mu \xi^{\mu\nu} = 0, \quad \xi^\mu{}_\mu = 0. \tag{8.29}$$

The second line in (8.29) indicates that the symmetric tensor $\xi^{\mu\nu}$ is orthogonal to U^μ and traceless, thus has indeed five independent parameters. These properties are similar to those characterising the shear stress tensor $\pi^{\mu\nu}$ commonly used in the formalism of the standard dissipative hydrodynamics. As the matter of fact, $\pi^{\mu\nu}$ becomes proportional to $\xi^{\mu\nu}$ for systems approaching local equilibrium. Similarly, in this case the parameter ϕ becomes proportional to the bulk viscous pressure Π.

8.4.4 Anisotropic matching principle

To derive the hydrodynamic equations obeyed by the parameters $\xi^{\mu\nu}$ and ϕ one most often uses the moments of the RTA kinetic equation. The number of included moments is equal to the number of unknown parameters. An alternative for this approach is the procedure where one first derives, directly from the RTA Boltzmann equation, the equations for the pressure corrections $\pi^{\mu\nu}$ and Π, and expresses them by the function f_a. This is the latest development for the leading order, known as the anisotropic matching principle [174], that may be supplemented by next-to-leading terms following the perturbative approach [175, 177].

For conformal, boost-invariant, and transversely homogeneous systems the bulk parameter ϕ can be set equal to zero, while the tensor $\xi^{\mu\nu}$ has the structure

$$\xi^{\mu\nu} = \xi_T \left(X^\mu X^\nu + Y^\mu Y^\nu \right) + \xi_L Z^\mu Z^\nu, \tag{8.30}$$

where $X^\mu = (0, 1, 0, 0)$ and $Z^\mu = (0, 0, 1, 0)$. Then, the distribution function can be written as

$$f_\mathrm{a} = \exp\left(-\frac{E}{\lambda} \right), \tag{8.31}$$

where

$$E^2 = (1 + \xi_X)(p \cdot X)^2 + (1 + \xi_Y)(p \cdot Y)^2 + (1 + \xi_Z)(p \cdot Z)^2 \tag{8.32}$$

with $\xi_X = \xi_Y = \xi_T$ and $\xi_Z = \xi_L$. We note that Eqs. (8.31) and (8.32) with $\xi_X \neq \xi_Z$ represent a

77

generalized ellipsoidal parameterization of the anisotropic distribution function proposed first in [170]. The symmetries of $\xi^{\mu\nu}$ imply that the anisotropy parameters ξ_I introduced in (8.32) satisfy the condition [170]

$$\sum_I \xi_I = \xi_X + \xi_Y + \xi_Z = 0 \,. \tag{8.33}$$

Consequently, the parameterizations (8.17) and (8.31) are connected through the following set of simple transformations

$$
\begin{aligned}
\xi_X &= \xi_Y = \xi_T = -\frac{\xi/3}{1+\xi/3}, \\
\xi_Z &= \xi_L = \frac{2\,\xi/3}{1+\xi/3}, \\
\lambda &= \Lambda(1+\xi/3)^{-1/2}.
\end{aligned}
\tag{8.34}
$$

Using anisotropic matching principle introduced above, one obtains two coupled ordinary differential equations for the effective temperature T and the anisotropy parameter ξ,

$$4\,\frac{\mathcal{R}(\xi)}{T}\frac{dT}{d\tau} = -\frac{1}{\tau}\left(\mathcal{R}(\xi) + \frac{\mathcal{R}_L(\xi)}{3}\right) \tag{8.35}$$

and

$$\frac{d\,\Delta P}{d\tau} = -\frac{T\,\Delta P}{c} - \frac{F}{\tau}, \tag{8.36}$$

Here ΔP is the difference of the longitudinal and transverse pressures. Using definitions given in [174] one finds that ΔP can be expressed as

$$\Delta P = -\frac{6k\pi\Lambda^4}{\xi}\left(\frac{\xi+3}{\xi+1} + \frac{(\xi-3)\arctan\sqrt{\xi}}{\sqrt{\xi}}\right). \tag{8.37}$$

Similarly, one finds the form of the function F appearing on the right-hand side of (8.36), namely

$$F = -2(1+\xi)\frac{\partial\Delta P}{\partial\xi}. \tag{8.38}$$

8.5   Comparisons with exact solutions of the RTA kinetic equation

Anisotropic hydrodynamics and viscous hydrodynamics predictions have been checked against exact solutions available for the RTA kinetic equation [114, 183]. Such studies have been done for the one-dimensional Bjorken geometry [115, 116, 184] and for the Gubser flow that includes transverse
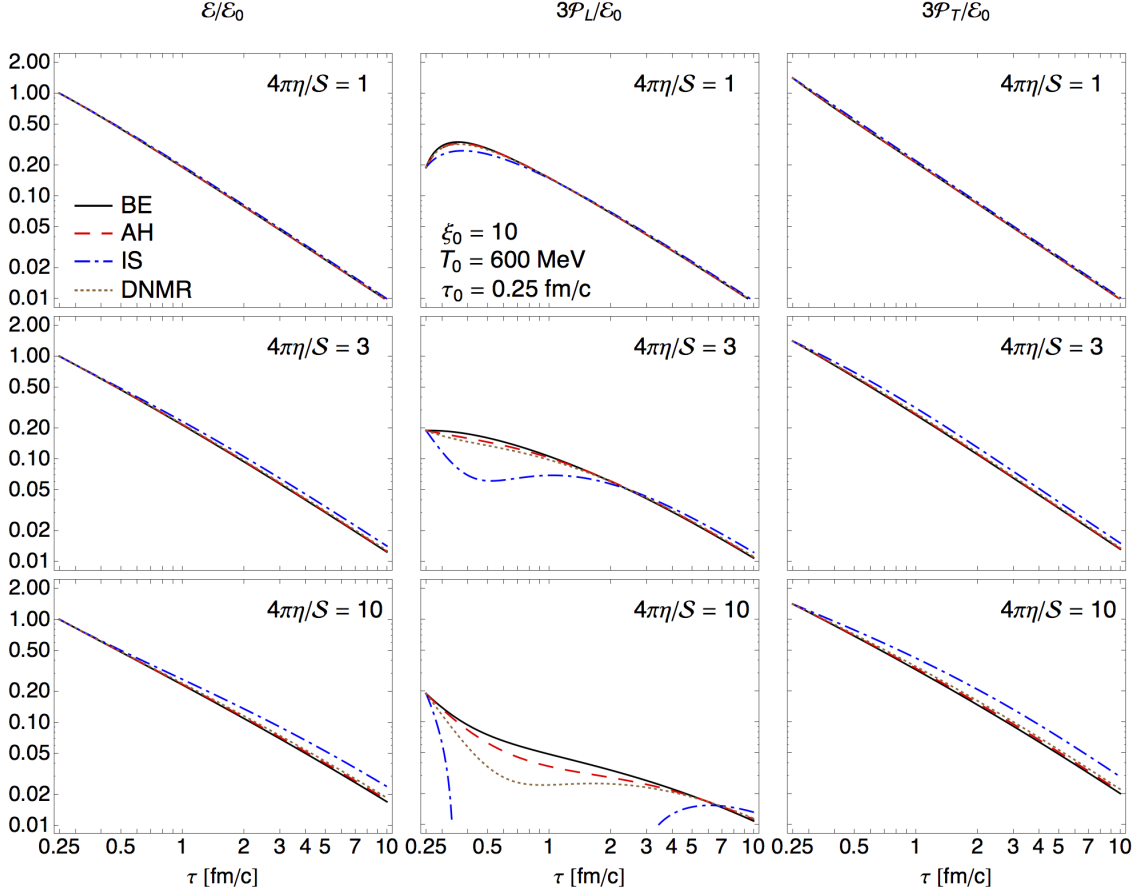
Figure 12: Time dependence of the energy density (first column), longitudinal pressure (second column) and the transverse pressure (third column) for three values of the shear viscosity: $4\pi\eta/\mathcal{S} = 1$ (first row), $4\pi\eta/\mathcal{S} = 3$ (second row), and $4\pi\eta/\mathcal{S} = 10$ (third row). The solid black, dashed red, dashed-dotted blue and dotted brown curves describe the results obtained with: RTA kinetic theory, AHYDRO, MIS, and DNMR.

expansion [185, 186]. The results of those studies show that AHYDRO in general better reproduces the results of the underlying kinetic theory than the standard viscous hydrodynamics.

In Fig. 12 we show the results for the proper-time dependence of the energy density (first column), longitudinal pressure (second column) and the transverse pressure (third column). All these quantities are normalised in such a way as to have the same late-time asymptotics. The results presented in the three rows (from up to down) correspond to three values of the shear viscosity: $4\pi\eta/\mathcal{S} = 1$, $4\pi\eta/\mathcal{S} = 3$, and $4\pi\eta/\mathcal{S} = 10$. The solid black curves show the results obtained by solving the RTA kinetic equations. They are compared with the results obtained within the framework of AHYDRO (dashed red curves), the MIS hydrodynamics (dashed-dotted blue lines), and the DNMR hydrodynamics (dotted brown curves). The AHYDRO approach is defined in this case by Eqs. (8.19) and (8.20).

All the results describe a one-dimensional, boost-invariant expansion with the initialization time

n	RTA	BRSSS	DNMR	MIS	AHYDRO
0	2/3	2/3	2/3	2/3	2/3
1	4/45	4/45	4/45	4/45	4/45
2	16/945	16/945	16/945	8/135	16/945
3	−208/4725	−1712/99225	-304/33075	112/2025	-176/6615

Table 1: Leading coefficients of gradient expansions for RTA, BRSSS, DNMR, MIS, and AHYDRO [139].

$\tau_0 = 0.25$ fm/c, the initial anisotropy parameter $\xi_0 = 10$, and the initial effective temperature $T_0 = 600$ MeV. One observes that the AHYDRO results follow most closely the exact kinetic-theory results. This is especially seen in the case of the longitudinal pressure and large viscosity. For $4\pi\eta/\mathcal{S} = 10$ the longitudinal pressure calculated in the MIS approach becomes negative, which is not allowed in the kinetic-theory framework. Although such large values of the QGP shear viscosity are excluded by the recent phenomenological models of heavy-ion collisions, one may find such values at the edges of the system where hadronic gas is present. Therefore, the use of the MIS approach should be avoided in such regions. Interestingly, a more complete DNMR approach much better reproduces the exact result.

8.6 Consistency with the gradient expansion

Recently, the gradient expansion has been studied for anisotropic hydrodynamics (in the formulation based on the anisotropic matching principle), its underlying kinetic theory in the relaxation time approximation, and for different formulation of standard viscous hydrodynamics [139]. The first four coefficients of the gradients expansion generated for these theories are shown in Table 1. One finds that the formulation of anisotropic hydrodynamics based on the anisotropic matching principle [174] yields the first three terms of the gradient expansion in agreement with those obtained for the RTA kinetic theory [118], see the second and the last columns. This finding gives further support for this particular hydrodynamic model as a good approximation of the kinetic-theory framework.

Leading coefficients of the gradient expansion have also been calculated for other versions of the hydrodynamic evolution equations. The results for BRSSS, DNMR and MIS are shown in the third, fourth and fifth column of Table 1, respectively. We find that both BRSSS and DNMR agree up to terms of second order in gradients ($n = 2$). It is important to stress, however, that there are different reasons for this agreement in the two cases. For BRSSS one fixes the free parameters (transport coefficients) in such a way as to get the agreement up to second order (and since MIS has fewer transport coefficients to adjust, it does not reproduce the second order exactly). In contrast, in the DNMR and AHYDRO constructions the values of the transport coefficients are obtained directly from the RTA kinetic equation (without any adjustment). Recall finally, that the third order theory due to Jaiswal [167] (see Sec. 8.3) matches the first three orders, as guaranteed by its construction.

We note at this point that in a recent work [187], the off-equilibrium behaviour described by different hydrodynamic models has been analysed and compared in numerical simulations of non-boost invariant

expansion. It was found that the results of anisotropic hydrodynamics and viscous hydrodynamics agree for the central close-to-equilibrium part of the system, however they differ at the edges where the approach of anisotropic hydrodynamics helps to control the undesirable growth of viscous corrections observed in standard frameworks.

9 Asymptotic nature of the late proper time expansion

Much of this review has been devoted to showing how the gradient expansion truncated at low orders provides an effective way to quantify the approach to equilibrium and at the same time provides a way of matching calculations in microscopic models with effective descriptions in terms of hydrodynamics. In the present Section we review recent progress in understanding large order behaviour of gradient expansions, which has led to the discovery of their asymptotic character both at the microscopic level [18] and in hydrodynamics [19]. It is important to realize that the divergence of the gradient expansion is connected to the phenomenon of hydrodynamization, reviewed in Sec. 5, which is the statement that hydrodynamics works even when leading order corrections to the perfect fluid limit are very large.

It has been observed long ago that divergent series can be meaningful, see e.g. Ref. [188]. Indeed, a useful way to think about such series is not as prescriptions to add up all the contributions in a naive way, but rather as a formal way to present a sequence of numbers which encode some information. We cannot attempt to review this subject here, but we will summarize and briefly explain the basic methods which have been used in literature to deal with the divergent series arising in the context of boost-invariant conformal hydrodynamics.

The main message is that the manner of divergence conveys information about the transient dynamics of both hydrodynamic and microscopic models. In the former case, as reviewed in Sec. 6, hydrodynamic modes are augmented with a non-hydrodynamic sector which acts as a regulator to maintain causality. It is most straightforward to begin with such setups, because here one has much better access to the full dynamics which generates the series, so the connection between the pattern of divergence and the non-hydrodynamic sector can be made completely explicit. This will be the subject of Sec. 9.1, where we will address BRSSS theory as well as anisotropic hydrodynamics and the HJSW theory reviewed in Secs. 8.4 and 7.5. Building intuition on these simpler examples, we will review microscopic calculations in holography, which initiated this line of research, and the most recent analysis of these issues performed for RTA kinetic theory.

9.1 Large order gradient expansion in hydrodynamics

A very fruitful point of view is to think of the gradient expansion calculated in a hydrodynamic theory, such as MIS, BRSSS, HJSW, DNMR or AHYDRO, precisely in the same way as if it had been obtained from a fundamental theory. This is useful, because both at the microscopic level and the level of hydrodynamics the hydrodynamic modes dominate at late times, the difference lying only in the

spectrum of transient modes. We can then study it in hydrodynamic theories where it is simple and where we have reliable information about it (from linearized analysis, for example). This leads to a very detailed understanding of the interplay between the structure of the non-hydrodynamic sector and large-order behaviour of the gradient expansion.

9.1.1 BRSSS theory

The simplest hydrodynamic theory to consider is MIS theory, but in this Section, following Refs. [19, 152, 189], we will instead deal with BRSSS theory since it captures more physics than MIS, yet is not much more difficult to analyse.

The gradient expansion of the pressure anisotropy $R(w)$,

$$R(w) = \sum_{n=1}^{\infty} \frac{r_n}{w^n}, \tag{9.1}$$

can in this case be calculated analytically directly from the differential equation Eq. (7.15). The leading terms of this expansion were already presented in Eq. (7.16). It is straightforward to calculate the expansion coefficients to very high order. In our presentation, following Ref. [19], we will adopt the $\mathcal{N} = 4$ SYM values of the transport coefficients. The basic feature of the resulting series is that at large order the expansion coefficients exhibit factorial growth. More precisely, one can check that at large n these coefficients grow with n in a way consistent with the Lipatov form [190]

$$r_n \sim \frac{\Gamma[n + \beta]}{A^n}, \tag{9.2}$$

where A and β are real parameters. Given the series coefficients r_n, one can easily check whether Eq. (9.2) applies by examining the ratios of neighbouring coefficients. Specifically, if Eq. (9.2) describes the large order behaviour, then one should find asymptotically linear behaviour:

$$\frac{r_{n+1}}{r_n} \sim \frac{1}{A}\, n + \frac{\beta}{A}. \tag{9.3}$$

For the case of the gradient series in BRSSS hydrodynamics, this linear behaviour can be seen in Fig. 13. It is worth noting that by fitting a straight line to the ratio (9.3) one can determine the parameters $A \approx 7.211759$ and $\beta \approx -0.625945$, which have a clear physical interpretation, described later on in this section.

The standard tool in dealing with factorially divergent series is the (generalized) Borel transform, see e.g. Ref. [188], which amounts to removing the leading order factorial growth of the series coefficients:

$$\mathcal{B}R(\xi) = \sum_{n=1}^{\infty} \frac{r_n}{\Gamma(n + \beta)}\, \xi^n. \tag{9.4}$$

This series will possess a non-vanishing radius of convergence, and will define an analytic function
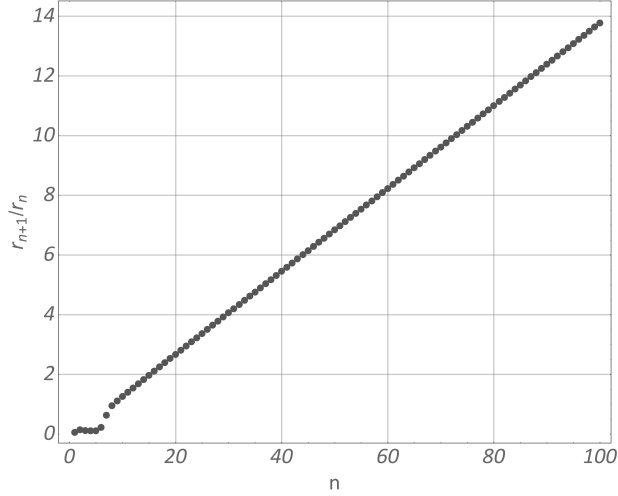
Figure 13: The large order behaviour of the hydrodynamic series for BRSSS hydrodynamics. The linear behaviour of r_{n+1}/r_n at large n, through Eq. (9.3), allows to recover A and β.

within the disc of radius A around the origin in the complex ξ plane. The inverse transform is given by the (generalized) Borel summation formula

$$\mathcal{S}R(w) = w^\beta \int_{\mathcal{C}} d\xi\, e^{-w\xi}\, \xi^{\beta-1}\, \tilde{\mathcal{B}}R(\xi), \tag{9.5}$$

where $\tilde{\mathcal{B}}R$ is the analytic continuation of the Borel transform Eq. (9.4) and $\mathcal{C}$ is the contour connecting 0 and ∞. The analytic continuation of $\mathcal{B}R(\xi)$ necessarily contains singularities that are responsible for the vanishing radius of convergence of the original series, which render the inverse Borel transform non-unique due to non-equivalent choice of integration contours $\mathcal{C}$.

In practice, the analytic continuation of the Borel transform is typically performed using Padé approximants. A Padé approximant is a rational function

$$\tilde{\mathcal{B}}R(\xi) = \frac{P_m(\xi)}{Q_n(\xi)}, \tag{9.6}$$

where $P_m(\xi)$ and $Q_n(\xi)$ are polynomials of order m and n respectively, with the constant term in Q_n scaled to unity and the remaining coefficients chosen so as to match a given polynomial of order $m + n + 1$ – in our case the truncated Borel transform of the gradient series.

The singularities of the Padé approximants are poles, but it is known that functions possessing branch point singularities result in Padé approximants featuring dense sequences of poles originating at the locations of the branch points, see e.g. Ref. [191]. For the case of the gradient expansion of BRSSS theory one finds a branch cut starting at $\xi \approx 7.211877$; this is shown in Fig. 14. The location of the branch point is numerically very close to the value of the parameter $A \approx 7.211759$ fitted using

83
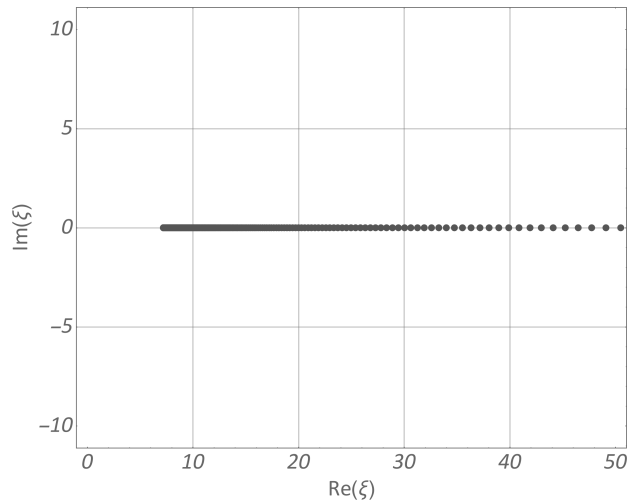
Figure 14: Poles of the symmetric Padé approximant to the Borel transform of the gradient series for BRSSS hydrodynamics truncated at 600 derivatives. One sees that the leading singularity of the branch-cut type. An in-depth analysis in Refs. [19,189] revealed that this singularity hides further branch-cut singularities with branch-points located at positive integer multiples of A from Eq. (9.2), see also Fig. 16.

Eq. (9.2).

In fact, the origin of the cut is consistent with the supposition that the analytically continued Borel transform contains a singular piece of the form

$$\tilde{\mathcal{B}}R(\xi) \sim \log\left(A - \xi\right) \tag{9.7}$$

where the parameter A describing the location of the branch point is the same as the one which appears in Eq. (9.3). One can convince oneself of this claim by calculating Padé approximants for Eq. (9.7) and studying the pattern of singularities.

The key observation is that the presence of a branch point singularity on the real axis introduces complex ambiguities in resummation, given by the difference in the values obtained for Eq. (9.5) by integrating above and below the cut. For large values of w the ambiguity is proportional to

$$AMB = e^{-w\,A}w^{\beta}, \tag{9.8}$$

where we have neglected subleading corrections in the large-w expansion. This ambiguity is a critically important feature of the hydrodynamic series in BRSSS theory and its presence is an indication of physics encoded in its large-order behaviour.

The form Eq. (9.8) implies that to cancel the ambiguity one needs exponential corrections to the gradient series. One can easily see that such corrections are in fact required by the differential equation which we are solving, Eq. (7.15). Indeed, we have already seen in Sec. 7 that there are non-analytic,

84

exponentially suppressed corrections to the hydrodynamic series following from the presence of the non-hydrodynamic MIS mode, given in Eq. (7.17), which we display here again for convenience:

$$\delta R(w) \sim e^{-\frac{3}{2C_{\tau_\pi}}w}\, w^{\frac{C_\eta - 2C_{\lambda_1}}{C_{\tau_\pi}}} \left\{ 1 + O\left(\frac{1}{w}\right) \right\}. \tag{9.9}$$

These have precisely the correct structure to eliminate the ambiguity in inverting the Borel transform (9.8) and suggests that one should make the following identifications:

$$A = \frac{3}{2\,C_{\tau_\pi}} \quad \text{and} \quad \beta = \frac{C_\eta - 2\,C_{\lambda_1}}{C_{\tau_\pi}}. \tag{9.10}$$

Evaluating these combinations with parameter values appropriate for $\mathcal{N} = 4$ SYM (which were used to generate the gradient expansion under discussion) gives excellent agreement with the values obtained by fitting A and β using Eq. (9.2). Both Eq. (9.8) and (9.9) receive corrections in $1/w$ which one also expects to match. One therefore sees that the branch-cut in the Borel plane represents the transient excitation of BRSSS theory evaluated at vanishing momentum, see Eq. (6.22). The fact that the exponential decay gets modified by an infinite series in $1/w$ follows from the fact that this excitation gets dressed by the hydrodynamic flow. This issue was addressed for the first time in the AdS/CFT-based calculations of Ref. [153].

The exponential correction Eq. (9.9) is in fact just the leading term in an infinite set of exponentially suppressed contributions which need to be added to the original asymptotic series Eq. (5.11). This naturally follows from the nonlinear nature of the BRSSS evolution equation, which in the present setup is given by Eq. (7.15). The resulting expression for the pressure anisotropy takes the form of a transseries:

$$R(w) = \sum_{m=0}^{\infty} \sigma^m\, e^{-mAw}\, \Phi_m(w), \tag{9.11}$$

where m labels the different transseries sectors and σ is a so-called transseries parameter, which is complex, see e.g. Refs. [192, 193]. In each sector we have a divergent series of the form

$$\Phi_m(w) = w^{m\beta} \sum_{n=0}^{\infty} \frac{r_n^{(m)}}{w^n}, \tag{9.12}$$

whose resummation involves an exponentially-suppressed ambiguity at large values of w, as in Eq. (9.8). The sector with $m = 0$ is the original gradient expansion Eq. (9.1), so that $r_n^{(0)} \equiv r_n$. The $m = 1$ sector corresponds to the only transient excitation that is present in the BRSSS theory, and the higher order sectors follow from the presence of nonlinear effects in Eq. (7.15).

This transseries structure is well known in physics due to its appearance in studies of large-order behaviour of perturbation theory in quantum mechanics. For this reason one sometimes speaks of Φ_0 as being the "perturbative" sector, and the Φ_m with $m > 0$ as the "instanton" sectors. In the same

spirit, the parameter A in Eq. (9.2) is sometimes referred to as an "action". As we shall see below, one often has many such "actions".

To make sense of the transseries expansion Eq. (9.11) one proceeds by performing a Borel summation in each sector. The basic idea is that the complex parameter σ carries physical information about the initial state. Eq. (7.15) requires specifying an initial condition to determine its solution: one real number, the value of R at some value of w. This provides one constraint on σ. To fully determine σ one has to impose the cancellation of the ambiguity in the choice of contour $\mathcal{C}$ when performing the integral in the inverse Borel transform for the perturbative series Φ_0. The resurgent structure of the transseries then guarantees that there is a choice of integration contours when resumming the $m = 1, 2, \ldots$ sectors in Eq. (9.11) such that the answer, $R(w)$, is real and unambiguous up to the physical choice of the initial condition.

The ideas reviewed above in the context of BRSSS theory carry over to more complicated cases in spirit, but need to be suitably adapted and generalized. Before we move on to this subject, let us remark that it is possible to explicitly carry out the Borel summation procedure, as outlined in this Section. This was done for the first three transseries sectors ($m = 0, 1, 2$) in Ref. [19]. It is interesting to note that in order to match this expression with the special attractor solution discussed in Sec. 7.4, one is required to set $\Re(\sigma) \approx 0.875$, while naively one might expect that the attractor should correspond to omitting the exponential terms. In consequence, instead of thinking about non-hydrodynamic modes in terms of perturbations about the gradient expansion one should perhaps think of them as perturbations around the hydrodynamic attractor. The presence of such attractor solutions in other models, see Ref. [136], certainly strengthens this idea.

9.1.2 Anisotropic hydrodynamics

The large order behaviour of the gradient expansion of the pressure anisotropy in boost-invariant anisotropic hydrodynamics for a conformal fluid was calculated in Ref. [139]. The calculation proceeds a little differently there, since it does not seem to be possible to write down a single differential equation for $R(w)$. Instead, one has to solve equations (8.35) and (8.36) as series in the proper-time τ and then use the result to find the coefficients r_n appearing in the expansion of $R(w)$. The analysis of this series then proceeds as in the case of BRSSS theory and leads to the same conclusion, namely that anisotropic hydrodynamics contains a single purely decaying non-hydrodynamic mode with the decay rate set by the relaxation time. This is the outcome expected on the grounds that the order of the boost-invariant evolution equations is the same as in the case of BRSSS (unlike the HJSW theory discussed in the following Section).

9.1.3 HJSW theory

It is interesting to consider the large order behaviour of the gradient expansion of the simplest hydrodynamic theory which avoids acausality by extending Navier-Stokes theory not by a single, purely decaying mode (as MIS, BRSSS and AHYDRO do), but by a pair of conjugate modes. The second of the
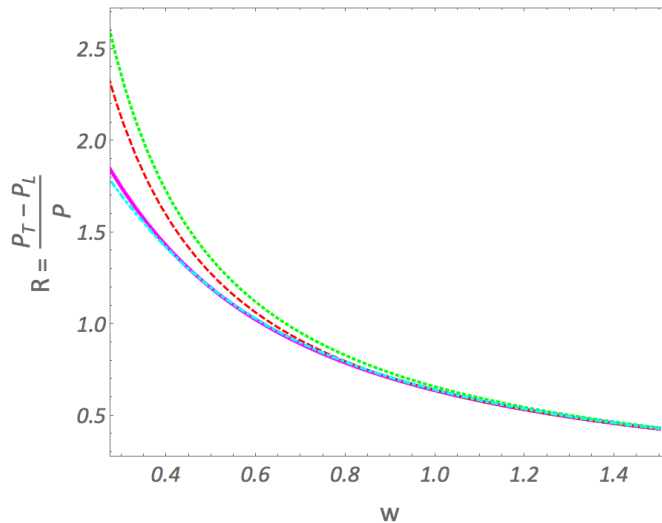
Figure 15: The hydrodynamic attractor (magenta), compared with the resummation result (cyan, dot-dashed) and the gradient expansion of order 1 (red, dashed) and 2 (green, dotted). Quite curiously, comparison required fitting $\Re(\sigma) \approx 0.875$ in Eq. (9.11).

models described in Sec. 7.5 is an example of such a theory. When restricted to boost-invariant flows one arrives at Eq. (7.23). It is easy to calculate higher order terms in the gradient series (7.25) numerically and as one would expect, this series diverges. If we use a transseries Ansatz of the type (9.11) we find two complex conjugate values for the "action":

$$A_{\pm} = \frac{3}{2}\left(\Omega_I \pm i\Omega_R\right).$$

We then have two types of "non-perturbative" contributions and thus, following Ref. [194], we find that we need a two-parameter transseries to fully describe the solutions to this equation:

$$R\left(w\right) = \sum_{n_{\pm}=0}^{\infty} \sigma_+^{n_+}\, \sigma_-^{n_-}\, \mathrm{e}^{-(n_+\, A_+ + n_-\, A_-)\, w}\, w^{n_+\, \beta_+ + n_-\, \beta_-}\, \Phi_{(n_+|n_-)}\left(w\right). \tag{9.13}$$

In the expression above $\Phi_{(n_+|n_-)}(w)$ are series expansions in w^{-1} in each sector; the "perturbative" sector is given by taking $n_+ = n_- = 0$. The coefficients of these expansions were studied in Ref. [152] and found to satisfy very nontrivial relations following from the theory of resurgence, similarly to the BRSSS case.

The presence of two transseries parameters is, of course, related to the fact that now the evolution equation for $R(w)$ is second order and requires specifying two initial conditions. This structure can be viewed as a model for the nonhydrodynamic sector found previously in the holographic study of hydrodynamic gradient expansion at strong coupling [18], which is the subject of Sec. 9.2.1.

87
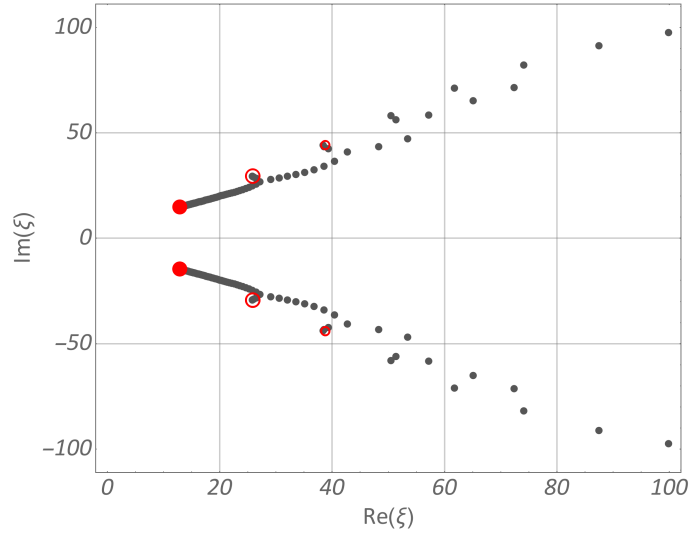
Figure 16: The plot shows singularities of the approximate analytic continuation of the Borel transform of hydrodynamic gradient expansion in the HJSW theory truncated at 600 derivatives. One can clearly see that the two leading singularities match $3/2\,i$ frequency of the lowest non-hydrodynamic excitation in the model at vanishing momentum $\mathbf{k}$ and unit temperature T (solid red dots). The new clearly visible feature as compared to the BRSSS case depicted in Fig. 14 is the presence of additional singularities starting at positive integer multiples of the leading branch points (empty red dots denoting the first two multiples). They necessarily follow from the nonlinear nature of the underlying equation and are reflected in the structure of transseries ansatz. Following this logic, they also exist in the BRSSS theory, but are impossible to locate in Fig. 14 since the relevant branch-cuts partially overlap.

9.2 Large order gradient expansion from microscopic models

9.2.1 Holographic CFTs

The holographic dual to the hydrodynamic gradient expansion for Bjorken flow is a special case of the fluid-gravity duality [102] in which T becomes a function of τ only and symmetry dictates $u^\mu \partial_\mu = \partial_\tau$. This finding leads to the following metric ansatz for its gravity dual [100, 195, 196]

$$ds^2 = \frac{L^2}{u^2}\left\{ -2d\tau du - a\, d\tau^2 + (\tau+u)^2 e^{\frac{2}{3}d-2b}\, dY^2 + e^{\frac{2}{3}d-b}\left(\left(dx^1\right)^2 + \left(dx^2\right)^2 \right) \right\},$$

where the off-diagonal bulk metric element implies the choice of the so-called generalized ingoing Eddington-Finkelstein coordinates[17] and the metric components a, b and d are functions of τ and u. As opposed to the original work [18], and in the spirit of the fluid-gravity duality, we will repackage this dependence as a dependence on $\tau\, T(\tau)$ and $u\, T(\tau)$ with $T(\tau)$ being the effective temperature from Eq. (5.5). The former is the familiar w-variable encountered in Sect. 5 which casts the hydrodynamic gradient expansion as the Taylor series around $w = \infty$. The latter quantity, $u\, T(\tau) \equiv \rho$, roughly measures the radial energy scale u in the units of local temperature $T(\tau)$. One can superficially understand this parametrisation as a statement that in the hydrodynamic regime we measure all dimensionful parameters with respect to the energy density or, equivalently, effective temperature. The key idea is to seek for the bulk metric in the gradient-expanded form

$$a(w,\rho) = a_0(\rho) + \frac{1}{w}a_1(\rho) + \frac{1}{w^2}a_2(\rho) + \dots$$

where the ellipsis denotes further terms with three or more derivatives. Analogous expressions hold also for b and d.

As shown originally in Ref. [18], it is possible to solve Einstein's equations (4.5) in a semi-analytic manner up to a very high order in the large-w expansion and infer from it the large order behaviour of the hydrodynamic derivative expansion of the normalised pressure anisotropy $R(w)$ of a strongly coupled expanding plasma[18]. We will not discuss here the detailed procedure and its implementation, but, instead, we want to indicate the following crucial ideas behind it. The starting point for the whole analysis is the metric describing the Bjorken perfect fluid solution:

$$a_0(\rho) = 1 - \pi^4\, \rho^4 \quad \text{and} \quad b_0(\rho) = d_0(\rho) = 0. \tag{9.14}$$

This solution has a horizon at $\rho = \frac{1}{\pi}$. Higher order corrections can now be calculated by solving at each order in the large-w expansion three linear second-order ordinary differential equations outside the horizon. The remaining two Einstein's equations turn out to be trivially obeyed. Lower order

---

[17]As a result, the bulk coordinates are distinct from the ones used in Eq. (4.2) despite being denoted by the same symbols.

[18]Ref. [18] parametrizes the problem differently, which, at least superficially, happens to lead to a more efficient algorithm for solving the relevant equations. The implementation presented here, which we introduce especially for the needs of the present review, is conceptually nicer, but most likely computationally slower.

solutions (e.g. zeroth order when solving for the first order solution) appear in the source terms and as a result the solution at a given order is determined by boundary conditions at $\rho = 0$ and $\rho = \frac{1}{\pi}$. As discussed in Sec. 4, the physical solution should not blow up outside the horizon, which can be taken care of by representing functions by sums of orthonormal polynomials bounded on this domain, see e.g. Refs. [104, 197] for reviews of these methods in the context of general relativity.

All the *physical* boundary conditions can be specified at $\rho = 0$ using Eq. (4.6). First, we want the plasma to live in flat Minkowski space. Second, the leading order expression given by Eq. (9.14) through the definition of ρ and Eq. (4.6) already accounts for the full dependence of the energy density on the effective temperature $T(\tau)$. As a result, when calculating higher order corrections, we need to ensure, through the use of Eq. (4.6), that this result remains intact. This corresponds to the Landau matching condition in relativistic hydrodynamics. Let us point out, as it will become apparent to the reader after reading the next Section, that the above way of phrasing the gradient expansion on the gravity side can be very closely mimicked within kinetic theory. This allows us to build up a very close parallel between these two a priori very distinct languages of describing collective systems.

The outcome of analogous calculations in Ref. [18], using a faster numerical implementation, is the form of the normalized pressure anisotropy $R(w)$ for strongly-coupled plasma up to terms having 240 derivatives of the fluid variables. The coefficients, again, exhibit factorial growth and, as can be seen in Fig. 17, they give rise to very intricate singularity structure in the Borel plane. The new feature, as compared with hydrodynamic theories reviewed to date, is the presence of more than one non-hydrodynamic excitation (see also Ref. [198] for a sharp manifestation of their presence). By inverting the Borel transform along two inequivalent contours one obtains the following large-w contribution associated with the two leading singularities:

$$\delta R \sim \mathrm{e}^{-A_\pm^{(1)}\, w}\, w^{\beta_\pm^{(1)}},$$

where $A^{(1)} = -14.7003 \pm 12.9435\, i$ and $\beta^{(1)} = 0.6867 \pm 0.7799\, i$. In the original Ref. [18] these values were matched to the behaviour of the lowest transient QNM evaluated in the Bjorken background, in complete agreement with the overall picture advocated in this review. The presence of other transient QNMs suggests the following form of the transseries [199]

$$R\left(w\right) = \sum_{n_\pm^{(1)}, n_\pm^{(2)},\ldots=0}^{\infty} \Phi_{\left(n_+^{(1)}|n_-^{(1)}|n_+^{(2)}|n_-^{(2)}|\ldots\right)}(w) \times$$
$$\times \prod_{j=1}^{\infty} \left(\sigma_+^{(j)}\right)^{n_+^{(j)}} \left(\sigma_-^{(j)}\right)^{n_-^{(j)}} \mathrm{e}^{-\left(n_+^{(j)} A_+^{(j)} + n_-^{(j)} A_-^{(j)}\right) w}\, w^{n_+^{(j)} \beta_+^{(j)} + n_-^{(j)} \beta_-^{(j)}}, \quad (9.15)$$

which generalizes Eq. (9.13) to a case in which infinitely many independent modes are present. Again, the "perturbative" series considered in Ref. [18] is represented by $\Phi_{(0|0|0|0|\ldots)}$ and "actions" $A_\pm^{(j)}$ represent frequencies of subsequent QNMs at vanishing momentum $\mathbf{k}$, as in Eq. (9.13). Different products present in Eq. (9.15) correspond to interactions between modes triggered by nonlinearities of Einstein's
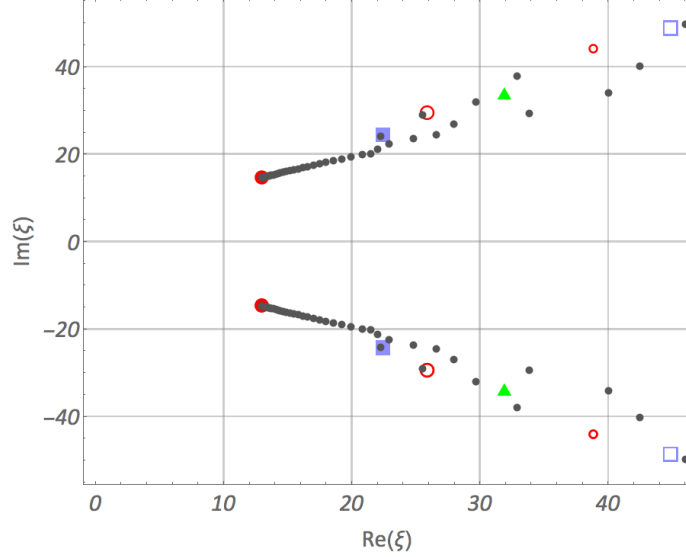
Figure 17: In this plot, grey dots denote singularities of the approximate analytic continuation of the Borel transform, given by Eq. (9.4) with $\beta = 1$, of the hydrodynamic gradient expansion in a hCFT such as $\mathcal{N} = 4$ SYM truncated at 240 derivatives obtained in Ref. [18]. Big red dot, pale blue square and green triangle correspond to $3/2\,i$ times ω/T for the three least damped transient QNMs at vanishing momentum **k**, see Sec. 4.3. Corresponding empty shapes denote integer multiples of relevant frequencies. One can clearly see that the position of the leading singularity – a pair of branch points – coincides with what would be given by the lowest non-hydrodynamic mode frequency, as in the studies of hydrodynamic theories. Quite remarkably, one also sees singularities lying very close to the positions corresponding to frequencies of the second transient mode and the doubled frequency of the first transient mode. One expects that upon increasing the number of orders and accuracy of the calculation, one would see the associated branch cuts, as well as signatures of higher QNMs. This points, quite emphatically, to a transseries structure. Note that some of the poles in the plot do not correspond to physical singularities and are artefacts of the approximate analytic continuation.

equations (4.5).

One can intuitively understand the proposal in Eq. (9.15) in the following way. BRSSS and AHYDRO theories give rise to first order ODEs for $R(w)$, which require providing one real number as an initial condition. They also have one transient mode and, through the transseries, there is a relation between the transseries parameter σ and a relevant initial condition. This is illustrated in Fig. 15 in the context of the attractor solution of BRSSS theory. The HJSW theory gives rise to a second order ODE for $R(w)$, which requires providing two real numbers as an initial condition, and there is one pair of oscillatory transient modes. This leads to a resurgent transseries which has two parameters. In holography, Einstein's equations (4.5) for the bulk metric ansatz (9.14) are second order PDEs in the ρ and w variables and require specifying a function of ρ (or, in practical calculations, a function of u) in order to solve the initial value problem [11, 103, 107, 108]. Such a function contains infinitely many real parameters. At the level of the energy-momentum tensor of the hCFT this freedom manifests itself in its early time dynamics through Eq. (5.15), since the $\mathcal{E}_n$ from this equation are in one-to-one correspondence with the form of the near-boundary expansion of the initial condition [108]. In the late-time dynamics, the same feature manifests itself through the presence of infinitely many modes in equilibrium, see Sec. 4.3. At least superficially, one can therefore think of Einstein's equations as equivalent to some tentative ODE of infinite order for $R(w)$. It remains to be seen if this perspective will bring further insights.

9.2.2 RTA kinetic theory

At the moment of writing this review, the latest development on the large-order behaviour of the hydrodynamic gradient expansion concern the RTA kinetic theory. We will review here the conformally-invariant case analysed in Ref. [118] with the aim to draw parallels with holography and present the Borel plane analysis of the gradient expansion as a novel tool in diagnosing excitations of time-dependent systems. It should be stressed that the asymptotic character of the gradient expansion in the RTA kinetic theory has been also observed in Ref. [200] in a non-conformal model with a constant relaxation time τ_{rel}. See also Ref. [201] in this context.

To obtain the solution of the RTA Boltzmann equation (5.18) at high orders of the gradient expansion it is far more efficient to proceed with the wisdom of hindsight and calculate the anisotropy directly as a function of the dimensionless evolution parameter (5.8), rather than as it was presented in Sec. 5.3.1 or in the original article [118]. It is convenient to view the distribution function as dependent on the boost-invariant dimensionless variable w, as well as on

$$v \equiv \frac{U \cdot p}{T} \quad \text{and} \quad \psi \equiv \frac{\left(p^0\right)^2 - \left(p^3\right)^2}{T^2},$$

i.e. to consider $f(w, v, \psi)$. To derive the requisite form of the Boltzmann equation starting with Eq. (3.20) one has to view the new variables w, v and ψ as functions of the boost-invariant combination $\sqrt{\left(x^0\right)^2 - \left(x^3\right)^2}$ of Cartesian coordinates x^0 and x^3. After the differentiation is carried out we can,

appealing to boost-invariance [114], one sets $x^3 = 0$ and $t = \tau$ to obtain

$$\left(\frac{2}{3} + \frac{1}{18}R\right)\partial_w f + \left(\frac{1}{w}\frac{\psi}{\upsilon} - \left(\frac{2}{3} + \frac{1}{18}R\right)\frac{\upsilon}{w}\right)\partial_\upsilon f + \left(\frac{2}{3} - \frac{1}{9}R\right)\frac{\psi}{w}\partial_\psi f = \frac{e^{-\upsilon} - f}{\gamma}\,, \qquad (9.16)$$

where derivatives of the temperature T have been eliminated in favour of the pressure anisotropy R defined in Eq. (5.4). The key idea now is to look for $R(w)$ and $f(w, \upsilon, \psi)$ in the gradient-expanded form, i.e. use the ansatz for $R(w)$ given by Eq. (5.11) and the following one for $f(w, \upsilon, \psi)$:

$$f(w, \upsilon, \psi) = f_0(\upsilon, \psi) + \frac{1}{w}f_1(\upsilon, \psi) + \frac{1}{w^2}f_2(\upsilon, \psi) + \ldots \qquad (9.17)$$

The leading terms in the above equation is the equilibrium distribution function, which in the introduced parametrization simply reads

$$f_0(\upsilon, \psi) = e^{-\upsilon}.$$

As it turns out, one can now iteratively solve the RTA Boltzmann equation (9.16) which at each order n gives a linear algebraic relation for $f_n(\upsilon, \psi)$ with the result depending on r_n. Imposing now the Landau matching condition, i.e. demanding that a given $f_n(\upsilon, \psi)$ does not contribute to the local energy density of plasma for $n > 0$ fixes the corresponding contribution r_n to the gradient expansion of the pressure anisotropy $R(w)$. In Ref. [118] an analysis of that type has been performed up to terms having 200 derivatives revealing vanishing radius of convergence.

Let us now point out a nice analogy between the distribution function in kinetic theory and bulk metric in holography that can be seen here in the context of the boost-invariant flow. In both cases the microscopic dynamics is captured by equations of motion in higher number of dimensions, albeit of a very different mathematical nature. In the context of holography, the additional variable has an interpretation of the energy scale in a hQFT, see Sec. 4. In the context of kinetic theory, there are three additional variables that represent on-shell particle momenta, see Sec. 3.3. Both in the holographic setup considered in the previous Section and in the kinetic theory setup of this section we measure these additional variables in units of the effective temperature, which sets the characteristic near-equilibrium scale in conformal theories. Discarding singular solutions in holography, which in Sec. 9.2.1 was achieved by using an appropriate numerical representation of bulk metric components, in both setups the corresponding implementation of the Landau matching condition fixes the transport coefficients. This analogy, very much inspired by the fluid-gravity duality [102] discussed in Sec. 7.2, should naturally extend to general hydrodynamic flows. Applying the Borel transform technique and appropriate analytic continuation to the large-order gradient series in the conformal RTA theory reveals the structure of singularities displayed in Fig. 18. One can see there a branch point singularity located at $3/2\,\gamma^{-1}$, where γ is the dimensionless proportionality constant setting the scaling of the relaxation time $\tau_{\rm rel}$ with temperature in conformal RTA, see Eq. (3.22). Following the intuition gained in the analysis of other setups reviewed earlier in this Section, one should seek the origin of this singularity in terms
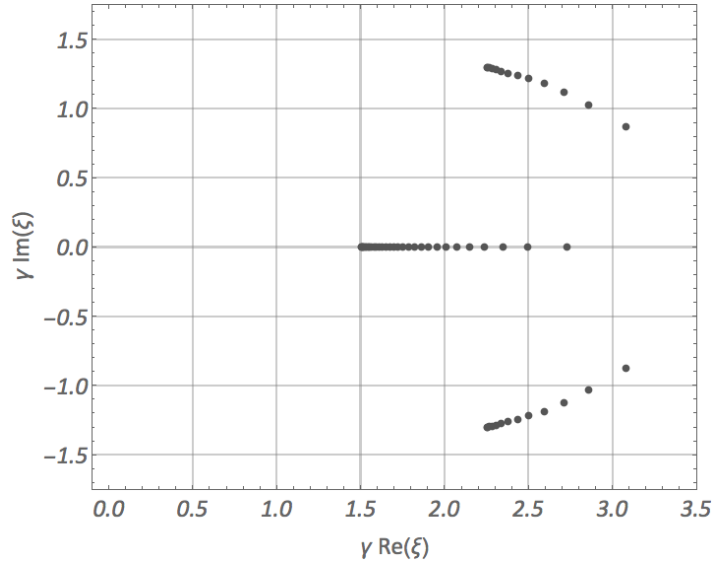
Figure 18: The plot shows singularities of the approximate analytic continuation of the Borel transform of hydrodynamic gradient expansion in the conformal RTA kinetic theory. The beginning of the leading singularity lying on the real axis is in an excellent agreement with $3/2\,i$ times the frequency of the transient excitation at vanishing momentum. The major puzzle at the moment of writing this review is the presence of other singularities lying off real axis and beginning at $\gamma\,A_{\pm} \approx 2.25 \pm 1.3\,i$, since they cannot be matched in a straightforward way with equilibrium modes of the model, c.f. Sec. 3.3.4.

of the single non-hydrodynamic mode present in the RTA kinetic theory. One subtlety that needs to be stressed is that in contrast with all the other known models, this mode is a pole only at vanishing $\mathbf{k} = 0$. Otherwise, it is represented in the retarded two-point function of the energy-momentum tensor as a branch-cut singularity, see Sec. 3.3.4. The consequence of this difference is not understood at the moment of writing the present review. An even more surprising outcome of the analysis in Ref. [118] is the presence of two symmetric singularities lying off the real axis on the Borel plane, see Fig. 18. Following the intuition developed in other studies, one would be tempted to interpret them as a signature of oscillatory modes present in the expanding plasma of the conformal RTA kinetic theory. The puzzle comes from the fact that no obvious equilibrium mode can be matched to this singularity and, perhaps, it is an excitation that originates from the underlying expansion of the system. Somewhat similar in spirit "emergent" modes were discussed earlier in Ref. [202] in the context of kinetic theory with different, more complicated collisional kernel.

Finally, the last point we wish to bring to the readers' attention is the question of initial conditions for the kinetic theory and the number of singularities in the Borel plane. In the hydrodynamic theories reviewed earlier in this section, a one-to-one correspondence was found between the number of initial conditions for $R(w)$ and the number of singularities in the Borel plane. The latter was found to match the number of modes in the system. In the present case, somewhat analogously to holography, the initial state in kinetic theory is encoded in the initial distribution function which contains infinitely many parameters. The universal hydrodynamic gradient expansion does not know about them and one should expect this information to enter through "non-perturbative" transient effects associated with infinitely many singularities on the Borel plane. This puzzling issue is currently under investigation [203].

9.2.3 Significance of the asymptotic character of hydrodynamic gradient expansion

The results reviewed in this section in the context of one-dimensionally expanding systems in diverse models and theories point univocally to the asymptotic character of hydrodynamic gradient expansion for generic flows and other models (not necessarily conformally-invariant). The phenomenological relevance of this finding stems from the fact that it makes the phenomenon of hydrodynamization, reviewed in Sec. 5, mathematically less surprising. Since the gradient series is not convergent anyway, smallness of subsequent terms is not a criterion for the applicability of hydrodynamics, which is rather determined by the separation of the nonhydrodynamic modes whose presence is – as we have seen – intimately connected with the divergence of the gradient series.

10 Summary and Outlook

10.1 Key lessons

The overarching theme of our review is broadly-understood hydrodynamic model building given insights from ab initio studies of time-dependent processes in microscopic frameworks: holography and

relativistic kinetic theory. The first key notion here is the idea of modes of equilibrium plasma reviewed in Secs. 3 and 4.3. There are two kinds of modes: transient ones and the ones which can be made long-lived by lowering their spatial variations. The latter are called hydrodynamic.

The second fundamental idea for our presentation is the notion of universal dynamics at late times described in Sec. 5. This universality lies in our ability to parametrize the dynamics by a smaller number of functions than the number of independent components of the expectation value of the energy-momentum tensor. The key to doing this is the gradient expansion. Bringing in the mode picture, the gradient expansion corresponds to a "condensation" of hydrodynamic modes and this why it is called the hydrodynamic gradient expansion (see Sec. 6).

A very surprising feature that becomes apparent when comparing ab initio solutions for the expectation value of the energy-momentum tensor with its predicted form within the hydrodynamic gradient expansion is that the latter, when truncated keeping only the first few orders, can do a great job despite the fact that the leading corrections are huge. This gives rise to the phenomenon of hydrodynamization: the violation of approximate local thermal equilibrium in the hydrodynamic regime – see Sec. 5. The phenomenological relevance of this finding lies in providing an explanation for the success of hydrodynamic modelling in ultrarelativistic heavy-ion collisions at RHIC and LHC where spatiotemporal variations and momentum anisotropies are very large initially [135] and, even more so, in the context of small systems (proton-nuclei and high-multiplicity proton-proton collisions) [137, 204].

The fourth notion (covered in Sections 7 and 8) are dissipative hydrodynamic theories with a well-posed initial value problem, which are or can be used in modelling a part of the evolution of nuclear matter at RHIC and LHC. The features that we want to emphasize is that each of these models necessarily comes with a set of transient modes and that depending on microscopic dynamics and phenomenological context one can fit the parameters of these modes to either try to match the truncated gradient expansion of an underlying theory or to capture features of the non-hydrodynamic sectors.

Finally, in Sec. 9 we reviewed recent developments demonstrating the asymptotic character of the hydrodynamic gradient expansion and a subtle interplay between the long-lived and the transient modes. This finding can be seen as a mathematical reason behind hydrodynamization.

10.2   Open directions

The developments presented here are very recent and open many promising directions for future research. Below we mention four among the ones that we find particularly exciting.

The fundamental notion advocated in this review are the modes of equilibrium systems (see Secs. 3 and 4.3). Whereas hydrodynamic modelling in the context of ultrarelativistic heavy-ion collisions provides us with access to some information about the hydrodynamic sector, one can safely say that nothing is known about the transient modes. It would be very interesting to investigate them in detail, also in the context of other systems. One should mention here a recent effort in this direction using data describing damped oscillations of trapped unitary Fermi gases [205].

On a more theoretical side, it would be very illuminating to understand more comprehensively the properties of modes in relativistic kinetic theory, since the only study available to date and reviewed in Sec. 3.3.4 concerns perhaps the simplest available collisional kernel. Related to this are studies of higher curvature corrections in holography and their influence on the spectrum of quasinormal modes, see Sec. 4.3. These developments fall into a broader class of efforts to bridge strong and weak-coupling results in QFTs, see e.g. Refs. [65, 118, 206].

Another promising of interesting future problems has to do with the breaking of conformal symmetry. For example, in the context of hydrodynamization, it has been observed that the bulk viscous term can give a very big contribution to the energy-momentum tensor [29][19]. It would be interesting to investigate it more comprehensively, also in the context of second order transport which is very diverse in non-conformal systems. Furthermore, in the analysis presented here a lot of mileage for one dimensionally expanding systems reviewed in Sec. 5 was gained by introducing considering pressure anisotropy R as a function of w-variable. In particular, it is this parametrization that allows to see the attractor solution. Trying to understand if a similar construction can be found when conformal symmetry is broken is certainly a very tempting question to ask.

In this review we pursued the perspective of attractor solutions for conformal boost-invariant flow seen in various theories or microscopic models as a notion of hydrodynamics beyond the gradient expansion [19, 136]. If this set of ideas is to develop, such attractor solutions should be found in the absence of conformal symmetry and for less symmetric flows than the Bjorken expansion. This is an outstanding problem to address and, perhaps, the slow roll method applied in this context in Ref. [19] would be a good starting point.

10.3 Closing words

The past 15 years, the golden age of relativistic hydrodynamics, brought numerous insights on how the hydrodynamic regime emerges from microscopic theories, many of which this review covered in detail. This set of developments constitutes now a mature discipline, but one cannot escape the impression that our understanding is very much model-based and will be superseded by a more comprehensive picture in the future. We hope that our review will help to inspire fellow researchers to further contribute to understanding non-equilibrium QFTs in general and QCD in particular.

Acknowledgements

---

[19]Ref. [29] describes this phenomenon as lack of equilibration, because what would be the equation of state in equilibrium is violated, but we prefer to view it as another instance of hydrodynamization.

pointing out that in Fig. 17 one can see traces of higher singularities. Finally, we would like to thank Viktor Svensson for proof-reading the manuscript and valuable comments.

Appendix A   Acronyms

RHIC	Relativistic Heavy-Ion Collider at Brookhaven National Laboratory
LHC	Large Hadron Collider at CERN
QCD	quantum chromodynamics
YM	Yang-Mills
SYM	supersymmetric Yang-Mills
QGP	quark-gluon plasma
EOS	equation of state
CGC	color glass condensate
(h)QFT	(holographic) quantum field theory
(h)CFT	(holographic) conformal field theory
AdS	anti-de Sitter (spacetime)
AdS/CFT	anti-de Sitter/conformal field theory (correspondence)
QNM	quasinormal mode
NS	Navier-Stokes (hydrodynamic equations)
MIS	Müller-Israel-Stewart (hydrodynamics)
BRSSS	Baier-Romatschke-Son-Starinets-Stephanov (hydrodynamics)
DNMR	Denicol-Molnar-Niemi-Rischke (hydrodynamics)
HJSW	Heller-Janik-Spalinski-Witaszczyk (hydrodynamics)
AHYDRO	anisotropic hydrodynamics
KT, EKT	kinetic theory, effective kinetic theory
RTA	relaxation time approximation (for kinetic theory)
RS	Romatschke-Strickland (ansatz for the distribution function)
RQMD	relativistic quantum molecular dynamics
ODE	ordinary differential equation
PDE	partial differential equation

Table 2: List of acronyms

Appendix B   Notation

EOS	equation of state
EQ	label specifying global thermal equilibrium
eq	label specifying local thermal equilibrium
$T^{\mu\nu}$	energy-momentum tensor
T	effective temperature
U^{μ}	flow vector defining the Landau hydrodynamic frame
$\Delta^{\mu\nu}$	operator projecting on the space orthogonal to U^{μ}
$\pi^{\mu\nu}$	shear stress tensor
$\sigma^{\mu\nu}$	shear flow tensor
Π	bulk pressure
$\mathcal{E}$	energy density
$\mathcal{P}(\mathcal{E})$	equilibrium pressure corresponding to the energy density $\mathcal{E}$ (functional form $\mathcal{P}(\mathcal{E})$ follows form the equation of state)
η	shear viscosity
ζ	bulk viscosity

Table 3: Symbols denoting physical concepts and variables (part 1)

$T_{\mathrm{a}}^{\mu\nu}$	leading-order energy-momentum tensor of anisotropic hydrodynamics
$\xi^{\mu\nu}$	anisotropy tensor
ϕ	bulk variable
$\tilde{\pi}^{\mu\nu}$	modified shear stress tensor
$\tilde{\Pi}$	modified bulk pressure

Table 4: Symbols and concepts used in AHYDRO

Appendix C   Conventions

Throughout the paper we use the natural system of units with $c = \hbar = k_B = 1$, except for few places where we use explicit notation to demonstrate the dependence of physical quantities on physical con-

stants. Three-vectors are denoted by the bold font, four-vectors are in the standard font, the dot denotes the scalar product of three- or four-vectors. The Minkowski metric is $\eta_{\mu\nu} = \text{diag}(-1, +1, +1, +1)$.

We use the standard parameterizations of the on-mass-shell four-momentum and spacetime coordinates of a particle,

$$
\begin{aligned}
p^\mu &= (E, p_x, p_y, p_L) = (E, \mathbf{p}) = (m_\perp \cosh y, p_x, p_y, m_\perp \sinh y), \\
x^\mu &= (x^0, x^1, x^2, x^3) = (t, x^1, x^2, z) = (t, \mathbf{x}) = (\tau \cosh Y, x^1, x^2, \tau \sinh Y).
\end{aligned}
\tag{C.1}
$$

Here $m_T = \sqrt{m^2 + p_T^2} = \sqrt{m^2 + (p^1)^2 + (p^2)^2}$ is the transverse mass, $\tau = \sqrt{(x^0)^2 - (x^3)^2}$ is the (longitudinal) proper time, y is the rapidity

$$
y = \frac{1}{2} \ln \frac{E + p_L}{E - p_L},
\tag{C.2}
$$

and Y is the spacetime rapidity,

$$
Y = \frac{1}{2} \ln \frac{x^0 + x^3}{x^0 - x^3}.
\tag{C.3}
$$

The flow of matter is described by the four-vector

$$
U^\mu = \gamma(1, v_1, v_2, v_3), \quad \gamma = (1 - v^2)^{-1}, \quad U \cdot U = -1.
\tag{C.4}
$$

We note that, due to the form of the metric used, the energy of a particle in the frame connected with the fluid element moving with the four-velocity U^μ is $-p \cdot U$. Most of other symbols and acronyms are listed in Tables 2–4.

Appendix D Boost invariant hydrodynamics

For scalar functions of the space-time coordinates (such as the energy density $\mathcal{E}(x)$, entropy density $\mathcal{S}(x)$, pressure $\mathcal{P}(x)$, or temperature $T(x)$) the boost invariance and transverse homogeneity imply that they depend on the longitudinal proper time $\tau = \sqrt{(x^0)^2 - (x^3)^2}$ only. For vector fields (such as the flow four-vector field $U^\mu(x)$) the situation is a bit more complicated. Combining the rule for the longitudinal Lorentz transformation of a four-vector, $U'^\mu(x') = L^\mu_\nu U^\nu(x)$, with the condition of boost invariance, $U'^\mu(x') = U^\mu(x')$, we find that the boost-invariant flow vector has the form

$$
U^\mu(x) = (x^0/\tau, 0, 0, x^3/\tau).
\tag{D.1}
$$

The form (D.1) has been specified also by the condition that U^μ is timelike and its spatial part vanishes at $x^3 = 0$ (in order to describe the flow in the center-of-mass reference frame). Note also that proper time τ - spacetime rapidity Y coordinates are curvilinear and lead to the following form of the

Minkowski metric line element:

$$ds^2 = -d\tau^2 + \tau^2 dY^2 + \left(dx^1\right)^2 + \left(dx^2\right)^2.$$

For not dissipative systems, the entropy current is conserved. If such systems are boost invariant and transversally homogenous, this property can be expressed by the equation

$$\partial_\mu(\mathcal{S}U^\mu) = \frac{d\mathcal{S}(\tau)}{d\tau} + \frac{\mathcal{S}(\tau)}{\tau} = 0, \tag{D.2}$$

which has a scaling solution

$$\mathcal{S}(\tau) = \frac{\mathcal{S}_0 \tau_0}{\tau}. \tag{D.3}$$

Here $\mathcal{S}_0$ is the entropy density at the initial proper time τ_0. Equations (D.1)–(D.3) form the foundation of the renowned Bjorken hydrodynamic model of heavy-ion collisions [93]. As we have just seen, they can be introduced as a consequence of boost-invariance and lack of dissipation.

For conformal systems in equilibrium, the entropy density scales with the third power of temperature, $\mathcal{S}(\tau) \sim T^3(\tau)$, hence, we find

$$T(\tau) = T_0 \left(\frac{\tau_0}{\tau}\right)^{1/3}. \tag{D.4}$$

Similar expressions can be found for the energy density and pressure,

$$\mathcal{E}(\tau) = \mathcal{E}_0 \left(\frac{\tau_0}{\tau}\right)^{4/3}, \quad \mathcal{P}(\tau) = \mathcal{P}_0 \left(\frac{\tau_0}{\tau}\right)^{4/3}. \tag{D.5}$$

Appendix E   Conformal invariance

Conformal symmetry a theory is covariance of its equations of motion under Weyl scaling of the metric:

$$g_{\mu\nu} \to e^{-2\phi}g_{\mu\nu}, \quad u^\mu \to e^\phi u^\mu, \quad T \to e^\phi T, \tag{E.1}$$

where ϕ depends on the coordinates x^μ [10, 207, 208]. A quantity which transforms homogeneously with a factor of $e^{s\phi}$ is said to transform with Weyl weight s.

A beautiful formalism allowing for manifest Weyl covariance in conformal hydrodynamics was introduced by Ref. [207] and applied to fluid-gravity duality in Ref. [208]. The basic tool is the Weyl-covariant derivative $\mathcal{D}_\mu$, which preserves the Weyl weight of the differentiated tensor. It is constructed using the vector field $\mathcal{A}_\nu$ defined by [207]

$$\mathcal{A}_\nu \equiv U^\lambda \partial_\lambda U_\nu - \frac{\partial_\lambda U^\lambda}{3} U_\nu. \tag{E.2}$$

This quantity is of order one in the gradient expansion and transforms as a connection under Weyl-

transformations

$$\mathcal{A}_\nu \to \mathcal{A}_\nu + \partial_\nu \phi. \tag{E.3}$$

Due to this property it can be used to compensate for derivatives of the Weyl factor when differentiating a Weyl-covariant tensor. For instance, one has

$$\mathcal{D}_\mu T \;\; = \;\; \partial_\mu T - \mathcal{A}_\mu T. \tag{E.4}$$

By adding suitable correction terms one can construct a Weyl-covariant derivative of any tensor which transforms homogeneously under Weyl scaling. The case of most interest in the context of this review is the Weyl-covariant derivative of $\pi_{\mu\nu}$, which reads

$$\mathcal{D}\,\pi_{\mu\nu} = U^\lambda (\partial_\lambda + 4\,A_\lambda)\,\pi_{\mu\nu} - 2A^\lambda U_{(\mu} \pi_{\nu)\lambda}.$$

The same formula applies also to $\frac{1}{T}\mathcal{D}\,\pi_{\mu\nu}$, which provides therefore a recipe for decoding Eqs. (7.20) and (7.22). For further details the reader is referred to the original literature cited above.

References

[1] L. D. Landau and E. M. Lifshitz, *Fluid Mechanics, Second Edition: Volume 6 (Course of Theoretical Physics)*. 1987.

[2] J. Casalderrey-Solana, H. Liu, D. Mateos, K. Rajagopal, and U. A. Wiedemann, *Gauge/String Duality, Hot QCD and Heavy Ion Collisions*. 2011. `arXiv:1101.0618 [hep-th]`.

[3] O. DeWolfe, S. S. Gubser, C. Rosen, and D. Teaney, "Heavy ions and string theory," *Prog. Part. Nucl. Phys.* **75** (2014) 86–132, `arXiv:1304.7794 [hep-th]`.

[4] P. Romatschke, "New Developments in Relativistic Viscous Hydrodynamics," *Int. J. Mod. Phys.* **E19** (2010) 1–53, `arXiv:0902.3663 [hep-ph]`.

[5] S. Jeon and U. Heinz, "Introduction to Hydrodynamics," *Int. J. Mod. Phys.* **E24** (2015) no. 10, 1530010, `arXiv:1503.03931 [hep-ph]`.

[6] A. Jaiswal and V. Roy, "Relativistic hydrodynamics in heavy-ion collisions: general aspects and recent developments," *Adv. High Energy Phys.* **2016** (2016) 9623034, `arXiv:1605.08694 [nucl-th]`.

[7] K. Yagi, T. Hatsuda, and Y. Miake, "Quark-gluon plasma: From big bang to little bang," *Camb. Monogr. Part. Phys. Nucl. Phys. Cosmol.* **23** (2005) 1–446.

[8] R. Vogt, *Ultrarelativistic heavy-ion collisions*. Elsevier, Amsterdam, 2007.

[9] W. Florkowski, *Phenomenology of Ultra-Relativistic Heavy-Ion Collisions*. 2010.

[10] R. Baier, P. Romatschke, D. T. Son, A. O. Starinets, and M. A. Stephanov, "Relativistic viscous hydrodynamics, conformal invariance, and holography," *JHEP* **04** (2008) 100, `arXiv:0712.2451 [hep-th]`.

[11] P. M. Chesler and L. G. Yaffe, "Boost invariant flow, black hole formation, and far-from-equilibrium dynamics in N = 4 supersymmetric Yang-Mills theory," *Phys.Rev.* **D82** (2010) 026006, `arXiv:0906.4426 [hep-th]`.

[12] P. M. Chesler and L. G. Yaffe, "Holography and colliding gravitational shock waves in asymptotically AdS$_5$ spacetime," *Phys. Rev. Lett.* **106** (2011) 021601, `arXiv:1011.3562 [hep-th]`.

[13] M. P. Heller, R. A. Janik, and P. Witaszczyk, "The characteristics of thermalization of boost-invariant plasma from holography," *Phys.Rev.Lett.* **108** (2012) 201602, `arXiv:1103.3452 [hep-th]`.

[14] P. Romatschke, "Do nuclear collisions create a locally equilibrated quark?gluon plasma?," *Eur. Phys. J.* **C77** (2017) no. 1, 21, `arXiv:1609.02820 [nucl-th]`.

[15] W. A. Hiscock and L. Lindblom, "Generic instabilities in first-order dissipative relativistic fluid theories," *Phys.Rev.* **D31** (1985) 725–733.

[16] M. Lublinsky and E. Shuryak, "How much entropy is produced in strongly coupled Quark-Gluon Plasma (sQGP) by dissipative effects?," *Phys. Rev.* **C76** (2007) 021901, `arXiv:0704.1647 [hep-ph]`.

[17] G. S. Denicol, J. Noronha, H. Niemi, and D. H. Rischke, "Origin of the Relaxation Time in Dissipative Fluid Dynamics," *Phys.Rev.* **D83** (2011) 074019, `arXiv:1102.4780 [hep-th]`.

[18] M. P. Heller, R. A. Janik, and P. Witaszczyk, "Hydrodynamic Gradient Expansion in Gauge Theory Plasmas," *Phys.Rev.Lett.* **110** (2013) no. 21, 211602, `arXiv:1302.0697 [hep-th]`.

[19] M. P. Heller and M. Spalinski, "Hydrodynamics Beyond the Gradient Expansion: Resurgence and Resummation," *Phys. Rev. Lett.* **115** (2015) no. 7, 072501, `arXiv:1503.07514 [hep-th]`.

[20] M. P. Heller, R. A. Janik, M. Spalinski, and P. Witaszczyk, "Coupling hydrodynamics to nonequilibrium degrees of freedom in strongly interacting quark-gluon plasma," *Phys.Rev.Lett.* **113** (2014) no. 26, 261601, `arXiv:1409.5087 [hep-th]`.

[21] K. Landsteiner, "Notes on Anomaly Induced Transport," *Acta Phys. Polon.* **B47** (2016) 2617, `arXiv:1610.04413 [hep-th]`.

[22] F. M. Haehl, R. Loganayagam, and M. Rangamani, "Adiabatic hydrodynamics: The eightfold way to dissipation," *JHEP* **05** (2015) 060, `arXiv:1502.00636 [hep-th]`.

[23] M. Stephanov and Y. Yin, "Hydrodynamics and critical slowing down," 2017. `arXiv:1704.07396 [nucl-th]`. `https://inspirehep.net/record/1594939/files/arXiv:1704.07396.pdf`.

[24] A. Buchel and C. Pagnutti, "Bulk viscosity of N=2* plasma," *Nucl. Phys.* **B816** (2009) 62–72, `arXiv:0812.3623 [hep-th]`.

[25] A. Buchel, M. P. Heller, and R. C. Myers, "Equilibration rates in a strongly coupled nonconformal quark-gluon plasma," *Phys. Rev. Lett.* **114** (2015) no. 25, 251601, `arXiv:1503.07114 [hep-th]`.

[26] R. A. Janik, G. Plewa, H. Soltanpanahi, and M. Spalinski, "Linearized nonequilibrium dynamics in nonconformal plasma," *Phys. Rev.* **D91** (2015) no. 12, 126013, `arXiv:1503.07149 [hep-th]`.

[27] T. Ishii, E. Kiritsis, and C. Rosen, "Thermalization in a Holographic Confining Gauge Theory," *JHEP* **08** (2015) 008, `arXiv:1503.07766 [hep-th]`.

[28] R. A. Janik, J. Jankowski, and H. Soltanpanahi, "Quasinormal modes and the phase structure of strongly coupled matter," *JHEP* **06** (2016) 047, `arXiv:1603.05950 [hep-th]`.

[29] M. Attems, J. Casalderrey-Solana, D. Mateos, D. Santos-Olivan, C. F. Sopuerta, M. Triana, and M. Zilhao, "Holographic Collisions in Non-conformal Theories," *JHEP* **01** (2017) 026, `arXiv:1604.06439 [hep-th]`.

[30] M. Attems, J. Casalderrey-Solana, D. Mateos, D. Santos-Olivan, C. F. Sopuerta, M. Triana, and M. Zilhao, "Paths to equilibrium in non-conformal collisions," *JHEP* **06** (2017) 154, `arXiv:1703.09681 [hep-th]`.

[31] P. Kovtun, G. D. Moore, and P. Romatschke, "The stickiness of sound: An absolute lower limit on viscosity and the breakdown of second order relativistic hydrodynamics," *Phys. Rev.* **D84** (2011) 025006, `arXiv:1104.1586 [hep-ph]`.

[32] J. I. Kapusta, B. Muller, and M. Stephanov, "Relativistic Theory of Hydrodynamic Fluctuations with Applications to Heavy Ion Collisions," *Phys. Rev.* **C85** (2012) 054906, `arXiv:1112.6405 [nucl-th]`.

[33] Y. Akamatsu, A. Mazeliauskas, and D. Teaney, "A kinetic regime of hydrodynamic fluctuations and long time tails for a Bjorken expansion," *Phys. Rev.* **C95** (2017) no. 1, 014909, `arXiv:1606.07742 [nucl-th]`.

[34] S. Bhattacharyya, V. E. Hubeny, R. Loganayagam, G. Mandal, S. Minwalla, T. Morita, M. Rangamani, and H. S. Reall, "Local Fluid Dynamical Entropy from Gravity," *JHEP* **06** (2008) 055, `arXiv:0803.2526 [hep-th]`.

[35] P. Figueras, V. E. Hubeny, M. Rangamani, and S. F. Ross, "Dynamical black holes and expanding plasmas," *JHEP* **04** (2009) 137, `arXiv:0902.4696 [hep-th]`.

[36] I. Booth, M. P. Heller, and M. Spalinski, "Black Brane Entropy and Hydrodynamics," *Phys. Rev.* **D83** (2011) 061901, `arXiv:1010.6301 [hep-th]`.

[37] I. Booth, M. P. Heller, G. Plewa, and M. Spalinski, "On the apparent horizon in fluid-gravity duality," *Phys. Rev.* **D83** (2011) 106005, `arXiv:1102.2885 [hep-th]`.

[38] P. M. Chesler, N. Kilbertus, and W. van der Schee, "Universal hydrodynamic flow in holographic planar shock collisions," *JHEP* **11** (2015) 135, `arXiv:1507.02548 [hep-th]`.

[39] P. M. Chesler, "How big are the smallest drops of quark-gluon plasma?," *JHEP* **03** (2016) 146, `arXiv:1601.01583 [hep-th]`.

[40] L. D. McLerran and R. Venugopalan, "Computing quark and gluon distribution functions for very large nuclei," *Phys. Rev.* **D49** (1994) 2233–2241, `arXiv:hep-ph/9309289 [hep-ph]`.

[41] L. D. McLerran and R. Venugopalan, "Gluon distribution functions for very large nuclei at small transverse momentum," *Phys. Rev.* **D49** (1994) 3352–3355, `arXiv:hep-ph/9311205 [hep-ph]`.

[42] F. Gelis, "The Initial Stages of Heavy Ion Collisions," *Acta Phys. Polon.* **B45** (2014) no. 12, 2257–2306.

[43] A. Bialas, M. Bleszynski, and W. Czyz, "Multiplicity Distributions in Nucleus-Nucleus Collisions at High-Energies," *Nucl. Phys.* **B111** (1976) 461–476.

[44] P. Romatschke and U. Romatschke, "Viscosity Information from Relativistic Nuclear Collisions: How Perfect is the Fluid Observed at RHIC?," *Phys. Rev. Lett.* **99** (2007) 172301, `arXiv:0706.1522 [nucl-th]`.

[45] S. Borsanyi, G. Endrodi, Z. Fodor, A. Jakovac, S. D. Katz, S. Krieg, C. Ratti, and K. K. Szabo, "The QCD equation of state with dynamical quarks," *JHEP* **11** (2010) 077, `arXiv:1007.2580 [hep-lat]`.

[46] P. Huovinen, P. F. Kolb, U. W. Heinz, P. V. Ruuskanen, and S. A. Voloshin, "Radial and elliptic flow at RHIC: Further predictions," *Phys. Lett.* **B503** (2001) 58–64, `arXiv:hep-ph/0101136 [hep-ph]`.

[47] D. Teaney, J. Lauret, and E. V. Shuryak, "A Hydrodynamic description of heavy ion collisions at the SPS and RHIC," `arXiv:nucl-th/0110037 [nucl-th]`.

[48] P. F. Kolb and R. Rapp, "Transverse flow and hadrochemistry in Au+Au collisions at $\sqrt{s_{\mathrm{NN}}} = 200$ GeV," *Phys. Rev.* **C67** (2003) 044903, `arXiv:hep-ph/0210222 [hep-ph]`.

[49] P. Kovtun, D. T. Son, and A. O. Starinets, "Viscosity in strongly interacting quantum field theories from black hole physics," *Phys. Rev. Lett.* **94** (2005) 111601, `arXiv:hep-th/0405231 [hep-th]`.

[50] H. Song, S. A. Bass, U. Heinz, T. Hirano, and C. Shen, "200 A GeV Au+Au collisions serve a nearly perfect quark-gluon liquid," *Phys. Rev. Lett.* **106** (2011) 192301, `arXiv:1011.2783 [nucl-th]`. [Erratum: Phys. Rev. Lett.109,139904(2012)].

[51] B. Alver and G. Roland, "Collision geometry fluctuations and triangular flow in heavy-ion collisions," *Phys. Rev.* **C81** (2010) 054905, `arXiv:1003.0194 [nucl-th]`. [Erratum: Phys. Rev.C82,039903(2010)].

[52] J. Noronha-Hostler, G. S. Denicol, J. Noronha, R. P. G. Andrade, and F. Grassi, "Bulk Viscosity Effects in Event-by-Event Relativistic Hydrodynamics," *Phys. Rev.* **C88** (2013) no. 4, 044916, `arXiv:1305.1981 [nucl-th]`.

[53] P. K. Kovtun and A. O. Starinets, "Quasinormal modes and holography," *Phys. Rev.* **D72** (2005) 086009, `arXiv:hep-th/0506184 [hep-th]`.

[54] S. Grozdanov, N. Kaplis, and A. O. Starinets, "From strong to weak coupling in holographic models of thermalization," *JHEP* **07** (2016) 151, `arXiv:1605.02173 [hep-th]`.

[55] S. A. Hartnoll and S. P. Kumar, "AdS black holes and thermal Yang-Mills correlators," *JHEP* **12** (2005) 036, `arXiv:hep-th/0508092 [hep-th]`.

[56] P. Romatschke, "Retarded correlators in kinetic theory: branch cuts, poles and hydrodynamic onset transitions," *Eur. Phys. J.* **C76** (2016) no. 6, 352, `arXiv:1512.02641 [hep-th]`.

[57] P. B. Arnold and L. G. Yaffe, "Effective theories for real time correlations in hot plasmas," *Phys. Rev.* **D57** (1998) 1178–1192, `arXiv:hep-ph/9709449 [hep-ph]`.

[58] S. Jeon and L. G. Yaffe, "From quantum field theory to hydrodynamics: Transport coefficients and effective kinetic theory," *Phys. Rev.* **D53** (1996) 5799–5809, `arXiv:hep-ph/9512263 [hep-ph]`.

[59] P. B. Arnold, G. D. Moore, and L. G. Yaffe, "Transport coefficients in high temperature gauge theories. 1. Leading log results," *JHEP* **11** (2000) 001, `arXiv:hep-ph/0010177 [hep-ph]`.

[60] P. B. Arnold, G. D. Moore, and L. G. Yaffe, "Effective kinetic theory for high temperature gauge theories," *JHEP* **01** (2003) 030, `arXiv:hep-ph/0209353 [hep-ph]`.

[61] P. B. Arnold, G. D. Moore, and L. G. Yaffe, "Transport coefficients in high temperature gauge theories. 2. Beyond leading log," *JHEP* **05** (2003) 051, `arXiv:hep-ph/0302165 [hep-ph]`.

[62] A. Czajka and S. Jeon, "Kubo formulas for the shear and bulk viscosity relaxation times and the scalar field theory shear τ_π calculation," *Phys. Rev.* **C95** (2017) no. 6, 064906, `arXiv:1701.07580 [nucl-th]`.

[63] A. Kurkela and E. Lu, "Approach to Equilibrium in Weakly Coupled Non-Abelian Plasmas," *Phys. Rev. Lett.* **113** (2014) no. 18, 182301, `arXiv:1405.6318 [hep-ph]`.

[64] A. Kurkela and Y. Zhu, "Isotropization and hydrodynamization in weakly coupled heavy-ion collisions," *Phys. Rev. Lett.* **115** (2015) no. 18, 182301, `arXiv:1506.06647 [hep-ph]`.

[65] L. Keegan, A. Kurkela, P. Romatschke, W. van der Schee, and Y. Zhu, "Weak and strong coupling equilibration in nonabelian gauge theories," *JHEP* **04** (2016) 031, `arXiv:1512.05347 [hep-th]`.

[66] P. L. Bhatnagar, E. P. Gross, and M. Krook, "A Model for Collision Processes in Gases. 1. Small Amplitude Processes in Charged and Neutral One-Component Systems," *Phys. Rev.* **94** (1954) 511–525.

[67] J. L. Anderson and H. R. Witting, "A relativistic relaxation-time model for the Boltzmann equation," *Physica* **74** (1974) 466.

[68] S. de Groot, W. van Leeuwen, and C. van Weert, *Relativistic Kinetic Theory: Principles and Applications*. 1980.

[69] R. Baier, A. H. Mueller, D. Schiff, and D. T. Son, "'Bottom up' thermalization in heavy ion collisions," *Phys. Lett.* **B502** (2001) 51–58, `arXiv:hep-ph/0009237 [hep-ph]`.

[70] J. M. Maldacena, "The Large N limit of superconformal field theories and supergravity," *Adv.Theor.Math.Phys.* **2** (1998) 231–252, `arXiv:hep-th/9711200 [hep-th]`.

[71] S. Gubser, I. R. Klebanov, and A. M. Polyakov, "Gauge theory correlators from noncritical string theory," *Phys.Lett.* **B428** (1998) 105–114, `arXiv:hep-th/9802109 [hep-th]`.

[72] E. Witten, "Anti-de Sitter space and holography," *Adv.Theor.Math.Phys.* **2** (1998) 253–291, `arXiv:hep-th/9802150 [hep-th]`.

[73] E. D'Hoker and D. Z. Freedman, "Supersymmetric gauge theories and the AdS / CFT correspondence," in *Strings, Branes and Extra Dimensions: TASI 2001: Proceedings*, pp. 3–158. 2002. `arXiv:hep-th/0201253 [hep-th]`.

[74] A. Czajka and S. Mrowczynski, "Universality of the hard-loop action," *Phys. Rev.* **D91** (2015) no. 2, 025013, `arXiv:1410.5117 [hep-ph]`.

[75] G. 't Hooft, "A Planar Diagram Theory for Strong Interactions," *Nucl. Phys.* **B72** (1974) 461.

[76] S. de Haro, S. N. Solodukhin, and K. Skenderis, "Holographic reconstruction of space-time and renormalization in the AdS / CFT correspondence," *Commun. Math. Phys.* **217** (2001) 595–622, `arXiv:hep-th/0002230 [hep-th]`.

[77] R. C. Myers, "Higher Derivative Gravity, Surface Terms and String Theory," *Phys. Rev.* **D36** (1987) 392.

[78] Y. Kats and P. Petrov, "Effect of curvature squared corrections in AdS on the viscosity of the dual gauge theory," *JHEP* **01** (2009) 044, `arXiv:0712.0743 [hep-th]`.

[79] M. Brigante, H. Liu, R. C. Myers, S. Shenker, and S. Yaida, "Viscosity Bound Violation in Higher Derivative Gravity," *Phys. Rev.* **D77** (2008) 126006, `arXiv:0712.0805 [hep-th]`.

[80] A. Buchel, R. C. Myers, and A. Sinha, "Beyond eta/s = 1/4 pi," *JHEP* **03** (2009) 084, `arXiv:0812.2521 [hep-th]`.

[81] S. Grozdanov and A. O. Starinets, "Second-order transport, quasinormal modes and zero-viscosity limit in the Gauss-Bonnet holographic fluid," *JHEP* **03** (2017) 166, `arXiv:1611.07053 [hep-th]`.

[82] X. O. Camanho, J. D. Edelstein, J. Maldacena, and A. Zhiboedov, "Causality Constraints on Corrections to the Graviton Three-Point Coupling," *JHEP* **02** (2016) 020, `arXiv:1407.5597 [hep-th]`.

[83] E. Witten, "Anti-de Sitter space, thermal phase transition, and confinement in gauge theories," *Adv. Theor. Math. Phys.* **2** (1998) 505–532, `arXiv:hep-th/9803131 [hep-th]`.

[84] S. W. Hawking, "Particle Creation by Black Holes," *Commun. Math. Phys.* **43** (1975) 199–220. [,167(1975)].

[85] J. D. Bekenstein, "Black holes and entropy," *Phys. Rev.* **D7** (1973) 2333–2346.

[86] S. W. Hawking, "Black Holes and Thermodynamics," *Phys. Rev.* **D13** (1976) 191–197.

[87] S. S. Gubser, I. R. Klebanov, and A. A. Tseytlin, "Coupling constant dependence in the thermodynamics of N=4 supersymmetric Yang-Mills theory," *Nucl. Phys.* **B534** (1998) 202–222, `arXiv:hep-th/9805156 [hep-th]`.

[88] P. Petreczky, "Lattice QCD at non-zero temperature," *J. Phys.* **G39** (2012) 093002, `arXiv:1203.5320 [hep-lat]`.

[89] J. D. Bekenstein, "Generalized second law of thermodynamics in black hole physics," *Phys. Rev.* **D9** (1974) 3292–3300.

[90] J. M. Bardeen, B. Carter, and S. W. Hawking, "The Four laws of black hole mechanics," *Commun. Math. Phys.* **31** (1973) 161–170.

[91] E. Berti, V. Cardoso, and A. O. Starinets, "Quasinormal modes of black holes and black branes," *Class. Quant. Grav.* **26** (2009) 163001, `arXiv:0905.2975 [gr-qc]`.

[92] D. Nickel and D. T. Son, "Deconstructing holographic liquids," *New J. Phys.* **13** (2011) 075010, `arXiv:1009.3094 [hep-th]`.

[93] J. D. Bjorken, "Highly Relativistic Nucleus-Nucleus Collisions: The Central Rapidity Region," *Phys. Rev.* **D27** (1983) 140–151.

[94] R. A. Janik and R. B. Peschanski, "Asymptotic perfect fluid dynamics as a consequence of AdS/CFT," *Phys. Rev.* **D73** (2006) 045013, `arXiv:hep-th/0512162`.

[95] J. Casalderrey-Solana, M. P. Heller, D. Mateos, and W. van der Schee, "From full stopping to transparency in a holographic model of heavy ion collisions," *Phys. Rev. Lett.* **111** (2013) 181601, `arXiv:1305.4919 [hep-th]`.

[96] P. Arnold, P. Romatschke, and W. van der Schee, "Absence of a local rest frame in far from equilibrium quantum matter," *JHEP* **10** (2014) 110, `arXiv:1408.2518 [hep-th]`.

[97] R. A. Janik, "Viscous plasma evolution from gravity using AdS/CFT," *Phys.Rev.Lett.* **98** (2007) 022302, `arXiv:hep-th/0610144 [hep-th]`.

[98] S. Nakamura and S.-J. Sin, "A Holographic dual of hydrodynamics," *JHEP* **09** (2006) 020, `arXiv:hep-th/0607123 [hep-th]`.

[99] M. P. Heller and R. A. Janik, "Viscous hydrodynamics relaxation time from AdS/CFT," *Phys. Rev.* **D76** (2007) 025027, `arXiv:hep-th/0703243 [HEP-TH]`.

[100] M. P. Heller, P. Surowka, R. Loganayagam, M. Spalinski, and S. E. Vazquez, "Consistent Holographic Description of Boost-Invariant Plasma," *Phys. Rev. Lett.* **102** (2009) 041601, `arXiv:0805.3774 [hep-th]`.

[101] I. Booth, M. P. Heller, and M. Spalinski, "Black brane entropy and hydrodynamics: The Boost-invariant case," *Phys. Rev.* **D80** (2009) 126013, `arXiv:0910.0748 [hep-th]`.

[102] S. Bhattacharyya, V. E. Hubeny, S. Minwalla, and M. Rangamani, "Nonlinear Fluid Dynamics from Gravity," *JHEP* **0802** (2008) 045, `arXiv:0712.2456 [hep-th]`.

[103] M. P. Heller, R. A. Janik, and P. Witaszczyk, "A numerical relativity approach to the initial value problem in asymptotically Anti-de Sitter spacetime for plasma thermalization - an ADM formulation," *Phys.Rev.* **D85** (2012) 126002, `arXiv:1203.0755 [hep-th]`.

[104] P. M. Chesler and L. G. Yaffe, "Numerical solution of gravitational dynamics in asymptotically anti-de Sitter spacetimes," *JHEP* **07** (2014) 086, `arXiv:1309.1439 [hep-th]`.

[105] V. Cardoso, L. Gualtieri, C. Herdeiro, and U. Sperhake, "Exploring New Physics Frontiers Through Numerical Relativity," *Living Rev. Relativity* **18** (2015) 1, `arXiv:1409.0014 [gr-qc]`.

[106] P. M. Chesler and L. G. Yaffe, "Horizon formation and far-from-equilibrium isotropization in supersymmetric Yang-Mills plasma," *Phys. Rev. Lett.* **102** (2009) 211601, `arXiv:0812.2053 [hep-th]`.

[107] J. Jankowski, G. Plewa, and M. Spalinski, "Statistics of thermalization in Bjorken Flow," *JHEP* **12** (2014) 105, `arXiv:1411.1969 [hep-th]`.

[108] G. Beuf, M. P. Heller, R. A. Janik, and R. Peschanski, "Boost-invariant early time dynamics from AdS/CFT," *JHEP* **10** (2009) 043, `arXiv:0906.4423 [hep-th]`.

[109] T. Lappi and L. McLerran, "Some features of the glasma," *Nucl. Phys.* **A772** (2006) 200–212, `arXiv:hep-ph/0602189 [hep-ph]`.

[110] B. Wu and P. Romatschke, "Shock wave collisions in AdS5: approximate numerical solutions," *Int. J. Mod. Phys.* **C22** (2011) 1317–1342, `arXiv:1108.3715 [hep-th]`.

[111] D. Grumiller and P. Romatschke, "On the collision of two shock waves in AdS(5)," *JHEP* **08** (2008) 027, `arXiv:0803.3226 [hep-th]`.

[112] A. Bialas and W. Czyz, "Boost Invariant Boltzmann-vlasov Equations for Relativistic Quark - Anti-quark Plasma," *Phys. Rev.* **D30** (1984) 2371.

[113] A. Bialas, W. Czyz, A. Dyrek, and W. Florkowski, "Oscillations of Quark - Gluon Plasma Generated in Strong Color Fields," *Nucl. Phys.* **B296** (1988) 611–624.

[114] G. Baym, "Thermal equilibration in ultra relativistic heavy-ion collisions," *Phys. Lett.* **B138** (1984) 18–22.

[115] W. Florkowski, R. Ryblewski, and M. Strickland, "Anisotropic Hydrodynamics for Rapidly Expanding Systems," *Nucl. Phys.* **A916** (2013) 249–259, `arXiv:1304.0665 [nucl-th]`.

[116] W. Florkowski, R. Ryblewski, and M. Strickland, "Testing viscous and anisotropic hydrodynamics in an exactly solvable case," *Phys. Rev.* **C88** (2013) 024903, `arXiv:1305.7234 [nucl-th]`.

[117] A. Jaiswal, "Relativistic dissipative hydrodynamics from kinetic theory with relaxation time approximation," *Phys. Rev.* **C87** (2013) no. 5, 051901, `arXiv:1302.6311 [nucl-th]`.

[118] M. P. Heller, A. Kurkela, and M. Spalinski, "Hydrodynamization and transient modes of expanding plasma in kinetic theory," `arXiv:1609.04803 [nucl-th]`.

[119] W. Broniowski, M. Chojnacki, W. Florkowski, and A. Kisiel, "Uniform Description of Soft Observables in Heavy-Ion Collisions at s(NN)**(1/2) = 200 GeV**2," *Phys. Rev. Lett.* **101** (2008) 022301, `arXiv:0801.4361 [nucl-th]`.

[120] P. Romatschke, "Relativistic Viscous Fluid Dynamics and Non-Equilibrium Entropy," *Class. Quant. Grav.* **27** (2010) 025006, `arXiv:0906.4787 [hep-th]`.

[121] G. Plewa and M. Spalinski, "Entropy currents from holography in hydrodynamics with charge," *JHEP* **07** (2013) 062, `arXiv:1304.6705 [hep-th]`.

[122] F. M. Haehl, R. Loganayagam, and M. Rangamani, "The eightfold way to dissipation," *Phys. Rev. Lett.* **114** (2015) 201601, `arXiv:1412.1090 [hep-th]`.

[123] L. Lindblom, "The Relaxation effect in dissipative relativistic fluid theories," *Annals Phys.* **247** (1996) 1, `arXiv:gr-qc/9508058 [gr-qc]`.

[124] P. Kostadt and M. Liu, "Causality and stability of the relativistic diffusion equation," *Phys. Rev.* **D62** (2000) 023003.

[125] R. P. Geroch, "On hyperbolic 'theories' of relativistic dissipative fluids," `arXiv:gr-qc/0103112 [gr-qc]`.

[126] I. Muller, "Zum Paradoxon der Warmeleitungstheorie," *Z. Phys.* **198** (1967) 329–344.

[127] W. Israel, "Nonstationary irreversible thermodynamics: A Causal relativistic theory," *Annals Phys.* **100** (1976) 310–331.

[128] W. Israel and J. M. Stewart, "Transient relativistic thermodynamics and kinetic theory," *Annals Phys.* **118** (1979) 341–372.

[129] R. Baier, P. Romatschke, and U. A. Wiedemann, "Dissipative hydrodynamics and heavy ion collisions," *Phys. Rev.* **C73** (2006) 064903, `arXiv:hep-ph/0602249 [hep-ph]`.

[130] G. S. Denicol, H. Niemi, E. Molnar, and D. H. Rischke, "Derivation of transient relativistic fluid dynamics from the Boltzmann equation," *Phys. Rev.* **D85** (2012) 114047, `arXiv:1202.4551 [nucl-th]`. [Erratum: Phys. Rev.D91,no.3,039902(2015)].

[131] G. Denicol, E. Molnar, H. Niemi, and D. Rischke, "Derivation of fluid dynamics from kinetic theory with the 14–moment approximation," *Eur. Phys. J. A* **48** (2012) 170, `arXiv:1206.1554 [nucl-th]`.

[132] G. S. Denicol, "Kinetic foundations of relativistic dissipative fluid dynamics," *J. Phys.* **G41** (2014) no. 12, 124004.

[133] W. Florkowski and R. Ryblewski, "Highly-anisotropic and strongly-dissipative hydrodynamics for early stages of relativistic heavy-ion collisions," *Phys. Rev.* **C83** (2011) 034907, `arXiv:1007.0130 [nucl-th]`.

[134] M. Martinez and M. Strickland, "Dissipative Dynamics of Highly Anisotropic Systems," *Nucl. Phys.* **A848** (2010) 183–197, `arXiv:1007.0889 [nucl-th]`.

[135] M. Strickland, "Anisotropic Hydrodynamics: Three lectures," *Acta Phys. Polon.* **B45** (2014) no. 12, 2355–2394, `arXiv:1410.5786 [nucl-th]`.

[136] P. Romatschke, "Far From Equilibrium Fluid Dynamics," `arXiv:1704.08699 [hep-th]`.

[137] M. Habich, G. A. Miller, P. Romatschke, and W. Xiang, "Testing Hydrodynamic Descriptions of of p+p Collisions at $\sqrt{s} = 7$ TeV," `arXiv:1512.05354 [nucl-th]`.

[138] M. Spalinski, "Small systems and regulator dependence in relativistic hydrodynamics," *Phys. Rev.* **D94** (2016) no. 8, 085002, `arXiv:1607.06381 [nucl-th]`.

[139] W. Florkowski, R. Ryblewski, and M. Spalinski, "Gradient expansion for anisotropic hydrodynamics," `arXiv:1608.07558 [nucl-th]`.

[140] S. Grozdanov and N. Kaplis, "Constructing higher-order hydrodynamics: The third order," *Phys. Rev.* **D93** (2016) no. 6, 066012, `arXiv:1507.02461 [hep-th]`.

[141] J. Bhattacharya, S. Bhattacharyya, S. Minwalla, and A. Yarom, "A Theory of first order dissipative superfluid dynamics," *JHEP* **05** (2014) 147, `arXiv:1105.3733 [hep-th]`.

[142] A. Buchel and J. T. Liu, "Universality of the shear viscosity in supergravity," *Phys. Rev. Lett.* **93** (2004) 090602, `arXiv:hep-th/0311175 [hep-th]`.

[143] A. Muronga, "Second order dissipative fluid dynamics for ultrarelativistic nuclear collisions," *Phys. Rev. Lett.* **88** (2002) 062302, `arXiv:nucl-th/0104064 [nucl-th]`. [Erratum: Phys. Rev. Lett.89,159901(2002)].

[144] A. Muronga, "Causal theories of dissipative relativistic fluid dynamics for nuclear collisions," *Phys. Rev.* **C69** (2004) 034903, `arXiv:nucl-th/0309055 [nucl-th]`.

[145] U. W. Heinz, H. Song, and A. K. Chaudhuri, "Dissipative hydrodynamics for viscous relativistic fluids," *Phys. Rev.* **C73** (2006) 034904, `arXiv:nucl-th/0510014 [nucl-th]`.

[146] P. Bozek, "Bulk and shear viscosities of matter created in relativistic heavy-ion collisions," *Phys. Rev.* **C81** (2010) 034909, `arXiv:0911.2397 [nucl-th]`.

[147] C. Shen, Z. Qiu, H. Song, J. Bernhard, S. Bass, and U. Heinz, "The iEBE-VISHNU code package for relativistic heavy-ion collisions," *Comput. Phys. Commun.* **199** (2016) 61–85, `arXiv:1409.8164 [nucl-th]`.

[148] L. Tinti, A. Jaiswal, and R. Ryblewski, "Quasiparticle second-order viscous hydrodynamics from kinetic theory," *Phys. Rev.* **D95** (2017) no. 5, 054007, `arXiv:1612.07329 [nucl-th]`.

[149] M. Alqahtani, M. Nopoush, R. Ryblewski, and M. Strickland, "3+1d quasiparticle anisotropic hydrodynamics for ultrarelativistic heavy-ion collisions," `arXiv:1703.05808 [nucl-th]`.

[150] S. Pratt, E. Sangaline, P. Sorensen, and H. Wang, "Constraining the Eq. of State of Super-Hadronic Matter from Heavy-Ion Collisions," *Phys. Rev. Lett.* **114** (2015) 202301, `arXiv:1501.04042 [nucl-th]`.

[151] S. A. Bass, J. E. Bernhard, and J. S. Moreland, "Determination of Quark-Gluon-Plasma Parameters from a Global Bayesian Analysis," in *26th International Conference on Ultrarelativistic Nucleus-Nucleus Collisions (Quark Matter 2017) Chicago,Illinois, USA, February 6-11, 2017.* 2017. `arXiv:1704.07671 [nucl-th]`. `https://inspirehep.net/record/1594915/files/arXiv:1704.07671.pdf`.

[152] I. Aniceto and M. Spalinski, "Resurgence in Extended Hydrodynamics," *Phys. Rev.* **D93** (2016) no. 8, 085008, `arXiv:1511.06358 [hep-th]`.

[153] R. A. Janik and R. B. Peschanski, "Gauge/gravity duality and thermalization of a boost-invariant perfect fluid," *Phys. Rev.* **D74** (2006) 046007, `arXiv:hep-th/0606149 [hep-th]`.

[154] A. R. Liddle, P. Parsons, and J. D. Barrow, "Formalizing the slow roll approximation in inflation," *Phys. Rev.* **D50** (1994) 7222–7232, `arXiv:astro-ph/9408015 [astro-ph]`.

[155] J. Noronha and G. S. Denicol, "Transient Fluid Dynamics of the Quark-Gluon Plasma According to AdS/CFT," `arXiv:1104.2415 [hep-th]`.

[156] B. Schenke and M. Strickland, "Photon production from an anisotropic quark-gluon plasma," *Phys. Rev.* **D76** (2007) 025023, `arXiv:hep-ph/0611332 [hep-ph]`.

[157] L. McLerran and B. Schenke, "The Glasma, Photons and the Implications of Anisotropy," *Nucl. Phys.* **A929** (2014) 71–82, `arXiv:1403.7462 [hep-ph]`.

[158] M. Martinez and M. Strickland, "Pre-equilibrium dilepton production from an anisotropic quark-gluon plasma," *Phys. Rev.* **C78** (2008) 034917, `arXiv:0805.4552 [hep-ph]`.

[159] E. Shuryak, "Monitoring parton equilibration in heavy ion collisions via dilepton polarization," `arXiv:1203.1012 [nucl-th]`.

[160] A. Nunez and A. O. Starinets, "AdS / CFT correspondence, quasinormal modes, and thermal correlators in N=4 SYM," *Phys. Rev.* **D67** (2003) 124013, `arXiv:hep-th/0302026 [hep-th]`.

[161] T. Epelbaum and F. Gelis, "Pressure isotropization in high energy heavy ion collisions," *Phys. Rev. Lett.* **111** (2013) 232301, `arXiv:1307.2214 [hep-ph]`.

[162] J. Berges, K. Boguslavski, S. Schlichting, and R. Venugopalan, "Universal attractor in a highly occupied non-Abelian plasma," *Phys. Rev.* **D89** (2014) no. 11, 114007, `arXiv:1311.3005 [hep-ph]`.

[163] A. Jaiswal, "Relativistic third-order dissipative fluid dynamics from kinetic theory," *Phys. Rev.* **C88** (2013) 021903, `arXiv:1305.3480 [nucl-th]`.

[164] W. Czyz and W. Florkowski, "Kinetic Coefficients for Quark - Anti-quark Plasma," *Acta Phys. Polon.* **B17** (1986) 819–837.

[165] G. S. Denicol, T. Koide, and D. H. Rischke, "Dissipative relativistic fluid dynamics: a new way to derive the equations of motion from kinetic theory," *Phys. Rev. Lett.* **105** (2010) 162501, `arXiv:1004.5013 [nucl-th]`.

[166] G. S. Denicol, W. Florkowski, R. Ryblewski, and M. Strickland, "Shear-bulk coupling in nonconformal hydrodynamics," *Phys. Rev.* **C90** (2014) no. 4, 044905, `arXiv:1407.4767 [hep-ph]`.

[167] A. Jaiswal, "Relaxation-time approximation and relativistic third-order viscous hydrodynamics from kinetic theory," *Nucl. Phys.* **A931** (2014) 1205–1210, `arXiv:1407.0837 [nucl-th]`.

[168] C. Chattopadhyay, A. Jaiswal, S. Pal, and R. Ryblewski, "Relativistic third-order viscous corrections to the entropy four-current from kinetic theory," *Phys. Rev.* **C91** (2015) no. 2, 024917, `arXiv:1411.2363 [nucl-th]`.

[169] M. Martinez, R. Ryblewski, and M. Strickland, "Boost-Invariant (2+1)-dimensional Anisotropic Hydrodynamics," *Phys. Rev.* **C85** (2012) 064913, `arXiv:1204.1473 [nucl-th]`.

[170] L. Tinti and W. Florkowski, "Projection method and new formulation of leading-order anisotropic hydrodynamics," *Phys. Rev.* **C89** (2014) no. 3, 034907, `arXiv:1312.6614 [nucl-th]`.

[171] M. Nopoush, R. Ryblewski, and M. Strickland, "Bulk viscous evolution within anisotropic hydrodynamics," *Phys. Rev.* **C90** (2014) no. 1, 014908, `arXiv:1405.1355 [hep-ph]`.

[172] L. Tinti, "(3?+?1)-dimensional framework for leading-order nonconformal anisotropic hydrodynamics," *Phys. Rev.* **C92** (2015) no. 1, 014908, `arXiv:1411.7268 [nucl-th]`.

[173] L. Tinti, R. Ryblewski, W. Florkowski, and M. Strickland, "Testing different formulations of leading-order anisotropic hydrodynamics," *Nucl. Phys.* **A946** (2016) 29–48, `arXiv:1505.06456 [hep-ph]`.

[174] L. Tinti, "Anisotropic matching principle for the hydrodynamics expansion," *Phys. Rev.* **C94** (2016) no. 4, 044902, `arXiv:1506.07164 [hep-ph]`.

[175] D. Bazow, U. W. Heinz, and M. Strickland, "Second-order (2+1)-dimensional anisotropic hydrodynamics," *Phys. Rev.* **C90** (2014) no. 5, 054910, `arXiv:1311.6720 [nucl-th]`.

[176] D. Bazow, U. W. Heinz, and M. Martinez, "Nonconformal viscous anisotropic hydrodynamics," *Phys. Rev.* **C91** (2015) no. 6, 064903, `arXiv:1503.07443 [nucl-th]`.

[177] E. Molnar, H. Niemi, and D. H. Rischke, "Derivation of anisotropic dissipative fluid dynamics from the Boltzmann equation," *Phys. Rev.* **D93** (2016) no. 11, 114025, `arXiv:1602.00573 [nucl-th]`.

[178] E. Molnar, H. Niemi, and D. H. Rischke, "Closing the equations of motion of anisotropic fluid dynamics by a judicious choice of moment of the Boltzmann equation," `arXiv:1606.09019 [nucl-th]`.

[179] H. W. Barz, B. Kampfer, B. Lukacs, K. Martinas, and G. Wolf, "Deconfinement transition in anisotropic matter," *Phys. Lett.* **B194** (1987) 15–19.

[180] B. Kampfer, B. Lukacs, G. Wolf, and H. W. Barz, "Description of the nuclear stopping process within anisotropic thermo hydrodynamics," *Phys. Lett.* **B240** (1990) 297–300.

[181] R. Ryblewski and W. Florkowski, "Highly anisotropic hydrodynamics – discussion of the model assumptions and forms of the initial conditions," *Acta Phys. Polon.* **B42** (2011) 115–138, `arXiv:1011.6213 [nucl-th]`.

[182] P. Romatschke and M. Strickland, "Collective modes of an anisotropic quark gluon plasma," *Phys. Rev.* **D68** (2003) 036004, `arXiv:hep-ph/0304092 [hep-ph]`.

[183] G. Baym, "Entropy production and the evolution of ultra relativistic heavy-ion collisions ," *Nucl. Phys.* **A418** (1984) 525C–537C.

[184] W. Florkowski, E. Maksymiuk, R. Ryblewski, and M. Strickland, "Exact solution of the (0+1)-dimensional Boltzmann equation for a massive gas," *Phys. Rev.* **C89** (2014) no. 5, 054908, `arXiv:1402.7348 [hep-ph]`.

[185] G. S. Denicol, U. W. Heinz, M. Martinez, J. Noronha, and M. Strickland, "New Exact Solution of the Relativistic Boltzmann Equation and its Hydrodynamic Limit," *Phys. Rev. Lett.* **113** (2014) no. 20, 202301, `arXiv:1408.5646 [hep-ph]`.

[186] G. S. Denicol, U. W. Heinz, M. Martinez, J. Noronha, and M. Strickland, "Studying the validity of relativistic hydrodynamics with a new exact solution of the Boltzmann equation," *Phys. Rev.* **D90** (2014) no. 12, 125026, `arXiv:1408.7048 [hep-ph]`.

[187] W. Florkowski, R. Ryblewski, M. Strickland, and L. Tinti, "Non-boost-invariant dissipative hydrodynamics," `arXiv:1609.06293 [nucl-th]`.

[188] J. P. Boyd, "The devil's invention: asymptotic, superasymptotic and hyperasymptotic series," *Acta Appl. Math* **56** (1999) 1–98.

[189] G. Basar and G. V. Dunne, "Hydrodynamics, resurgence, and transasymptotics," *Phys. Rev.* **D92** (2015) no. 12, 125011, `arXiv:1509.05046 [hep-th]`.

[190] L. N. Lipatov, "Divergence of the Perturbation Theory Series and the Quasiclassical Theory," *Sov. Phys. JETP* **45** (1977) 216–223. [Zh. Eksp. Teor. Fiz.72,411(1977)].

[191] H. S. Yamada and K. S. Ikeda, "A Numerical Test of Pade Approximation for Some Functions with singularity," `arXiv:1308.4453 [math-ph]`.

[192] G. V. Dunne, "Resurgence and Trans-series in Quantum Theories," *Lectures given at the Schladming Winter School 2015* .

[193] I. Aniceto and R. Schiappa, "Nonperturbative Ambiguities and the Reality of Resurgent Transseries," *Commun. Math. Phys.* **335** (2015) no. 1, 183–245, `arXiv:1308.1115 [hep-th]`.

[194] I. Aniceto, R. Schiappa, and M. Vonk, "The Resurgence of Instantons in String Theory," *Commun. Num. Theor. Phys.* **6** (2012) 339–496, `arXiv:1106.5922 [hep-th]`.

[195] S. Kinoshita, S. Mukohyama, S. Nakamura, and K.-y. Oda, "A Holographic Dual of Bjorken Flow," *Prog. Theor. Phys.* **121** (2009) 121–164, `arXiv:0807.3797 [hep-th]`.

[196] S. Kinoshita, S. Mukohyama, S. Nakamura, and K.-y. Oda, "Consistent Anti-de Sitter-Space/Conformal-Field-Theory Dual for a Time-Dependent Finite Temperature System," *Phys. Rev. Lett.* **102** (2009) 031601, `arXiv:0901.4834 [hep-th]`.

[197] P. Grandclement and J. Novak, "Spectral methods for numerical relativity," *Living Rev. Rel.* **12** (2009) 1, `arXiv:0706.2286 [gr-qc]`.

[198] A. Buchel, M. P. Heller, and J. Noronha, "Entropy Production, Hydrodynamics, and Resurgence in the Primordial Quark-Gluon Plasma from Holography," *Phys. Rev.* **D94** (2016) no. 10, 106011, `arXiv:1603.05344 [hep-th]`.

[199] M. P. Heller, "Holography, Hydrodynamization and Heavy-Ion Collisions," *Acta Phys. Polon.* **B47** (2016) 2581, `arXiv:1610.02023 [hep-th]`.

[200] G. S. Denicol and J. Noronha, "Divergence of the Chapman-Enskog expansion in relativistic kinetic theory," `arXiv:1608.07869 [nucl-th]`.

[201] J.-P. Blaizot and L. Yan, "Onset of hydrodynamics for a quark-gluon plasma from the evolution of moments of distribution functions," `arXiv:1703.10694 [nucl-th]`.

[202] D. Bazow, M. Martinez, and U. W. Heinz, "Transient oscillations in a macroscopic effective theory of the Boltzmann equation," *Phys. Rev.* **D93** (2016) no. 3, 034002, `arXiv:1507.06595 [nucl-th]`. [Phys. Rev.D93,034002(2016)].

[203] M. P. Heller and V. Svensson, "work in progress,".

[204] P. Bozek, "Collective flow in p-Pb and d-Pd collisions at TeV energies," *Phys. Rev.* **C85** (2012) 014911, `arXiv:1112.0915 [hep-ph]`.

[205] J. Brewer and P. Romatschke, "Nonhydrodynamic Transport in Trapped Unitary Fermi Gases," *Phys. Rev. Lett.* **115** (2015) no. 19, 190404, `arXiv:1508.01199 [hep-th]`.

[206] S. Grozdanov and W. van der Schee, "Coupling constant corrections in holographic heavy ion collisions," `arXiv:1610.08976 [hep-th]`.

[207] R. Loganayagam, "Entropy Current in Conformal Hydrodynamics," *JHEP* **05** (2008) 087, `arXiv:0801.3701 [hep-th]`.

[208] S. Bhattacharyya, R. Loganayagam, I. Mandal, S. Minwalla, and A. Sharma, "Conformal Nonlinear Fluid Dynamics from Gravity in Arbitrary Dimensions," *JHEP* **12** (2008) 116, `arXiv:0809.4272 [hep-th]`.